UNIVERSITÄT DUISBURG ESSEN

Open-Minded

Disintegration behavior of polymer compounds used in biodegradable mulch films

Master Thesis

M.Sc. Environmental Toxicology (EnviTox)

Submitted by:

Maximilian Paul Stapf

Born in Filderstadt, Germany

Matriculation Number: 3107831

Supervised by:	Dr. Gerrit Renner,
	University of Duisburg-Essen
In cooperation with:	Dr. Stephan Kabasci,
	Fraunhofer UMSICHT
Date of submission:	20.04.2023

This Master Thesis has been prepared and written according to the Examination Regulation of the Master Program Environmental Toxicology at the University Duisburg-Essen. This includes all experiments and studies carried out for the Master Thesis.

The Thesis has been written at the Fraunhofer Institute for Environmental, Safety and Energy Technology UMSICHT, Oberhausen, Germany.

1st Assessor: Dr. Gerrit Renner

2nd Assessor: Dr. Stephan Kabasci

Head of Examination Board at 1st Assessors' University: *

* Not to be completed by the student.

Declaration

I declare that I have prepared this Master Thesis self-dependent according to § 20 of the Examination Regulation of the Master Program Environmental Toxicology published at 06. October 2011 at the Faculty of Biology at the University of Duisburg-Essen.

I declare that I did not use any other means and resources than indicated in this thesis. All external sources of information have been indicated appropriately in the text body and listed in the references.

Location, Date

Signature of the student

Abstract

Plastic mulch films are widely used in agriculture and their application comes with a variety of advantages like increased soil temperature, retention of soil moisture and reduced weed pressure. Most mulch films are made from poly(ethylene) (PE) which is persistent in soil when not being properly removed from the fields. To combat the threat of plastic pollution, biodegradable polymers were designed to be easily degraded into water and carbon dioxide by microorganisms. Because of the relevance of biodegradable mulch films, this work focused on the soil disintegration behavior of three biodegradable polymers that can be processed into a mulch film compound. Therefore, film like samples of poly(butylene-sebacate-co-terephthalate) (PBST), poly(butylene-adipate-co-terephthalate) (PBAT) and poly(3-hydroxybutyrate-co-3-hydroxyhexanoate) (PHA) were incubated on the soil surface and were buried in the soil to imitate the application of a mulch film and after being tilled into the soil after use. The incubation for 16 weeks at 23 °C and 50 % air humidity was conducted with regular topsoil and a mix of topsoil and agricultural soil from a test field for biodegradability studies to mimic natural conditions. First indications of material changes were found in surface modifications of PBST that were observed with light and scanning electron microscopy (SEM) as well as changes in the mechanical properties measured by a tension test. Thermal properties measured by differential scanning calorimetry (DSC) and functional groups measured by Fourier-transform infrared spectroscopy (FT-IR) remained almost constant in all samples under all conditions. Gel permeation chromatography (GPC) revealed a decrease in the molecular weight only in samples made from PHA. Comparing the polymers for the application in a biodegradable mulch film compound, a high percentage of PBST would make the material suitable for a short-term application due to the quick fragmentation. PBAT has shown slower degradation than PBST in this study. However, due to the acceleration of degradation by ultraviolet radiation reported in literature, the material may be equally suitable for short-term application. PHA may be processed for medium-term application based on its high degree of stability. The differences between surface and soil incubation were not clearly evident. In tendency, the degradation in soil seemed to be rather slower than on the surface. Further, it seemed like the influence of the agricultural soil type promoted faster material changes, although being challenging to point out clear evidence. Still, the influence of microbial communities and ultraviolet radiation is to be investigated in future studies.

Zusammenfassung

Mulchfolien sind in der Landwirtschaft weit verbreitet und bieten eine Vielzahl von Vorteilen, z.B. erhöhte Bodentemperatur und Bodenfeuchtigkeit sowie verringertes Unkrautwachstum. Die meisten Mulchfolien bestehen aus Poly(ethylen) (PE), das sich in der Erde anreichert, wenn die Folien nicht korrekt entfernt werden. Um dem entgegenzuwirken, wurden bioabbaubare Polymere entwickelt, die durch Mikroorganismen zu Wasser und Kohlenstoffdioxid abgebaut werden können. Hinsichtlich der Relevanz bioabbaubarer Mulchfolien fokussierte sich diese Arbeit auf das Desintegrationsverhalten von drei bioabbaubaren Polymeren, die als Compound in einer Mulchfolie verarbeitet werden können. Dazu wurden Folien-ähnliche Proben aus Poly(butylen-sebacat-co-terephthalat) (PBST), Poly(butylen-adipat-co-terephthalat) (PBAT) und Poly(3-hydroxybutyrat-co-3-hydroxyhexanoat) (PHA) sowohl auf als auch in Erde inkubiert, um die mögliche Anwendung als Mulchfolie nachzustellen. Die Inkubation für 16 Wochen bei 23 °C und 50 % Luftfeuchtigkeit wurde in Mutterboden und in einem Mix aus Mutterboden und Erde von einem Testfeld durchgeführt, um natürliche Bedingungen nachzuahmen. Erste Anzeichen von Materialveränderungen wurden bei PBST als Oberflächenmodifikationen bei der Untersuchung mittels Licht- und Rasterelektronen-mikroskopie (SEM) beobachtet. Gleichzeitig zeigten sich Veränderungen bei den mechanischen Eigenschaften, die mittels Zugversuchs gemessen wurden. Thermische Eigenschaften, gemessen mit Dynamischer Differenzkalorimetrie (DSC), und funktionelle Gruppen, gemessen mit Fourier-Transformations-Infrarotspektroskopie (FT-IR), blieben fast unverändert bei allen Proben. Die Abnahme des Molekulargewichts konnte durch Gel-Permeations-Chromatographie (GPC) nur in Proben aus PHA festgestellt werden. Bei einem möglichen Einsatz als Mulchfolien-Compound würde sich ein hoher Anteil an PBST für eine kurzzeitige Anwendung eignen, da sich das Material schnell zersetzt hat. PBAT zeigte zwar langsameren Abbau, aber durch beschleunigten Abbau unter Einfluss von UV-Strahlung, wie in der Literatur erwähnt, wäre eine kurzzeitige Anwendung ebenfalls denkbar. Im Gegensatz dazu könnte PHA aufgrund der hohen Stabilität für einen mittelfristigen Einsatz verarbeitet werden. Unterschiede zwischen der Inkubation auf oder in der Erde waren nicht eindeutig, allerdings schien der Abbau in der Erde langsamer abzulaufen als auf der Oberfläche. Weiterhin schien die landwirtschaftliche Erde schnellere Materialveränderungen zu bewirken, wobei klare Anzeichen schwer erkennbar waren. Demnach sollte zukünftig der Einfluss von Mikroorganismen und von UV-Strahlung weiter untersucht werden.

Acknowledgement

Firstly, I want to express my gratitude to Dr. Gerrit Renner from the University of Duisburg-Essen and Dr. Stephan Kabasci from the Fraunhofer Institute for Environmental, Safety and Energy Technology UMSICHT for the possibility to write this Master thesis. Secondly, I would like to express my full appreciation to Pia Borelbach for introducing me to the topic of biodegradable mulch films and for guiding me through the experimental setup.

I am also grateful for the constant support of Christian Brzoska, Sebastian Drabben, Jan Luskovec and Uwe Kleinwegen concerning all sorts of technical instruments. Thanks should also go to the student coworkers for frequent discussions and unlimited motivation.

Lastly, I would like to acknowledge Melli for her universal support, professional revision and belief in me.

Index

List of figures ..... **VII**

List of tables ..... **VIII**

List of abbreviations ..... **IX**

1 Introduction **1**

1.1 Plastics and the use in agriculture 1

1.2 Mulch films 1

1.3 Bioplastics and possible applications 3

1.4 The current state of biodegradable plastics 5

1.5 Steps of abiotic and biotic degradation 6

1.6 Measurement of degradation 9

1.7 Scope 10

2 Materials and devices **12**

2.1 Materials 12

2.2 Chemicals 12

2.3 Devices 13

2.4 Software 14

3 Methods **15**

3.1 Experimental setup 15

3.2 Used polymers 15

3.3 Preparations 16

3.4 Experimental conditions 18

3.5 Description of the methods 19

3.5.1 Soil moisture 19
3.5.2 pH control 19
3.5.3 Sampling and cleaning 20
3.5.4 Optical imaging 20
3.5.5 Scanning electron microscopy (SEM) 20
3.5.6 Tensile test 21
3.5.7 Differential scanning calorimetry (DSC) 21
3.5.8 Gel permeation chromatography (GPC) 22
3.5.9 Fourier-transform infrared spectroscopy (FT-IR) 23

4 Results **24**

4.1 Soil conditions 24

4.2 Visual inspection 26

4.3 Surface characterization 30

4.3.1 Light microcospy 30
4.3.2 SEM 32
4.4 Mechanical properties 35
4.5 Thermal properties 37
4.5.1 Glass transition temperature 37
4.5.2 Crystallization temperature 39
4.5.3 Melting temperature 42
4.5.4 Crystallinity 44
4.6 Molecular weight 44
4.7 Functional groups 46
5 Discussion 48
5.1 Soil conditions 48
5.2 Visual inspection and surface characterization by light microscopy 49
5.3 Surface characterization by SEM 50
5.4 Mechanical properties 51
5.5 Thermal properties 53
5.6 Molecular weight 56
5.7 Functional groups 58
6 Conclusion 60
7 Literature 62
8 Appendix 68

List of figures

Figure 1: Major fields of applications for plastics in agriculture and the most commonly used polymers, specifically in crop production (FAO 2021, PAPILLONS 2021). 2
Figure 2: Allocation of plastic types referring to the terms bio-based and biodegradable (EUBP 2022). 4
Figure 3: Interaction of abiotic and biotic factors affecting the disintegration and degradation of bioplastics (Ghosh & Jones 2021). 7
Figure 4: The main steps of biodegradation on a molecular level (Samir et al. 2022). 9
Figure 5: Structural formula of the three used polymers 15
Figure 6: Images of the three polymer types and the two sample forms of strips (top) and rectangles in film holders (bottom) before the incubation. 16
Figure 7: Temperature profile of the measurement cell and respective temperature gradient for DSC analysis 22
Figure 8: Weight course of the soil boxes. 24
Figure 9: Soil humidity during the incubation. 25
Figure 10: Change in pH during incubation. 26
Figure 11: Pictures of the control films of poly(ethylene) and cellulose. 27
Figure 12: Pictures of the sample strips from start to end of the incubation. 29
Figure 13: Close-up view of the surface of different samples. 31
Figure 14: SEM images of the surface of the three materials before incubation. 32
Figure 15: SEM images of the surface of the materials after incubation time. 34
Figure 16: Tension test of the elastic modulus. 35
Figure 17: Tensile strength at first maximum. 36
Figure 18: Comparison of the glass transition temperature of the surface samples. 38
Figure 19: Comparison the glass transition temperature of the in-soil samples. 39
Figure 20: Comparison of the crystallization temperature of the surface samples. 40
Figure 21: Comparison of the crystallization temperature of the in-soil samples. 41
Figure 22: Comparison of the melting temperature of the surface samples. 42
Figure 23: Comparison of the melting temperature of the in-soil samples. 43
Figure 24: Comparison of the molecular weight M_n of the samples 45
Figure 25: Infrared spectra of the three polymer types before and after incubation. 47
Figure 26: Layout diagram of the samples incubated on the soil surface (1.5 cm x 11 cm strips). 68
Figure 27: Layout diagram of the samples incubated on the soil surface (2 cm x 2 cm plates) and buried in the soil (3.7 cm x 3.5 cm rectangles fixed in film holders and 0.6 cm diameter circles collected in a net). 68
Figure 28: The diagram shows the heat flow of the sample chamber compared to the reference chamber according to the set temperature. 70
Figure 29: The diagram shows the heat flow of the sample chamber compared to the reference chamber according to the set temperature. 71
Figure 30: The diagram shows the heat flow of the sample chamber compared to the reference chamber according to the set temperature. 72
Figure 31: Images of the samples incubated in film holders in the soil before the incubation and after 16 weeks. 73

List of tables

Table 1: List of all used material. 12
Table 2: List of all used chemicals. 12
Table 3: List of all used devices. 13
Table 4: List of all used evaluation software. 14
Table 5: List of all combinations of polymer types, soil types and sample locations referring to their corresponding abbreviation. 18
Table 6: Measurement plan according to the sampling weeks. 69
Table 7: Overview of the temperature course during the measurement. 69
Table 8: Melting enthalpies in J / g from the second heating curve 72
Table 9: Identified peaks in the IR spectrum of poly(butylene-sebacate-co-terephthalate) (PBST). 74
Table 10: Identified peaks in the IR spectrum of poly(butylene-adipate-co-terephthalate) (PBAT) 74
Table 11: Identified peaks in the IR spectrum of poly(3-hydroxybutyrate-co-3-hydroxyhexanoate) (PHA). 75

List of abbreviations

Abbreviation	Meaning
ΔH_m	Change in melting enthalpy
δ	Bending
ν	Stretching
σ_m	Tensile strength at first maximum
°C	Degree Celsius
A	Area
Å	Angstrom
as	Asymmetric
ATR	Attenuated total reflection
bioPE	Bio-based poly(ethylene)
bioPET	Bio-based poly(ethylene-terephthalate)
BMF	Biodegradable mulch films
Bo1	Regular topsoil
Bo2	Mix of regular topsoil and agricultural soil
CH_4	Methane
cm	Centimeter
cm^2	Square centimeter
CO_2	Carbon dioxide
DSC	Differential scanning calorimetry
E_t	Tensile modulus
FT-IR	Fourier-transform infrared spectroscopy
g	Gram
GPC	Gel permeation chromatography
H_2O	Water
H_2O_2	Hydrogen peroxide
HFIP	1,1,1,3,3,3-hexafluoro-2-propanol
IN	Incubation buried in soil
J	Joule
K	Kelvin
kg	Kilogram
KTFAc	Potassium trifluoroacetate
kV	Kilovolt
$L_{critical}$	Critical thickness
LDPE	Low density poly(ethylene)
M	Molecular weight
mA	Milliampere
mg	Milligram
min	Minute
mL	Milliliter
mm	Millimeter
M_n	Number-average molecular weight

MPa	Megapascal
M_w	Weight-average molecular weight
mW	Milliwatt
M_z	Z-average molecular weight
N	Newton
OF	Incubation on the surface
PBAT	Poly(butylene-adipate-co-terephthalate)
PBST	Poly(butylene-sebacate-co-terephthalate)
PCL	Poly(caprolactone)
PDI	Polydispersity index
PE	Poly(ethylene)
PHA	Poly(hydroxyalkanoate) specifically poly(3-hydroxybutyrate-co-3-hydroxyhexanoate)
PHB	Poly(hydroxybutyrate)
PHBV	Poly(3-hydroxybutyrate-co-3-hydroxyvalerate)
PLA	Poly(lactic-acid)
PMF	Plastic mulch film
PP	Poly(propylene)
RI	Refractive index
s	Second
s	Symmetric
SEM	Scanning electron microscopy
t_c	Crystallization temperature
T_g	Glass transition temperature
t_m	Melting temperature
UV	Ultra-violet
µL	Microliter
µm	Micrometer

1 Introduction

1.1 Plastics and the use in agriculture

Plastics are ubiquitously used in modern society and economy. In 2021, the global plastics production was overall estimated as 391 million tons with an increasing trend (Plastics Europe 2022). Plastics are materials composed of synthetically or semi-synthetically produced, organic polymers. These polymers are chemical substances which are made up of multiple macro molecules. Plastics consist of several polymers, e.g. the frequently used plastic poly(ethylene) (PE) is composed of ethylene units that recur several times. They have easily adaptable features like durability, hardness, shapeability and elasticity varied by selection of the primary material, what makes them so popular in various fields of application (Koenders et al. 2020). In 2021, worldwide the largest sector of use for plastics with approximately 44 % of the annual global production was packaging, followed by building and construction with 18 %. The agricultural sector, which plays the central role within this project, showed a percentage of 4 % (Plastics Europe 2022).

Beyond the advantages as an easily adaptable material, plastics are also light weight, cost-effective, easy to install and manage and show mostly good mechanical resistance. These features make them ideal for usage in agricultural practices (Vox et al. 2016).

Plastics are involved in agriculture, e.g. as seedling trays, nursery pots, covering films for greenhouses and tunnels, shading and protective nets, silage films, bale nets, packaging containers and sacks and also soil mulching and solarization films, as can be seen in Figure 1 (FAO 2021, Malinconico 2017, Picuno 2014, Schettini & Vox 2010, Vox et al. 2016).

1.2 Mulch films

Exceeding two million tons per year, the amount of plastics used for agriculture within the various above-mentioned fields shows its importance of research (Francioni et al. 2021). Plastic mulch films (PMF) account for the majority of the plastic used in agriculture according to Kasirajan and Ngouajio (2012) and are used worldwide (Gao et al. 2019, Wang et al. 2021).

They have several positive effects on quality and yield of crops. Firstly, regulating soil temperatures by impacting the light reflection or absorption can help maintaining the optimal soil temperature for roots (Kasirajan & Ngouajio 2012, Mansoor et al. 2022). Black or transparent mulch films heat up the soil artificially for earlier germination while white mulch films contribute to reduced soil temperature and, therefore, slower germination and plant growth (Johnson & Fennimore 2005). Secondly, PMFs can increase and hold soil moisture, ensuring sufficient water availability for plant growth and reduced irrigation costs. Additionally, all kinds of mulching prevent soil erosion by wind and run-off, thus mitigating weathering (Kijchavengkul et al. 2008, Mansoor et al. 2022). Thirdly, efficient weed control by building a barrier preventing germination of weed is another key benefit (Bandopadhyay et al. 2018, Malinconico 2017, Martín-Closas et al. 2017).

Figure 1: Major fields of applications for plastics in agriculture and the most commonly used polymers, specifically in crop production (FAO 2021, PAPILLONS 2021).

Most of the PMFs are composed of low-density PE (LDPE) which is very durable, flexible, chemical resistant and most notably cost effective (Kasirajan & Ngouajio 2012). A huge disadvantage concerning these PE mulch films is the fact that they are not naturally

decomposable in the soil and need to be properly removed and disposed (Briassoulis & Degli Innocenti 2017, Francioni et al. 2021). This process can be expensive and labor-intensive as the operator and manual labor hours concerning PMF removal require an average of 42 hours per hectare based on the studies of Velandia et al. (2020). Moreover, a total removal and recycling de facto seems not to be possible due to the practically impossible separation of plastic from the soil debris and crop residues. In addition, abiotic factors like weathering break the plastic down and therefore a particular amount of macro- and microscopic residues will remain in the environment (Bandopadhyay et al. 2018, Qin et al. 2022, Wei & Zimmermann 2017). Meanwhile, a huge variety of biodegradable mulch films (BMF) have been designed to cope with this issue.

The desired idea of a circular economy, which is also implemented within the "EU Green Deal", where products and materials should be maintained at their highest value for the longest time possible to reduce pollution and preventing loss of material out of the system (Bucknall 2020), is also directed to plastics. Since most of the plastics are made from fossil fuel and the field of bioplastics consisting of renewable sources is not sufficiently applied to date, it is important to have a look on biodegradable plastics. They still can consist of fossil energy sources like crude oil, yet they can be biodegraded without causing any negative consequences due to their perseverance (Moshood et al. 2022).

1.3 Bioplastics and possible applications

The increasing use and the inappropriate disposal of conventional plastics contribute to greenhouse gas emissions due to incineration and a widely distributed pollution of the environment. This shows the significance of the transition towards biobased and biodegradable polymers. As a response to the accumulating plastic waste, the future ideal of plastics is a circular approach where all produced plastic is recycled to form a closed carbon cycle (Meereboer et al. 2020).

The growing market of bioplastics covers a range from electronic to medical applications and environmental protection (Samir et al. 2022). Most applications are found in food service (cutlery, cups, food containers), for bags and packaging. Further, the application in agriculture and horticulture (mulch films and pots) is expected to include another large volume market (Ghosh & Jones 2021).

The frequently used term bioplastics includes different materials along with their associated properties and implementations which can be bio-based or biodegradable or fulfill both characteristics (EUBP 2022). Bio-based plastics are made from renewable resources including starch, cellulose, agricultural and food waste, and microbial production of monomers (Samir et al. 2022). However, biodegradable plastics can be decomposed by microorganisms that are occurring in the environment. Thereby, the polymers are broken down into CO_2, water and biomass depending on the chemical structure of the material and the surrounding conditions like pH, temperature and humidity (EUBP 2022). Thus, it is important to differ between the resource basis and the degradation potential of a material. A seen in Figure 2, there are three main groups of bioplastics besides conventional plastics. Petroleum-based polymers like poly(ethylene) (PE) and poly(propylene) (PP) are produced from crude oil and show no biodegradation while there are petroleum-based polymers like poly(butylene-adipate-co-terephthalate) (PBAT) and poly(caprolactone) (PCL) that are biodegradable. Further there are bio-based but non-biodegradable plastics like bio-based PE (bioPE) or poly(ethylene-terephthalate) (bioPET) and bio-based biodegradable plastics like poly(lactic-acid) (PLA) or poly(hydroxyalkanoates) (PHA) (EUBP 2022). In the future, the petroleum-based production of

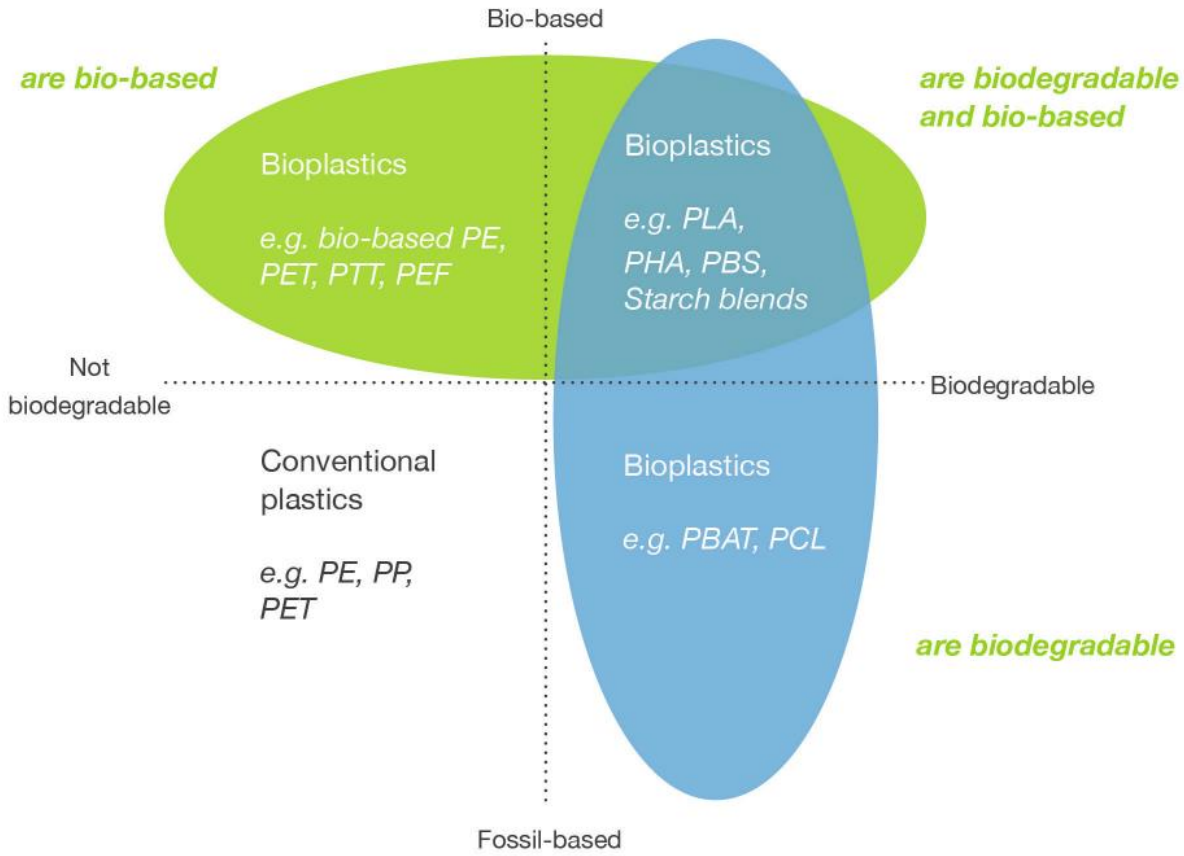

Figure 2: Allocation of plastic types referring to the terms bio-based and biodegradable (EUBP 2022).

polymers could be replaced by bio-based methods like the production of PCL to further reduce the dependence on fossil fuel (Emadian et al. 2017).

1.4 The current state of biodegradable plastics

Although biodegradable plastics have been on the market for several decades, they still represent a niche compared to conventional plastics. It is still a difficult task to equip the material with desired physical and chemical properties that last during their whole service life from the manufacturer to the consumers and to the waste collectors. After the product was used and declared as waste it should be either completely recycled to restart the cycle or completely disintegrate and serve as food for microorganisms (Ghosh & Jones 2021, Meereboer et al. 2020). Additionally, if the biodegradable plastic leaks into nature due to littering, insufficient waste separation or abrasion, it should not pose a threat to the environment but start to disintegrate as well (Ghosh & Jones 2021).

In addition to the general benefits from plastic materials being versatile and cheap, biodegradable plastics offer extra solutions for former unsolved questions. Because the recycling of plastic requires clean and homogenous material, many agricultural plastic products and products that are contaminated with food residues must be disposed on landfills. If these products were replaced by biodegradable materials, they could be considered as homogenous waste compartment and could be disposed in the organic waste stream and converted into bio-fertilizer (Ghosh & Jones 2021).

By the EU Waste Framework Directive (2008/98/EC) landfills were declared as least preferred option for waste treatment. Reasons are the contribution to climate change when the waste is thermally processed in incineration plants, the production of harmful gas and toxic leachate (Ghosh & Jones 2021). Again, the replacement by biodegradable alternatives would reduce the growth of landfills and diminish their environmental impact either by recycling or composting (Dilkes-Hoffman et al. 2019). However, also recycling has its limitations since the material's properties can change with increasing numbers of recycling what affects the quality of the material (Schyns & Shaver 2021). Composting instead represents a finite solution for the handling of plastic waste. Further, accidentally littered biodegradable products can prevent long-term accumulation of plastics as the material is designed to be mineralized by microorganisms (Ghosh & Jones 2021).

1.5 Steps of abiotic and biotic degradation

When referring to biodegradation the process is often displayed as single step transforming a biodegradable material directly into CO_2, water and biomass. Indeed, the expression of biodegradation presumes the occurrence biological activity, but the actual decomposition is a result of abiotic and biotic factors together, as Figure 3 shows. Therefore, abiotic degradation often is a key factor before biotic degradation can take place (Lucas et al. 2008). The main abiotic factors influencing a material are mechanical, light, thermal and chemical degradation.

Although mechanical degradation often shows no direct alterations on the material on a macroscopic level it can activate or accelerate other degradation processes (Briassoulis 2005). Especially compression, tension and shear forces under field conditions are constantly tearing on the material (Lucas et al. 2008). While the influence of mechanical degradation is steady but low, light degradation by ultraviolet (UV) radiation is one of the most relevant effects. Photoionization and chain scission can prepare the molecular structure for further degradation and crosslinking reactions can quickly change the mechanical properties (Lucas et al. 2008).

While most abiotic degradation ways are determined by the surrounding environment, thermal degradation depends on the type of material. Important factors are the melting temperature (t_m) and the glass transition temperature (T_g). Generally, the melting temperature is always higher than the temperature in the environment. Still, the temperature in industrial compost can exceed the melting temperature for a few thermoplasts like PCL with t_m of ca. 60 °C (Lucas et al. 2008). Lower temperatures can influence the macromolecular constitution of the polymers as well. Changes in the mobility of the polymer chains occur at the glass transition temperature and this material specific temperature varies strongly between different materials, e.g. 5 °C for poly(hydroxybutyrate) (PHB) and 50 °C for PLA. Higher temperatures can lead to improved accessibility of biological degradation while lower temperatures can promote brittleness and cracks (El-Hadi et al. 2002, Iovino et al. 2008).

Another very important factor influencing the abiotic degradation is chemical transformation. Oxygen from the atmosphere can attack covalent bonds of the polymers and together with degradation from UV radiation chain scission and crosslinking reactions can form (Lucas et al. 2008). Furthermore, present water molecules can reverse esterification and split up functional groups like esters, ethers and other functional groups resulting in shortened chain length and

reduced molecular weight (M). Especially amorphous parts of the material are prone to oxidation and hydrolysis (Lucas et al. 2008).

When it comes to material properties affecting both abiotic and biotic degradation the carbon backbone of the polymer plays the biggest role. Further, the polymer and surface variables, as seen in Figure 3, determine the susceptibility of the material for its abiotic and biotic degradation behavior. Therefore, T_g, t_m, M, crystallinity, functional groups, surface morphology and copolymers can considerably influence the degradation rate. Generally, small M, many functional groups, high surface area for microbial attacks, a low T_g and crystallinity facilitate biotic degradation (Ghosh & Jones 2021, Lucas et al. 2008, Samir et al. 2022). Additionally, parameters of the microenvironment like the surrounding pH influence the abiotic hydrolysis or biotic enzyme rate (Ghosh & Jones 2021).

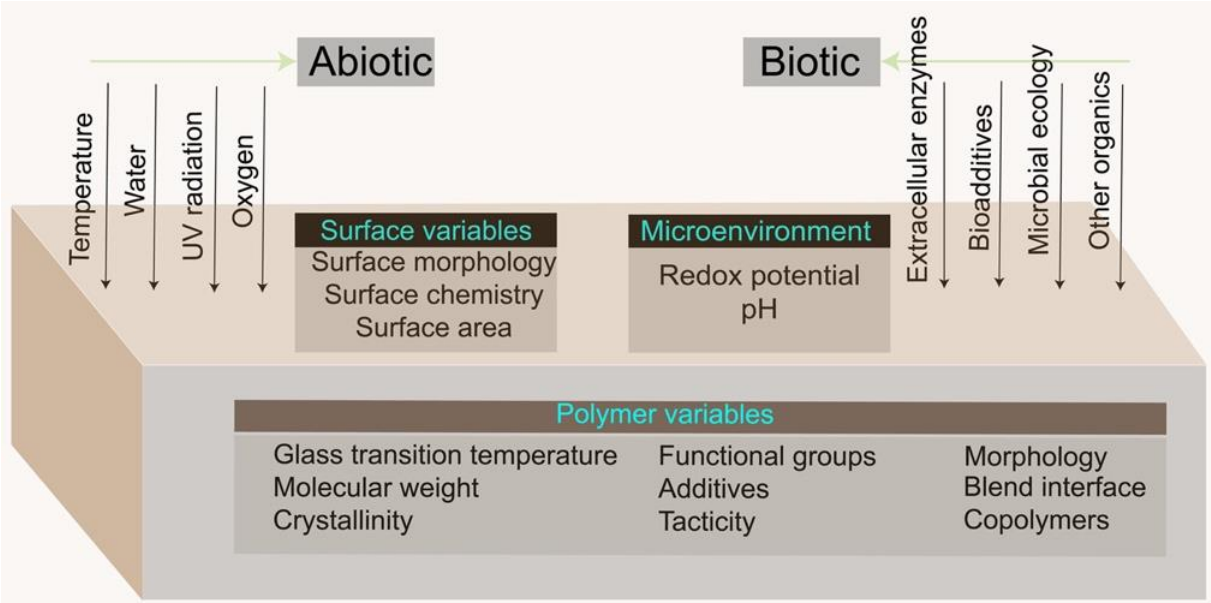

Figure 3: Interaction of abiotic and biotic factors affecting the disintegration and degradation of bioplastics (Ghosh & Jones 2021).

Particularly the dimension of the polymer matrix is an important factor when it comes to degradation. While enzymes mostly are too large to penetrate the structure of polymers, they can only attach to the surface of a material. In contrast, water molecules and other smaller chemicals like acids or radicals can permeate into the material (Meereboer et al. 2020). Thus, depending on the geometry abiotic degradation undergoes either surface or bulk erosion. Surface erosion steadily decreases the size while the molecular weight remains unaffected. During bulk erosion chain scission occurs throughout the whole thickness of the material and

the molecular weight decreases rapidly because diffusion proceeds faster than the cleavage of bonds. For poly(hydroxyesters), a thickness above the critical dimension $L_{critical}$ of 7.4 cm implies surface erosion, while a thickness below $L_{critical}$ implies bulk erosion (Von Burkersroda et al. 2002).

When the process of abiotic degradation has resulted in reduced molecular weight of polymers and enhanced availability of functional groups through hydrolysis microbial degradation can start, as seen in Figure 4 (Samir et al. 2022). Biotic degradation consists of biodeterioration, biofragmentation and assimilation. Thereby, biodeterioration describes a step affecting mostly the surface of the material, that interacts often at the same time with abiotic degradation and can be divided into chemical and enzymatic deterioration (Lucas et al. 2008).

Some microorganisms can infiltrate soft or brittle material with their filament network and enlarge pores and cracks (Bonhomme et al. 2003). Others build up biofilm structures and excrete organic acids that will increase polymer hydrolysis. At the same time, water swells up the polymer matrix and oligomers from bond cleavage are released (Lucas et al. 2008). Pores will form and will allow extracellular enzymes to enter (Auras et al. 2004). Enzyme classes involved in biodegradation include depolymerases, hydrolases and peroxidases (Amobonye et al. 2021).

The next step of biofragmentation describes a lytic process that is responsible for the breakdown of long-chain polymers into smaller molecules so they can be taken up by microorganisms (Lucas et al. 2008). Therefore, enzymes and free radicals are excreted to cleave the polymer bonds. Some of the enzymes are explicitly produced by the cells as a response to a specific substrate that was recognized by a signaling pathway while others are produced and segregated permanently (Lucas et al. 2008). Further, some enzymes can be attached to surfaces by a binding domain (Meereboer et al. 2020).

Generally, hydrolases use a nucleophilic attack at the ester bond so an H_2O molecule can cleave it. Oxygenases add additional alcohol or peroxyl groups to the polymers to facilitate the fragmentation and transport and peroxidases use H_2O_2 to break the polymer chains. Further, some enzymes catalyze oxidation reactions that produce free radicals that can start chain reactions of the polymer molecules (Lucas et al. 2008). The unspecific reactions of radicals are important especially for the fragmentation of crystalline regions where enzyme attacks are hindered due to the highly organized structure (Meereboer et al. 2020). Because not all

microorganisms are able to depolymerize and metabolize polyesters completely on their own, the complete polymer biodegradation is mostly a result of different interacting species (Lucas et al. 2008).

When the polymer chains are broken down into monomers and small oligomers, they can be taken up into the microbial cells what is called assimilation. Then, the absorbed molecules can be used for the metabolism or the composition of the cells what allows growth and reproduction. To convert the molecules, they are oxidized in a catabolic pathway either under aerobic or anaerobic conditions, as seen in Figure 4. Both pathways result in CO_2 and water. In aerobic respiration, oxygen is used as electron acceptor, while in anaerobic respiration mostly CH_4 is used as electron acceptor (Lucas et al. 2008). According to Meereboer et al. (2020) anaerobic biodegradation is less studied due to lower abundance of anaerobic environmental conditions where biodegradable plastics could occur. On industrial scale, two types of anaerobic environment are represented by landfills or biogas plants (Meereboer et al. 2020).

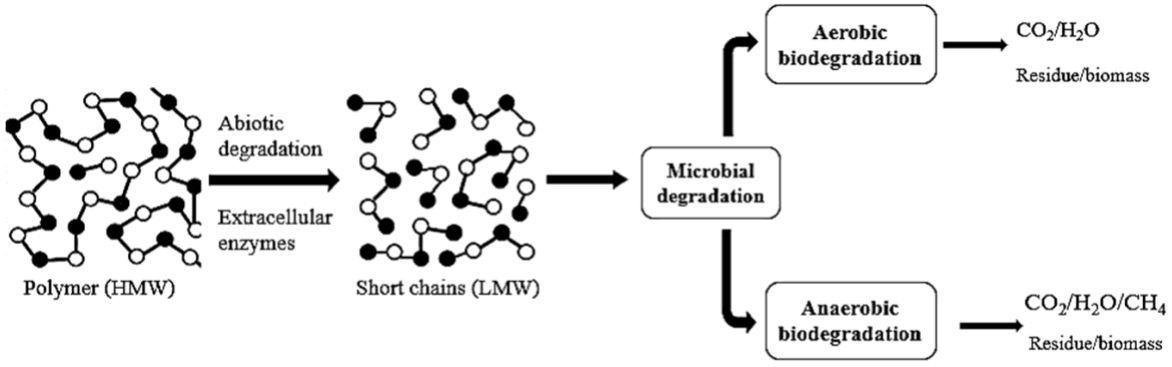

Figure 4: The main steps of biodegradation on a molecular level (Samir et al. 2022).

1.6 Measurement of degradation

"The unique proof that a polymer is consumed by microorganisms is the release of carbon dioxide" (Lucas et al. 2008). Thus, this test method is only suitable on a laboratory scale because soil and compost may also release CO_2 independently from the biodegradation of plastics and the usage of radio-labelled carbon compounds is often too expensive (Lucas et al. 2008). Other degradation tests are described by standards such as ISO 16929 where product samples are buried in a pilot compost and then residues are sieved by a 2 mm sieve after the incubation time (ASTM 6400, ISO 16929). To distinguish from the term degradation, the term

disintegration is used instead, which describes the fragmentation of a sample into very small pieces (ISO 17088).

Test protocols come with strictly defined conditions to ensure transparence and reproducibility. Unfortunately, these conditions for degradation are often excessive, e.g. high temperatures, or not comparable to a natural environment, e.g. shredding and grinding of plastic samples to increase the surface before mixing with compost or soil. Field applications of soil or compost biodegradation, though, show a variety of changing parameters, like unstable temperature and humidity, different matrix composition and microorganisms, that can influence the process of biodegradation and impede the predictability. Additionally, biodegradable materials should always be tested for negative impacts on the ecosystem (Ghosh & Jones 2021).

To facilitate the observation of ongoing degradation, alterations of different physical and chemical characteristics can serve as criteria. First remarkable changes concern physical properties, like toughness, when the material becomes more brittle. Although these features are expressed irregularly, they are attributed to molecular changes that contain reduction of molecular weight, crystallinity and intermolecular forces (Laycock et al. 2017). Therefore, a tensile test is a simple method to observe changes in the behavior of changing tensile strength. Further, surface analysis for cracks and pitting conducted with optical or scanning electron microscopy (SEM) show where degradation starts (Meereboer et al. 2020). To prove the hypothesis of reduced polymer chain length the molecular weight of samples can be measured with gel permeation chromatography (GPC) and changes affecting the macromolecular properties can be monitored by differential scanning calorimetry (DSC). Additionally, methods like Fourier-transform infrared spectroscopy (FT-IR) support the measurement of chemical changes due to chain scission or oxidation (Laycock et al. 2017). These methods provide a free experimental setup and are easily adaptable for different samples.

1.7 Scope

Overall, this work aims at comparing the disintegration behavior of three polymers that can be processed into a mulch film compound. Based on the present theories about degradation of biodegradable polymers, questions concerning the possible application of the single polymers in a biodegradable mulch film arise:

- When are the first signs of disintegration visible and in which way?
- Can the incubation type and the soil type affect the speed of disintegration?
- Which methods are suitable to show early material changes?

Answers to the questions will be argued in the following chapters.

2 Materials and devices

2.1 Materials

Table 1: List of all used material.

Material	Manufacturer	Location
FloraSelf mulch film	Hornbach Baumarkt AG	Bornheim, Germany
Garden sieve 3 mm	Tool Jungle / GreenTuch	
Glassless mounts CS II	Reflecta GmbH	Eutingen, Germany
Household sieve 1 mm	Gnaumore	
Plastic crate EG 4317	Auer GmbH	Amerang, Germany
Rotilabo brush 15 mm diam.	Carl Roth GmbH + Co. KG	Karlsruhe, Germany
Syringe filter PTFE 0.2 µm	Carl Roth GmbH + Co. KG	Karlsruhe, Germany
Syringe filter PTFE 0.45 µm	Carl Roth GmbH + Co. KG	Karlsruhe, Germany
Topsoil	Baustoffe Ruhr GmbH	Essen, Germany
Welted glasses + lid 5 mL	Carl Roth GmbH + Co. KG	Karlsruhe, Germany
Welted glasses + lid 50 mL	Carl Roth GmbH + Co. KG	Karlsruhe, Germany

2.2 Chemicals

Table 2: List of all used chemicals.

Chemical	Manufacturer	Location
1,1,1,3,3,3-hexafluoro-2-propanol	Fluorochem Ltd.	Hadfield, UK
Buffer solution pH 4 and 7	Working solution	
$CaCl_2$ for analysis 1.02382	Merck KGaA	Darmstadt, Germany
Potassium trifluoroacetate	Merck KGaA	Darmstadt, Germany

2.3 Devices

Table 3: List of all used devices.

Device	Manufacturer	Location
Balance ENTRIS224I-1S	Sartorius AG	Göttingen, Germany
BT1-FR 1.0 TH.140 tensile test machine	ZwickRoell GmbH & Co. KG	Ulm, Germany
Cressington 108 auto sput. coat.	Tescan GmbH	Dortmund, Germany
Digital film thickness gauge 4mm-0.001	Käfer Messuhrenfabrik GmbH & Co. KG	Villingen-Schwenningen, Germany
DSC 204 F1 Phoenix®	Netzsch-Gerätebau GmbH	Selb, Germany
DUO 2.5 vacuum pump	Pfeiffer Vacuum GmbH	Asslar, Germany
G1310B isocratic pump	Agilent Technologies	Waldbronn, Germany
GPC column 100 Å	PSS GmbH	Mainz, Germany
GPC column1000 Å	PSS GmbH	Mainz, Germany
GPC column300 Å	PSS GmbH	Mainz, Germany
Hole puncher LEITZ 5008	Leitz Acco Brands GmbH & Co KG	Stuttgart, Germany
Humidity tester MLS 50-3	Kern & Sohn GmbH	Balingen, Germany
Lab balance 15 kg	Sartorius AG	Göttingen, Germany
LP-S-20 hydraulic press	Labtech Eng. Company LTD	Samutprakarn, Thailand
pH 1000 sensor SE 100 N	Knick Elektronische Messgeräte GmbH & Co KG	Berlin, Germany
pH meter 766 Calimatic	Knick Elektronische Messgeräte GmbH & Co KG	Berlin, Germany
Tensor 27 FT-IR with ATR	Bruker GmbH	Ettlingen, Germany
Vega 3 XMU SEM	Tescan Orsay Holding, a.s.	Brno, Czech Republic
VHX-6000 dig. micr.	Keyence Deutschland GmbH	Neu-Isenburg, Germany

Wide angle camera 12 MP MLVE3ZD/A	Apple Inc.	Cupertino, USA
Xforce HP load cell	ZwickRoell GmbH & Co. KG	Ulm, Germany
XS205 DualRange balance	Mettler Toledo GmbH	Gießen, Germany

2.4 Software

Table 4: List of all used evaluation software.

Software	Manufacturer	Location
Keyence V. 3.0.0.115 V. 2.02	Keyence Deutschland GmbH	Neu-Isenburg, Germany
OPUS V. 7.8.44	Bruker GmbH	Ettlingen, Germany
Proteus® V. 8.0.3 21342.302	Netzsch-Gerätebau GmbH	Selb, Germany
testXpert® 3 V. 1.51	ZwickRoell GmbH & Co. KG	Ulm, Germany

3 Methods

3.1 Experimental setup

In this work, the disintegration behavior of three different polymers in soil was investigated. The used polymers are possible components for a compound used in a biodegradable plastic mulch film for agriculture. The single components were used for better estimation of disintegration. Further, two types of topsoil were used to compare the influence of adaption to biodegradable plastics. During the incubation time several optical and material-related analysis were performed.

3.2 Used polymers

The following biodegradable polymers with their corresponding structural formula, as seen in Figure 5, were used in this work:

- Poly(butylene-sebacate-co-terephthalate) (PBST) BASF ecoflex® FS Blend C 2200.
- Poly(butylene-adipate-co-terephthalate) (PBAT) Wango A 400.
- Poly(3-hydroxybutyrate-co-3-hydroxyhexanoate) (PHA) Kaneka Biopolymer Aonilex X 131A / X 151A.

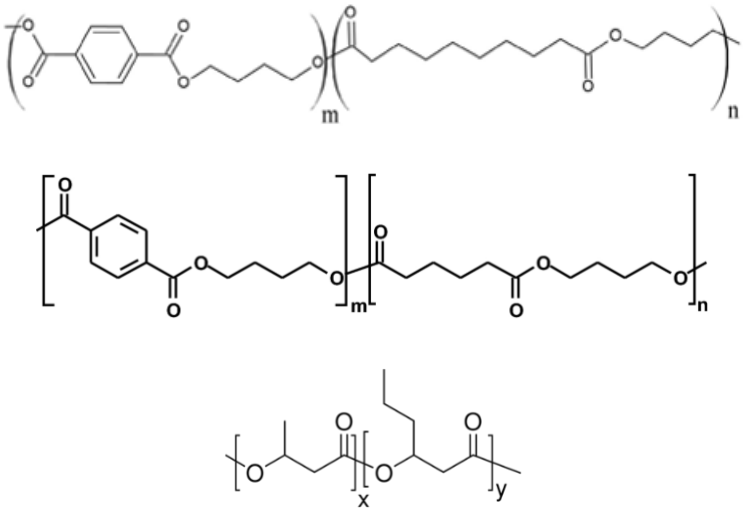

PBST

(Lim & Park 2023)

PBAT

(Reineke & Schlömann 2020)

PHA

(Merck 2023)

Figure 5: Structural formula of the three used polymers: Poly(butylene-sebacate-co-terephthalate) (PBST), poly(butylene-adipate-co-terephthalate) (PBAT) and poly(3-hydroxybutyrate-co-3-hydroxyhexanoate) (PHA).

The polymers were received as granulates and were pressed in form. Therefore, the granulate was heated up for two minutes, was ventilated for ten seconds and pressed into sheets of 15 cm x 18 cm with about 200 µm thickness for two minutes under 50 bar pressure. After two minutes of cooling down the sheets were removed from the press and were cut into strips of 1.5 cm x 11 cm and rectangles of 3.7 cm x 3.5 cm, as seen in Figure 6. Further, 2 cm x 2 cm squares were cut and 6 mm circles were stamped out with a hole puncher.

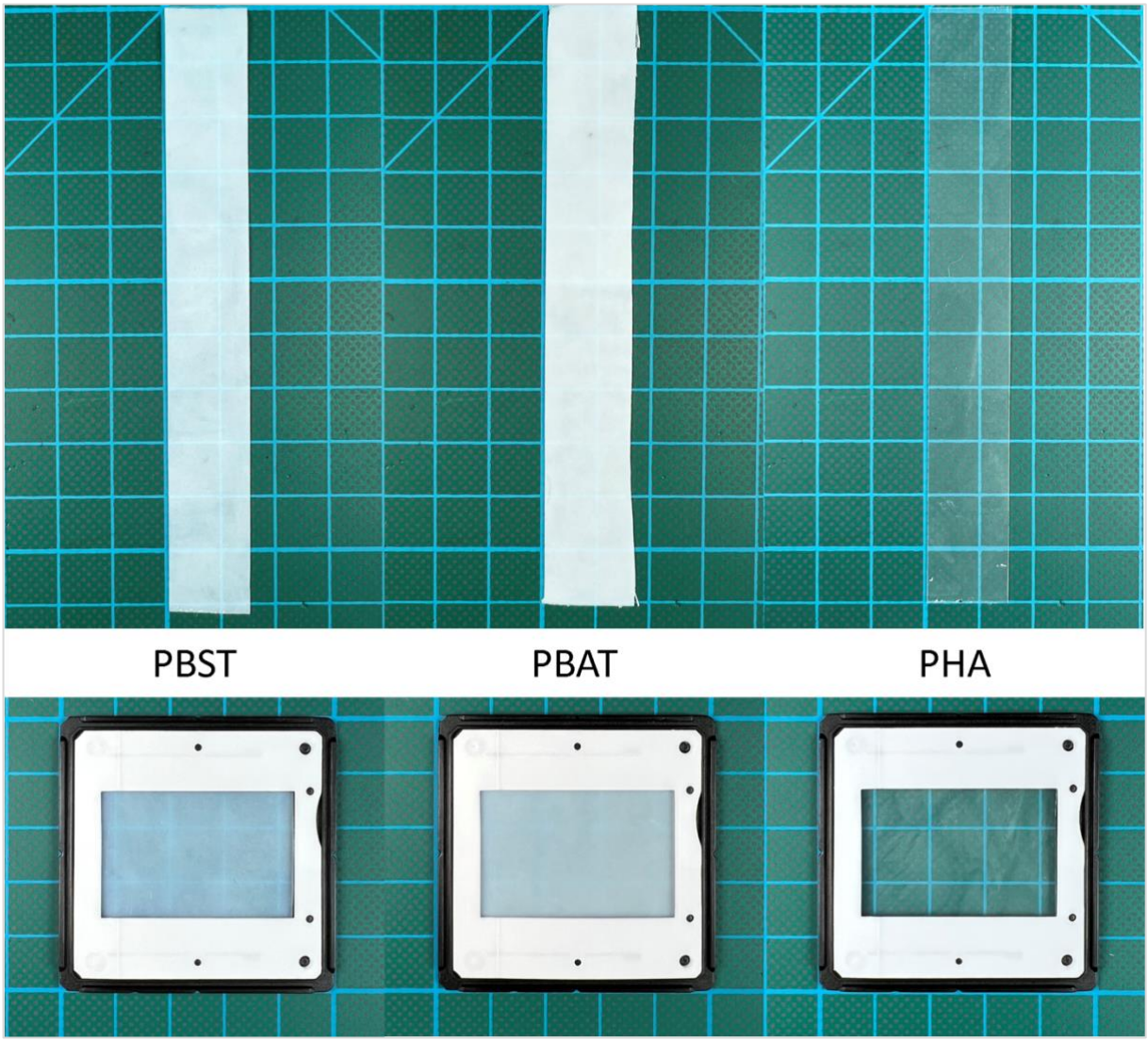

Figure 6: Images of the three polymer types and the two sample forms of strips (top) and rectangles in film holders (bottom) before the incubation. From left to right: Poly(butylene-sebacate-co-terephthalate) (PBST), poly(butylene-adipate-co-terephthalate) (PBAT) and poly(3-hydroxybutyrate-co-3-hydroxyhexanoate) (PHA). One square of the scale paper in the background equals 1 cm².

3.3 Preparations

Native topsoil was used in this experiment to recreate an environment that is close to the soil of agricultural fields. For the spatial separation of the different polymers a single plastic box

was used for each polymer. For handling purposes, separate boxes were also used for the incubation on the soil surface and in the soil. Besides the regular topsoil, a sample from an agricultural test field was used where biodegradable plastics are frequently applied to. This soil sample allows to inoculate the regular topsoil with potentially biodegrading microorganisms. Both soil types were separately sieved with a 3 mm sieve and watered with tap water to reach proper water content. Soil moisture and pH were measured before distributing the soil into the according containers. Considering all possible variations, twelve plastic boxes with the inner size of 37 cm x 27 cm were filled with about 10 kg of the topsoil. To six boxes each 200 g of the agricultural soil were added and homogenously mixed with the topsoil. For simplification, the boxes containing the mix of topsoil and agricultural soil are called 'agricultural soil' in this work. Samples of each polymer were distributed on the surface and within both types of soil.

The 1.5 cm x 11 cm plastic strips were placed lengthwise in three rows with 15 strips each on top of the soil. Two additional strips were placed vertically in the same box, as seen in the layout plan in the appendix (Figure 26). In this way, as many samples as possible could fit into one box and almost the whole soil surface was covered in plastic film. The rectangular samples were fixed in film holders and buried in a second box (Figure 27). To serve as control, samples of a commercial poly(ethylene) film and a cellulose film were also cut into 3.7 cm x 3.5 cm rectangles and placed in film holders to be buried in the soil.

The circular 6 mm samples were put in a mesh bag. In this way, the fine samples could be buried in the box and later taken out of the soil without risking mechanical damage. The remaining 2 cm x 2 cm pieces were placed on top of the soil with the buried film holders.

To finish the soil preparation, all boxes were sprayed with tap water to wet the samples and the weight of each box was noted to set a reference weight to keep control of the soil moisture. For clarity, the boxes were numbered according to Table 5.

Table 5: List of all combinations of polymer types, soil types and sample locations referring to their corresponding abbreviation. According to the denomination of samples the polymers refer to poly(butylene-sebacate-co-terephthalate) (PBST), poly(butylene-adipate-co-terephthalate) (PBAT) and poly(3-hydroxybutyrate-co-3-hydroxyhexanoate) (PHA).

Box No.	Abbreviation	Polymer	Soil type	Sample location
1	PBST_Bo1_OF	PBST	regular	surface
2	PBAT_Bo1_OF	PBAT	regular	surface
3	PHA_Bo1_OF	PHA	regular	surface
4	PBST_Bo1_IN	PBST	regular	in-soil
5	PBAT_Bo1_IN	PBAT	regular	in-soil
6	PHA_Bo1_IN	PHA	regular	in-soil
7	PBST_Bo2_OF	PBST	agriculture	surface
8	PBAT_Bo2_OF	PBAT	agriculture	surface
9	PHA_Bo2_OF	PHA	agriculture	surface
10	PBST_Bo2_IN	PBST	agriculture	in-soil
11	PBAT_Bo2_IN	PBAT	agriculture	in-soil
12	PHA_Bo2_IN	PHA	agriculture	in-soil

3.4 Experimental conditions

The plastic pieces were incubated on and in regular topsoil filled into plastic boxes for a duration of 16 weeks. To maintain constant climatic conditions, the boxes with soil and the samples were stored in the measurement room with air condition at 23 °C and 50 % air humidity.

Once a week the soil was watered with tap water to compensate the weight loss by evaporation. To avoid floating of the samples, watering was stopped when the water accumulated on top of the soil surface.

Samples were taken after one, two, four, six, eight, ten, twelve and 16 weeks.

3.5 Description of the methods

After every sampling the spot on the soil where the samples were taken from was scraped off and analyzed for soil moisture. Then, the samples were cleaned and dried, followed by optical examination with a digital microscope. After drying overnight, the strips and rectangles were cut into pieces for further analysis: Scanning electron microscopy to investigate surface modifications, dynamic scanning calorimetry to trace alterations in melting, crystallization and glass transition temperature as well as degree of crystallinity, Fourier-transform infrared spectroscopy to observe the composition of functional groups and gel permeation chromatography to detect changes in the molecular weight due to degradation. Further, the tensile strength of the strips was measured with a tensile test.

Additionally, the pH of the soil was measured before, during and after the experiment.

3.5.1 Soil moisture

On the one hand, to ensure a constant level of soil moisture, the soil boxes were weighed every week and the missing weight from evaporation was compensated by watering with tap water. On the other hand, soil samples were taken immediately after sampling from the respective soil surface or gap where the sample was situated to measure the soil moisture. Therefore, about 10 g soil were gently scraped off and were temporarily stored in a glass sample beaker with plastic lid to prevent undesired desiccation. When all soil samples were taken, 5 g of each were weighed in consecutively with the humidity tester and were heated up to 120 °C. The measurement was stopped when the mass change was < 1 mg / 2 min and the relative humidity in % was noted. The residual moisture of the soil was calculated as seen in equation 1 according to (JoVE 2023).

Eq. 1: $\text{Soil moisture} = \frac{(m_{wet} - m_{dry})}{m_{wet}}$ %, m_{wet} in g and m_{dry} in g.

3.5.2 pH control

Measurements of the soil pH were conducted before the experiment was set up, after eight weeks and in the end after 16 weeks. Therefore, 20 g of soil from each box were weighed into a separate glass beaker and filled up with 200 mL 0.01 M $CaCl_2$ solution. The mixture was set

aside for one hour while frequently being stirred with a glass stick. After the calibration of the pH meter with pH 4 and pH 7 buffer solution, the electrode was placed in the according glass beaker. The pH and temperature were noted when stable.

3.5.3 Sampling and cleaning

Samples were taken according to the sampling plan, as seen in the appendix (Table 6). The plastic strips on the soil surface were marked with a permanent pen on the upside to ensure which side was in contact with the soil. Then, the strips were carefully lifted with forceps and transferred into a sieve. When all samples of one box were taken, the material was carefully rinsed under tap water and spread out on a paper cleaning cloth. Remaining soil particles were removed with a brush on both sides and the samples were rinsed once again. The slide frames containing the plastic rectangles were pulled out of the soil using forceps and were also rinsed with tap water. Before continuing, the contact surface was encircled with a permanent marker to mark the overlap of the frames. Further cleaning was performed similarly to the strips.

After the cleaning procedure, the plastic pieces were gently patted dry with a paper towel and were stored as well in new paper sheets at around 23 °C and 50 % humidity.

3.5.4 Optical imaging

For the inspection of the sample surface pictures were taken using a digital microscope with up to 200-fold magnification. First, software-assembled panorama pictures were taken from both sides using 50-fold magnification. Afterwards, single pictures of surface alterations were taken.

For better comparison, pictures of the samples on a scale paper were recorded separately with a mobile device.

3.5.5 Scanning electron microscopy (SEM)

Further examination of the surface morphology was performed with a scanning electron microscope. The samples were prepared in a sputter coater under vacuum and were coated

with gold particles for 180 s with 30 mA. Images were taken with an acceleration voltage of 20 kV and a secondary electron detector.

3.5.6 Tensile test

The tensile test was conducted according to DIN 527-3 to check the mechanical properties of the sample strips and if they changed during the incubation time in the soil (DIN 527-3). Before the measurement the samples were stored overnight at 23 °C and 50 % air humidity according to the test protocol. Then, the thickness of the samples films was measured with a digital thickness gauge and the samples were mounted between the upper and lower clamp of the test machine with a distance of 80.0 mm. Next, the initial tension was adjusted to zero and set to 0.1 N. The testing speed of the tensile modulus was 1 mm / min and the following testing speed was 200 mm / min. The samples were stretched until the breaking point. While extending the samples the respective force was measured and different parameters are calculated by the testXpert® software. If possible, five strips from the same sampling date were measured and results were combined to form mean and standard deviation values.

For this work the tensile modulus E_t and the tensile strength at first maximum σ_m was compared among the same polymer types. According to DIN 527-1, the tensile modulus E_t can be derived from the fraction of the stress by the strain of the sample, as seen in equation 2 – 4 (DIN 527-1). Stress and strain are measured by the tensile test machine.

Eq. 2: $$E_t = \frac{\sigma}{\varepsilon}$$ MPa, stress σ in MPa and strain ε in %.

Eq. 3: $$\sigma = \frac{F}{A}$$ MPa, force F in N and cross-sectional area A in mm^2.

Eq. 4: $$\varepsilon = \frac{\Delta L_0}{L_0}$$ %, elongation ΔL_0 in mm and start length L_0 in mm.

3.5.7 Differential scanning calorimetry (DSC)

Possible changes of glass transition temperature, crystallization temperature and melting point were examined with differential scanning calorimetry. Therefore, samples were cut with a 5 mm circle punch and a hammer to create pieces of about 5 mg. The weight of each sample

was measured with an analytical balance and the sample was then inserted into small aluminum pan. The pan was closed with its counterpart and a small hole was stung into the lid to allow the discharge of gas. After filling the autosampler, a temperature program for the measurement was conducted for each sample, as seen in Figure 7. The temperature range started from -60 °C increasing to 200 °C with the exact description found in the Appendix (Table 7). The sample chamber was flushed with 20 mL / min nitrogen gas.

The relative crystallinity was calculated according to equation 5 by comparing the measured melting enthalpy from the second heating curve with the melting enthalpy of a 100 % crystalline sample:

Eq. 5: $$X_c = \frac{\Delta H_m}{\Delta H_m^0}$$ %, measured enthalpy ΔH_m in J /g, measured enthalpy of 100 % crystalline sample ΔH_m^0 in J / g.

Reference values for ΔH_m^0 were 142 J / g for PBST, 114 J / g for PBAT and 146 J / g for PHA, respectively (Chivrac et al. 2006, Heidarzadeh et al. 2017, Xu et al. 2018).

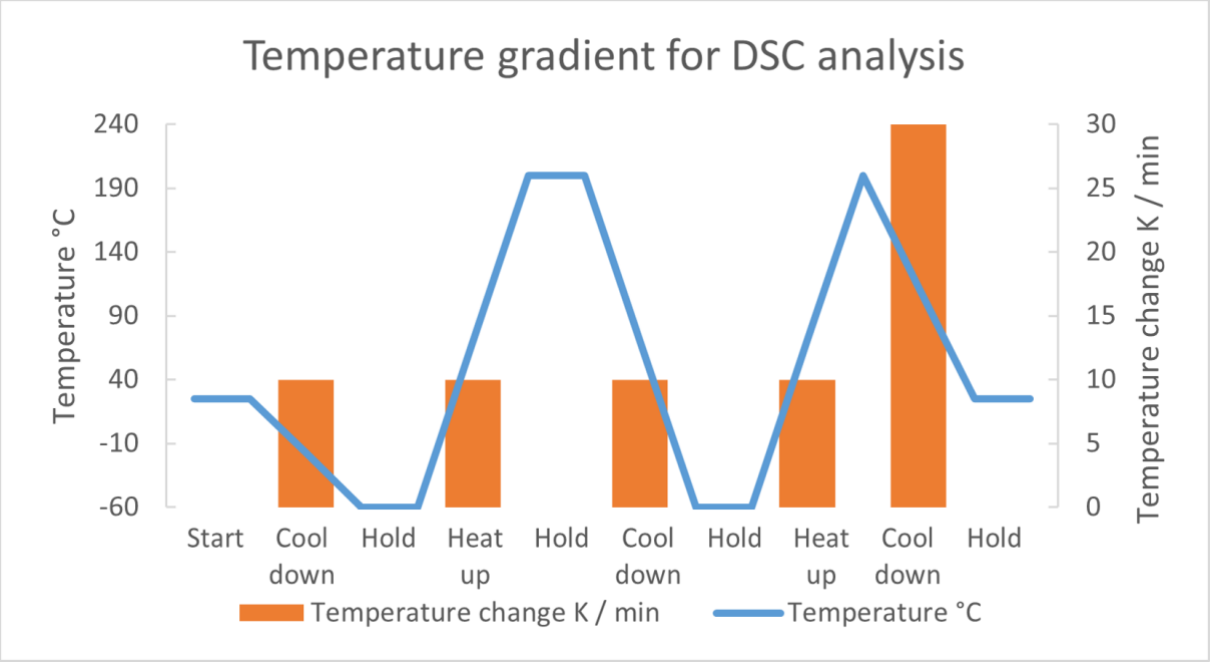

Figure 7: Temperature profile of the measurement cell and respective temperature gradient for DSC analysis.

3.5.8 Gel permeation chromatography (GPC)

Molecular weights of the samples were examined with GPC. Firstly, around 8 mg of each sample was weighed into a 5 mL welted glass with lid and the weight was noted. Secondly, the

samples were dissolved overnight in 3 mL 1,1,1,3,3,3-hexafluoro-2-propanol (HFIP) with 0.05 M potassium trifluoroacetate (KTFAc). Thirdly, the dissolved samples were filtered through a 0.45 µm and 0.2 µm PTFE membrane filter to remove any particulate impurities. Then, 100 µL of each sample were injected by an isocratic pump into the GPC with a flow rate of 1 mL / min. The GPC contained three columns with 1000 Å, 300 Å and 100 Å that were connected in series. A refractive index (RI) detector was used and with WinGPC® software the number-average (M_n), the weight-average (M_w) and the z-average (M_z) molecular weight as well as the polydispersity index (PDI) were calculated.

3.5.9 Fourier-transform infrared spectroscopy (FT-IR)

To track possible changes of the functional groups of the polymers, infrared spectra were taken. Therefore, the samples were pressed onto an attenuated total reflection (ATR) crystal and 16 spectra with a resolution of 4 cm^{-1} were combined. Recorded absorbance spectra from 4000 cm^{-1} to 400 cm^{-1} were processed with OPUS software.

4 Results

4.1 Soil conditions

The soil conditions pH and moisture were examined during the incubation time. The weight of the boxes filled with soil was measured weekly to maintain constant humidity of the soil and weight loss due to water evaporation was compensated by watering with tap water. Figure 8 shows the weight of each of the twelve boxes between the start and the end of week 15. Weight was not recorded after the final sampling date in week 16. Box labels were according to Table 5 (see chapter Preparations). First noticeable in Figure 8 are the two main starting weights of approximately 11.4 kg for the regular soil and 11.6 kg for the agricultural soil. The weight of the boxes then started to diverge from the first week on and average 200 – 300 g of water were lost and refilled every week. The highest reduction was found in the first two weeks and in the last two weeks. An average loss of 480 g per box in form of soil and water was detected. The ongoing decrease in weight partly resulted from a small loss of soil during sampling. Interestingly, the highest weight every week was measured for box eight containing

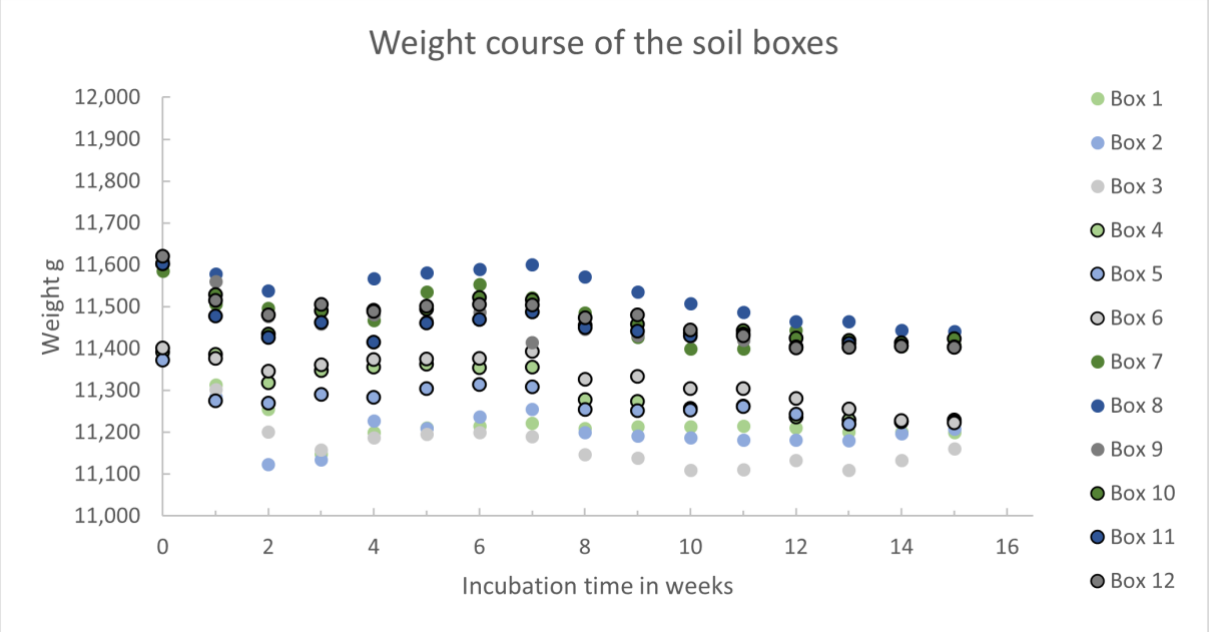

Figure 8: Weight course of the soil boxes. Scatter chart showing the weight course of the soil boxes in g over 15 weeks incubation time. According to the denomination of the samples, the boxes one to three contained regular soil with samples on the surface in form of strips of poly(butylene-sebacate-co-terephthalate) (PBST), poly(butylene-adipate-co-terephthalate) (PBAT) and poly(3-hydroxybutyrate-co-3-hydroxyhexanoate) (PHA), respectively. The boxes four to six contained regular soil with rectangular samples in the soil made from PBST, PBAT and PHA, respectively. Boxes seven to nine contained agricultural soil with samples on the surface in form of strips of PBST, PBAT and PHA, respectively. The boxes ten to twelve contained agricultural soil with rectangular samples in the soil made from PBST, PBAT and PHA, respectively.

the agricultural soil with PBAT samples on the surface. The lowest weight was measured for box two and five in the first three weeks containing regular topsoil with PBAT on the surface and in the soil, respectively, and box three for the following weeks with PHA samples on the surface.

Additionally, after every sampling some soil from around the plastic samples was scraped off to determine the soil moisture. The initial residual water content of the soil was around 20.2 % before it was distributed into the twelve boxes. Soil moisture varied strongly between minimum 11.9 % and maximum 21.3 % showing no obvious trend. As seen in Figure 9, especially week two, six and eight showed outlier which lied clearly above the other data points. Further, it looked like the boxes with plastic samples on the soil surface had a higher water content in the soil compared to the boxes with the samples in the soil.

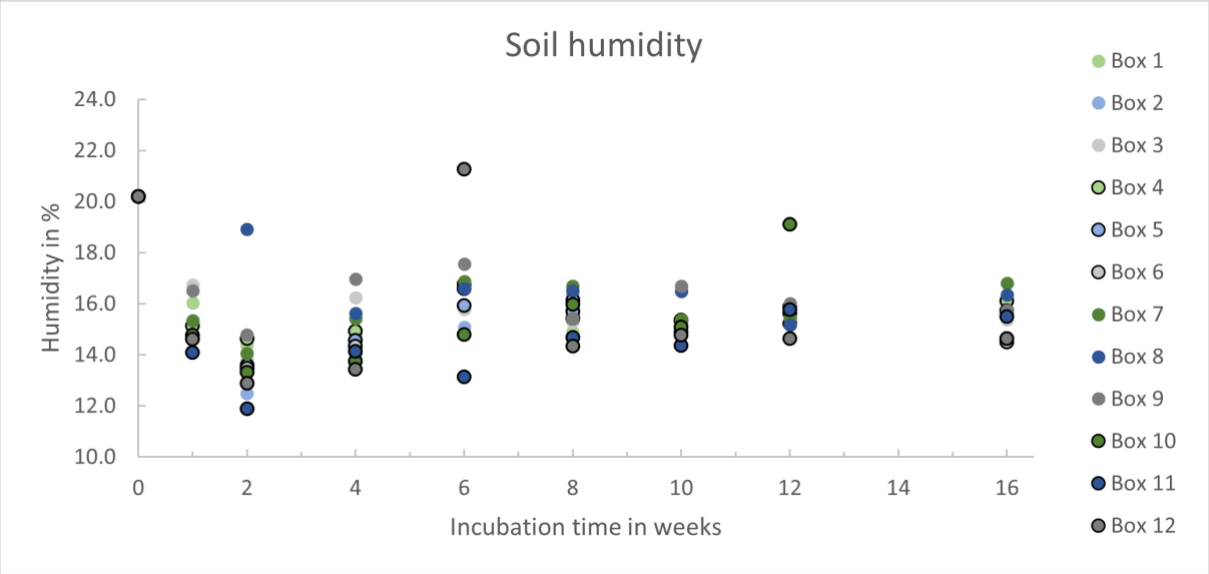

Figure 9: Soil humidity during the incubation. Scatter chart showing the soil humidity of the soil boxes in % over 16 weeks incubation time. According to the denomination of the samples, the boxes one to three contained regular soil with samples on the surface in form of strips of poly(butylene-sebacate-co-terephthalate) (PBST), poly(butylene-adipate-co-terephthalate) (PBAT) and poly(3-hydroxybutyrate-co-3-hydroxyhexanoate) (PHA), respectively. The boxes four to six contained regular soil with rectangular samples in the soil made from PBST, PBAT and PHA, respectively. Boxes seven to nine contained agricultural soil with samples on the surface in form of strips of PBST, PBAT and PHA, respectively. The boxes ten to twelve contained agricultural soil with rectangular samples in the soil made from PBST, PBAT and PHA, respectively.

The soil pH was also recorded to follow possible changes during the incubation time. Therefore, the pH was measured before the start, in the middle (week eight) and in the end (week 16), as seen in Figure 10. Start value of the soil was 7.8 before being distributed into the

boxes. While most pH values increased during the first half and then began to decrease again, others slowly increased towards the end of the incubation time. Maximum value was 8.2 for box two in week eight and minimum value was 7.7 for box six in week eight. Average temperatures during the measurement were 26.2 °C in the beginning, 19.0 °C in the middle and 18.7 °C in the end.

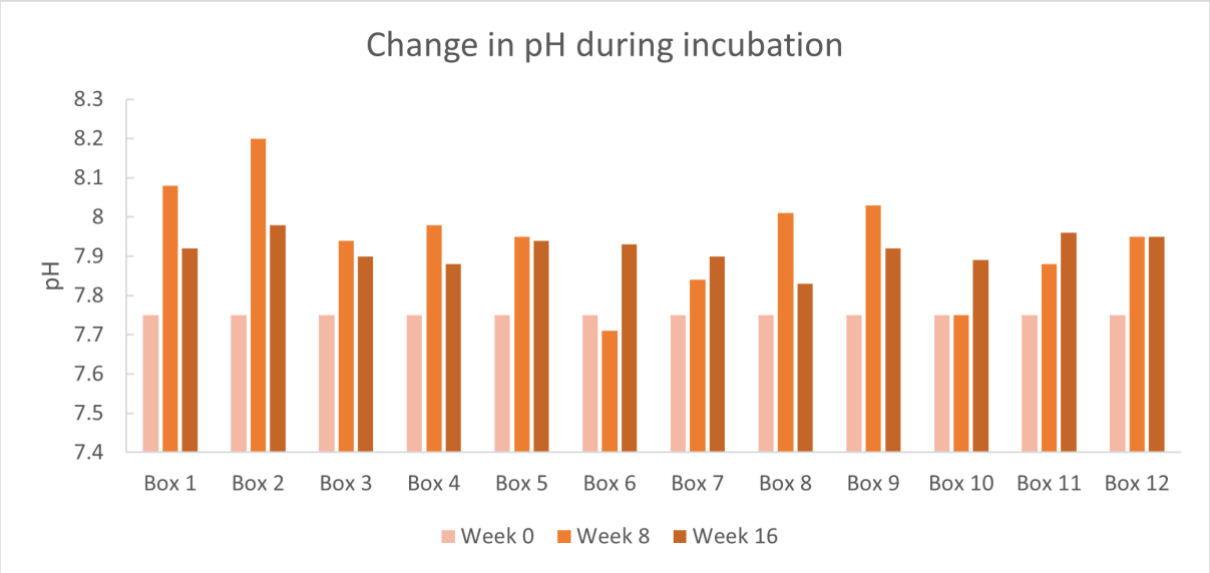

Figure 10: Change in pH during incubation. Bar chart showing the pH values of each soil box during the incubation time, represented by examples of week zero (light orange), week eight (orange) and week 16 (dark orange). According to the denomination of the samples, the boxes one to three contained regular soil with samples on the surface in form of strips of poly(butylene-sebacate-co-terephthalate) (PBST), poly(butylene-adipate-co-terephthalate) (PBAT) and poly(3-hydroxybutyrate-co-3-hydroxyhexanoate) (PHA), respectively. The boxes four to six contained regular soil with rectangular samples in the soil made from PBST, PBAT and PHA, respectively. Boxes seven to nine contained agricultural soil with samples on the surface in form of strips of PBST, PBAT and PHA, respectively. The boxes ten to twelve contained agricultural soil with rectangular samples in the soil made from PBST, PBAT and PHA, respectively.

4.2 Visual inspection

During sampling the strips were already inspected visibly and after being cleaned and dried overnight pictures of both sides of the samples were taken on a scale paper. In this way cracks, color changes and alterations of the texture were recorded.

First, the control samples of PE and cellulose were compared in their film holder. The negative control of PE showed no differences to the initial film piece after 16 weeks in both soils. As seen in Figure 11, the surface was shiny under both conditions and all staining could be brushed off during the cleaning steps. Instead, no residues of the cellulose film were found.

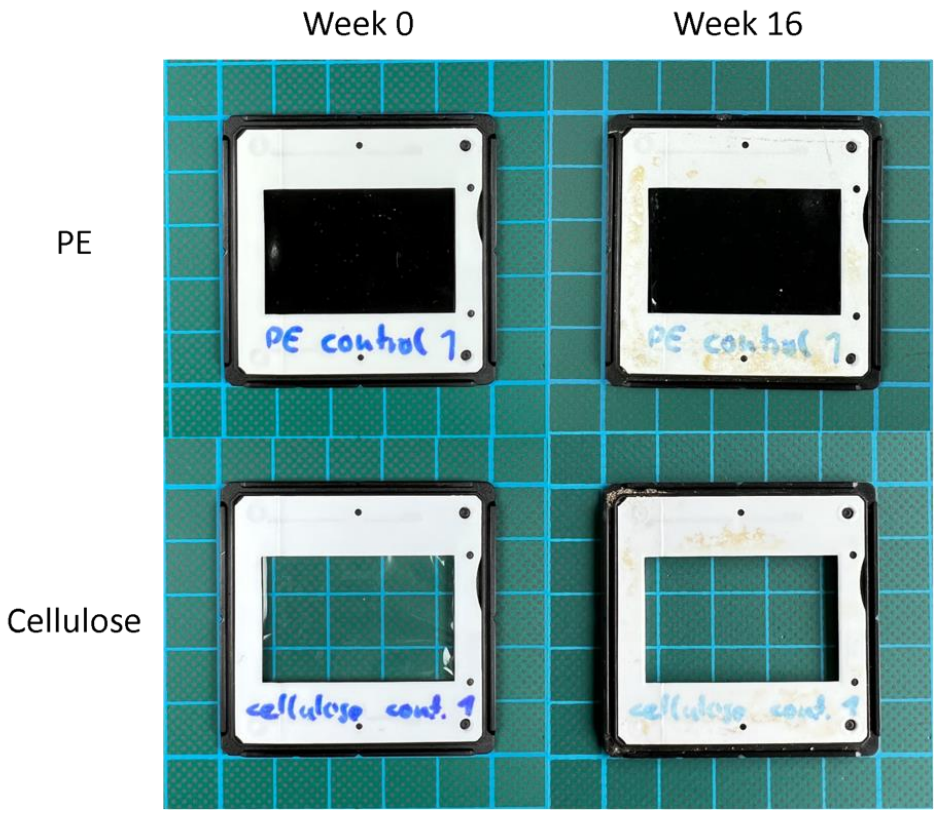

Figure 11: Pictures of the control films of poly(ethylene) and cellulose. Poly(ethylene) (PE) and cellulose film were used as control. Pictures of the control samples were taken before the experiment and after 16 weeks of incubation. One square of the scale paper equals 1 cm².

Second, the pictures of the downside of the samples, accordingly the contact surface between soil and sample, were directly compared by arranging the pictures of the respective sampling date next to each other. Figure 12 shows the samples of PBST, PBAT and PHA according to the incubation in regular topsoil and agricultural topsoil during the time course of 16 weeks.

Starting with the PBST samples it can be noticed that first changes appeared simultaneously in both soils. Color changes already appeared after one week and after four weeks the first fine cracks formed. While it took until week ten in the regular soil to form the first hole, samples in the agricultural soil developed first holes after six weeks already. After twelve weeks the strips showed blackish staining especially in the agricultural soil. Finally, after 16 weeks the samples from the regular topsoil showed cracks and discolorations and small pieces were breaking off. The samples in the agricultural soil showed similar but particularly stronger effects. Generally, the forms of sample deterioration occurred randomly on the whole sample surface without a clear pattern.

Continuing with the PBAT samples, definitely less changes on the sample surface were noticeable. In a similar manner, first color changes appeared in both soils after the first week. While the staining of the plastic strips in the regular topsoil only slightly increased, the samples in the agricultural soil showed more staining with ongoing incubation time. The first and only cracks were observed on the fringe of the strips after 16 weeks in the agricultural soil. Sometimes, soil particles and biofilm were stuck on the edges of the samples and were not removable by the applied cleaning method.

The PHA samples provided completely different sample characteristics. While PBST and PBAT samples were semi-transparent, soft and flexible with rubbery surface, the PHA samples showed more stiffness, were almost clear and the surface was smooth and shiny. Generally, no differences on the surface between the samples from both types of soil were visible. First changes appeared after the first week in the soil. The samples became less transparent as they were covered with turbid spots. It looked like these spots merged after two weeks and made the whole surface blurrier. Sometimes, patterns of the spots formed brighter areas on the surface. Further, the soil debris on the edges of the samples sometimes resisted the cleaning method and appeared as light-brown frame. Overall, no cracks or discolorations were noticeable during the incubation time.

Interestingly, samples mounted in the film holders that were incubated in the soil showed less staining and less cracks than samples that were placed on the soil surface. Further, the surface alterations of PBST and PBAT samples only evolved where within the frame where the samples had direct contact to the soil. However, PHA samples showed a blurry surface all over the sample independent of soil contact (see appendix Figure 31).

The 2 cm x 2 cm squares from the soil surface and the circular samples that were buried in a net were not used for the assessment.

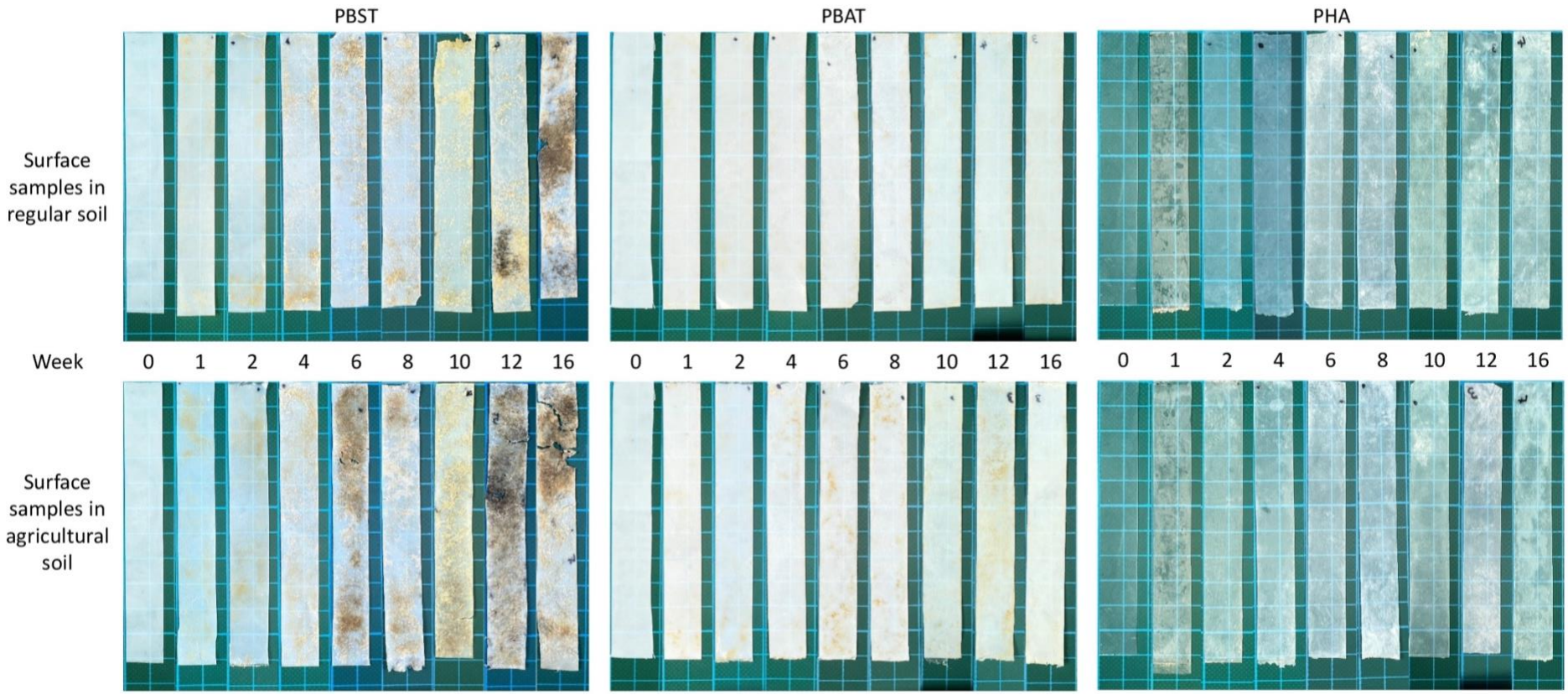

Figure 12: Pictures of the sample strips from start to end of the incubation. The upper row shows arranged images of the downside of the strips after every sampling date in order of poly(butylene-sebacate-co-terephthalate) (PBST), poly(butylene-adipate-co-terephthalate) (PBAT) and poly(3-hydroxybutyrate-co-3-hydroxyhexanoate) (PHA), respectively, from the regular soil. The lower row shows arranged images of the downside of the strips after every sampling date in order of PBST, PBAT and PHA from the agricultural soil. One square of the scale paper equals 1 cm^2.

4.3 Surface characterization

4.3.1 Light microcospy

Sample surfaces were examined and photographed with a digital microscope for a closer view of possible surface modifications. A chronological sequence of the sample strips during the incubation in soil was already shown in Figure 12, therefore only images from samples before the incubation and after 16 weeks of incubation were arranged in Figure 13. This section deals with higher resolution images of the end-effects on the sample surface with a 100- or 200-fold amplification.

Starting with the reference samples of PBST, PBAT and PHA, which were examined before they got in contact with soil, but also received the cleaning procedure, PBST and PBAT surfaces looked almost similar with a crystal-like structure, while the PHA reference looked almost transparent with a shiny surface.

Looking at the images of the PBST samples, it is immediately visible that material changed after the 16 weeks with soil contact. The strips that were placed on the soil surface both revealed a blurry surface with discoloration and stains of different sizes. Additionally, the sample incubated on the agricultural soil in particular showed deep cracks reaching into the material. Further, the rectangles that were incubated in the slide frames in the soil showed less attributes of disintegration, but also white stains were found and the sample from the agricultural soil also developed some cracks.

In comparison to the similar surface of the reference material, the PBAT samples developed less surface alterations. The strips from both soil types kept their initial color and only the surface was covered in small dots. It looked like the sample incubated on the regular topsoil featured some areas with minor cavities, whereas the samples incubated on the agricultural soil evolved some cracks starting to enter the material. Similar indications were also found for the two samples that were incubated in the film holders. The color of the films remained but the surface became blurry and small dots distributed all over the surface. Additionally, the samples from both soil types showed areas where minor cavities seemed to evolve.

However, the PHA samples owned a flat surface before the incubation but quickly developed a turbid surface covered in small circles that remembered of burst blisters. Generally, no discoloration or staining was found in any PHA sample and the same surface alterations occurred independently of soil type or way of incubation.

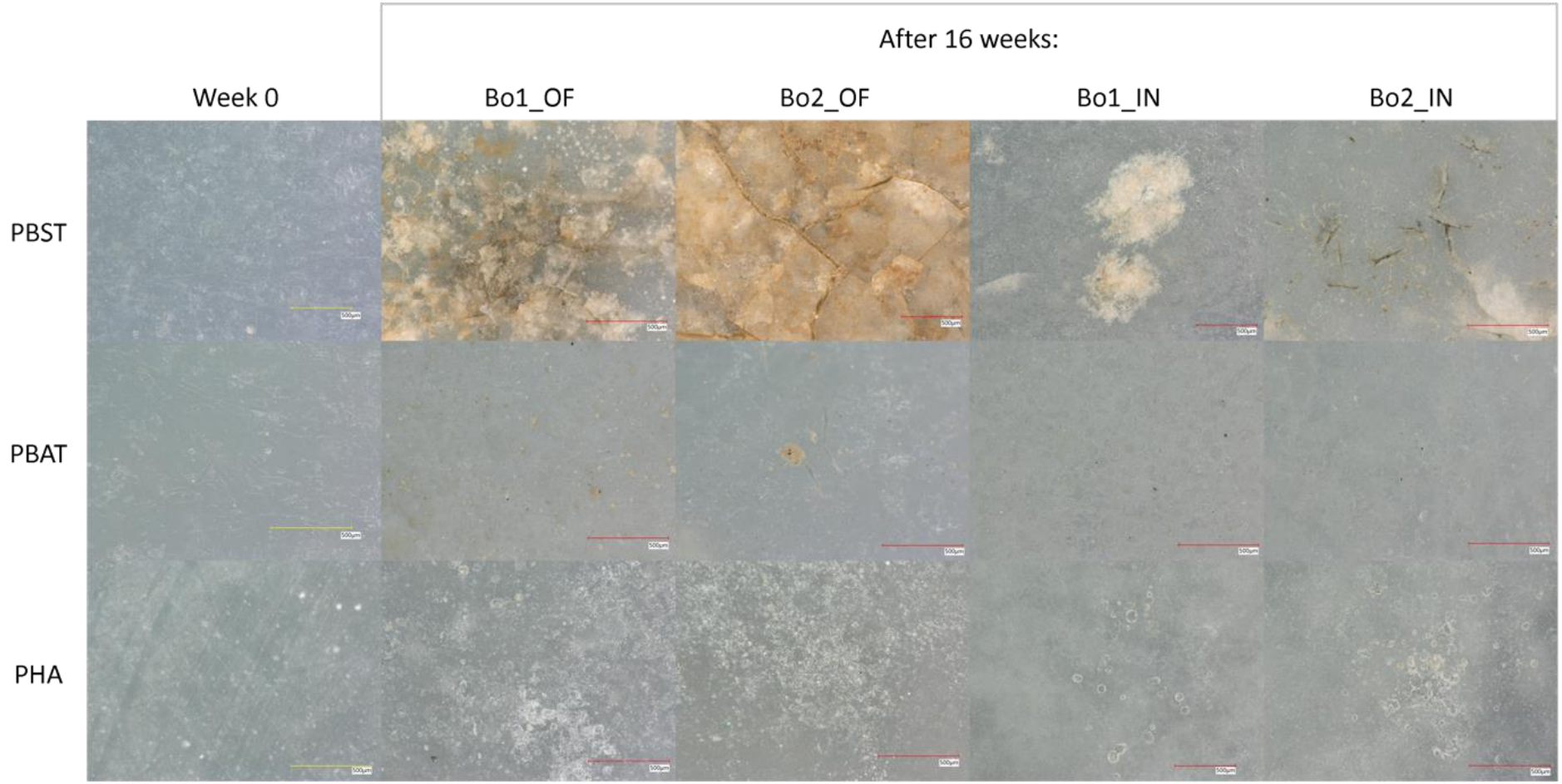

Figure 13: Close-up view of the surface of different samples. Images were taken with a digital microscope with 100- or 200-fold amplification. Therefore, the scale always represents 500 µm. From left to right, the three rows show the surface of the raw material before incubation, the downside of the samples incubated for 16 weeks on the surface of regular (Bo1_OF) and agricultural soil (Bo2_OF) and the surface of the samples incubated for 16 weeks mounted in film holders and placed in regular (Bo1_IN) and agricultural soil (Bo2_IN), respectively. From top to bottom, the following polymers are displayed in order of poly(butylene-sebacate-co-terephthalate) (PBST), poly(butylene-adipate-co-terephthalate) (PBAT) and poly(3-hydroxybutyrate-co-3-hydroxyhexanoate) (PHA), respectively.

4.3.2 SEM

Further examination of the sample surfaces was conducted with images of a scanning electron microscope. To compare the surface of the samples from different materials and the different soil types, images with the same resolution were taken and arranged next to each other. As a reference, the surface of PBST, PBAT and PHA before the incubation can be seen in Figure 14.

Similar surface properties were found when comparing the three polymer samples. Small particles were found on the surface of PBST and PBAT, whereas the PHA surface showed tiny holes. Overall, the surfaces were found to be even and flat with a few bumps and scratches.

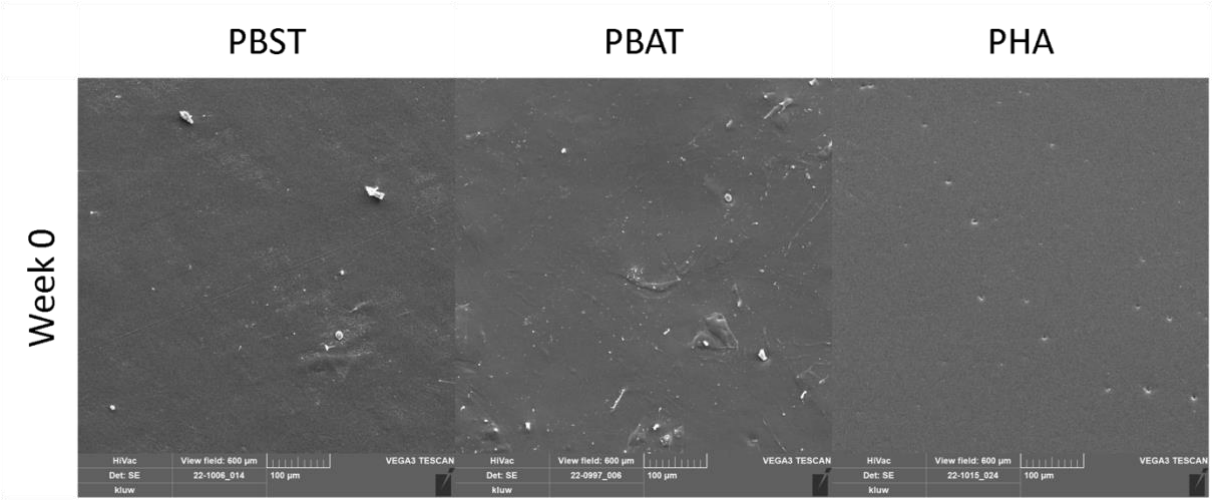

Figure 14: SEM images of the surface of the three materials before incubation. *Images of poly(butylene-sebacate-co-terephthalate) (PBST), poly(butylene-adipate-co-terephthalate) (PBAT) and poly(3-hydroxybutyrate-co-3-hydroxyhexanoate) (PHA) were taken in week zero, before the materials had contact with soil. Resolution was similar for all images with the scale indicating 100 µm.*

In contrast, the SEM images after 16 weeks revealed completely different surface properties of all samples, as seen in Figure 15. Starting with PBST, the strips that were incubated on the regular soil showed cavities of different sizes with diameters up to 100 µm distributed all over the surfaces. In between, some superficial cracks were found. The strips that were incubated on the surface of the agricultural soil showed similar surface alterations, but less and smaller cavities were found. However, the holes seemed to be deeper and to contain some soil debris. The rectangular samples buried in the regular soil provided images which followed the previous findings of superficial cracks and craters. The holes looked shallower and were smaller in diameter, though. Images of the samples buried in the agricultural soil confirmed the surface modifications showing superficial cracks and dimples. However, the holes were bigger and looked deeper compared to the same samples type from the regular soil.

Images of the PBAT strips that were incubated on the surface of regular soil for 16 weeks also showed a rough surface covered in small dimples although they were smaller compared to the holes of PBST samples. Interestingly, cracks only formed within the cavities. The surface of the strips from the agricultural soil showed deeper cavities but no cracks. Furthermore, the number of cavities seemed to be increased. Different observations were made for the rectangular samples incubated in the regular topsoil. Instead of single dimples, many cracks were found on the surface and they even connected to cavity-like forms. Additionally, some residual artefacts were found. Interestingly, images of the rectangular samples from the agricultural soil revealed a similar look compared to the surface incubated strips. The surface was covered in holes of different sizes and a few cracks were visible. Moreover, the cavities looked as deep as in the strips from the agricultural soil and some fractures were found.

Lastly, surface observation of the PHA sample strips incubated on the regular topsoil showed a rough surface with several tiny holes. The holes certainly looked less deep compared to the other samples and they connected to a pattern. The images from the strips from the agricultural soil showed a more distinct pattern of a sponge-like surface with differently sized holes in it. Additionally, some deeper dimples formed below the surface structure. Less surface alteration was found on samples buried in the regular soil. Although the whole surface showed seemed to be rough, only some areas showed defined cavities that were connected. Further, some fragments were found on the surface. A similarly rough surface structure was also found on samples that were buried in the agricultural soil. While only a few small holes were observed, the surface looked more bumpy and also contained more undefined surface structures.

Overall, surfaces from all samples showed changes in roughness compared to the surfaces of the reference images. Moreover, especially samples from the incubation on the soil surface showed distinct holes of different depths and diameters. Special occurrence of surface alterations was found on samples that were exposed to the agricultural soil.

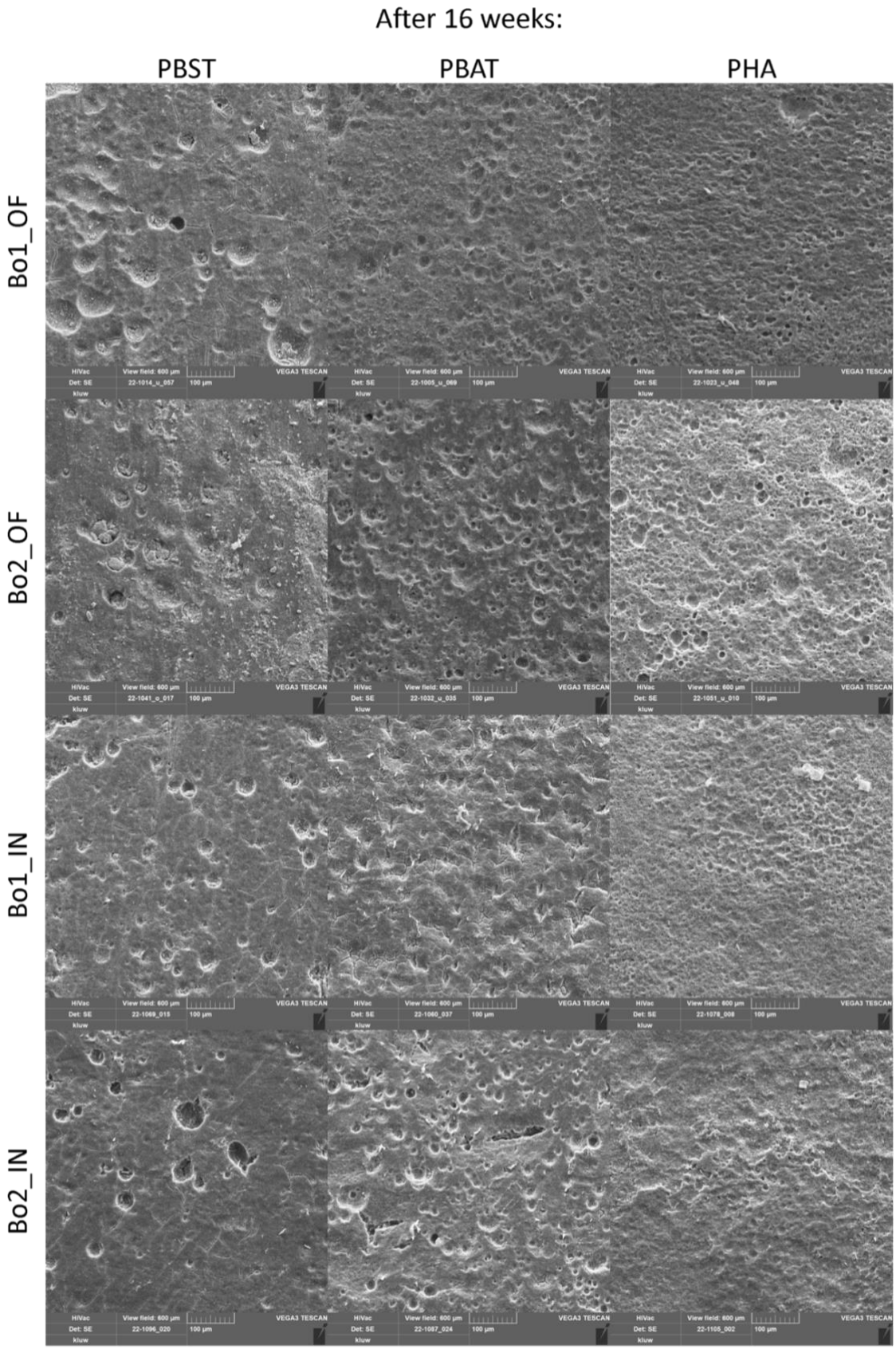

Figure 15: SEM images of the surface of the materials after incubation time. Images of the downside of the films made from poly(butylene-sebacate-co-terephthalate) (PBST), poly(butylene-adipate-co-terephthalate) (PBAT) and poly(3-hydroxybutyrate-co-3-hydroxyhexanoate) (PHA) were taken after 16 weeks of incubation. Resolution was similar for all images with the scale indicating 100 µm. The abbreviations in the form of "Bo1_OF" indicate the soil types of regular soil (Bo1) or agricultural soil (Bo2) and sample location on the surface (OF) or buried in the soil (IN).

4.4 Mechanical properties

The material-specific properties E_t and σ_m were determined by a tensile strength test after every sampling procedure. Therefore, five strips of each sampling date were measured and the values were averaged. However, for the measurement after week 16 only four strips could be used. Further, the measurement of PBST samples from the agricultural soil after week twelve and from both soil types after week 16 was stopped manually because the strips broke under small tension during the measurement and the test device continued without noticing. Standard deviations for the measurements were calculated but may be too small to be visible in the diagrams.

The samples showed three different starting points of the elastic modulus of 61.0 ± 7.5 MPa for PBST, 96.2 ± 8.9 MPa for PBAT and 802.8 ± 93.6 MPa for PHA, as seen in Figure 16. The same reference measurement was used for both soil types. The elastic modulus values of the PBST samples were the lowest of all samples and were similar to each other in both soil types until week four. Then, the samples incubated in the agricultural soil started to weaken after week six while the samples from the regular soil showed the first decline after week twelve. After the final incubation week, the strips from the agricultural soil showed a E_t of 0.6 ± 0.4 MPa and the strips from the regular topsoil showed values of 42.5 ± 26.9 MPa.

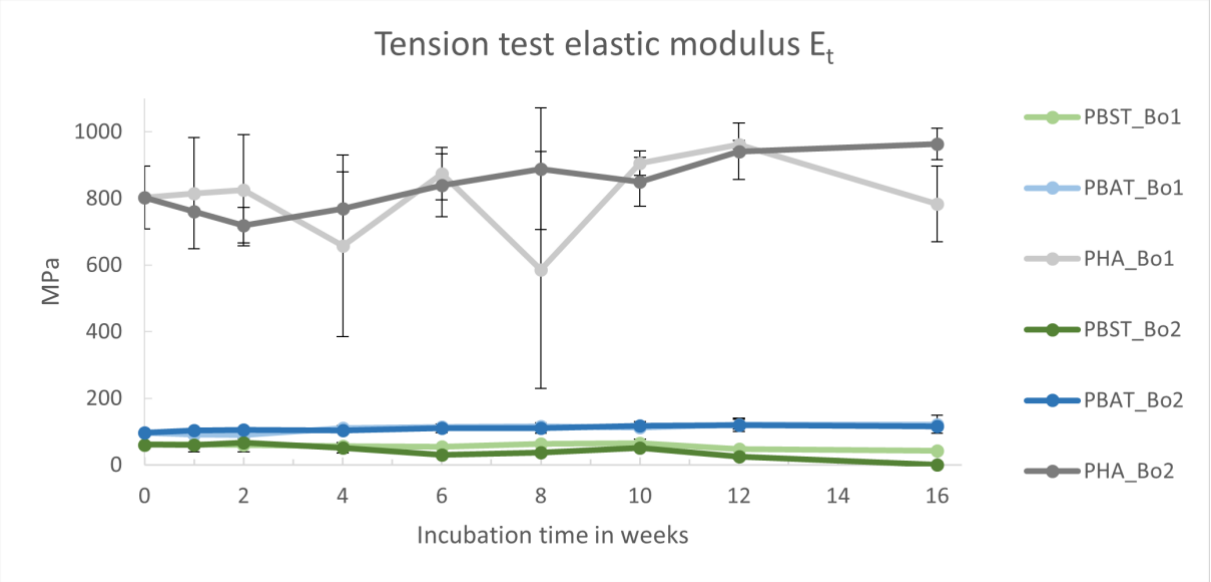

Figure 16: Tension test of the elastic modulus. Results of the elastic modulus E_t in MPa of the sample strips over the incubation time of 16 weeks. The elastic modulus of the samples of each sampling date was measured in replicates of five. According to the denomination of the samples, the abbreviations in the form of "PBST_Bo1" indicate the polymer types of poly(butylene-sebacate-co-terephthalate) (PBST), poly(butylene-adipate-co-terephthalate) (PBAT) or poly(3-hydroxybutyrate-co-3-hydroxyhexanoate) (PHA), and the soil types regular topsoil (Bo1) or agricultural topsoil (Bo2).

In contrast, PBAT samples from both soil types showed a slightly increasing trend of the elastic modulus during the incubation time. The measurement values raised up to 121.5 ± 2.7 MPa and 116.3 ± 6.1 MPa for strips from the regular and agricultural soil, respectively, therefore showing growth of 26 % and 21 %. However, the standard deviation was relatively high.

The PHA samples showed the highest measurement values of the three polymer types but also the highest deviation. No clear difference of the influence of the soil type was visible since all data points show alternating trends. In the end, the PHA strips incubated on the regular topsoil showed a small decrease in the elastic modulus towards 783.3 ± 113.8 MPa and PHA strips incubated on the agricultural soil increased their elastic modulus up to 963.3 ± 47.5 MPa.

The measurement of the tensile strength at first maximum is depicted in Figure 17. Starting points were 19.7 ± 11.3 MPa for PBST, 8.2 ± 0.4 MPa for PBAT and 23.7 ± 0.7 MPa for PHA samples. Generally, the tensile strength for the PHA samples remained the highest during the whole incubation time. The lowest tensile strength in the beginning was found for PBAT but the tensile strength of the PBST samples quickly fell below.

Interestingly the deviation between the PBST samples was biggest in the reference measurements after the first week. Also, data points dropped after the first week and approached almost zero after six weeks. Simultaneously, the tensile strength of the samples

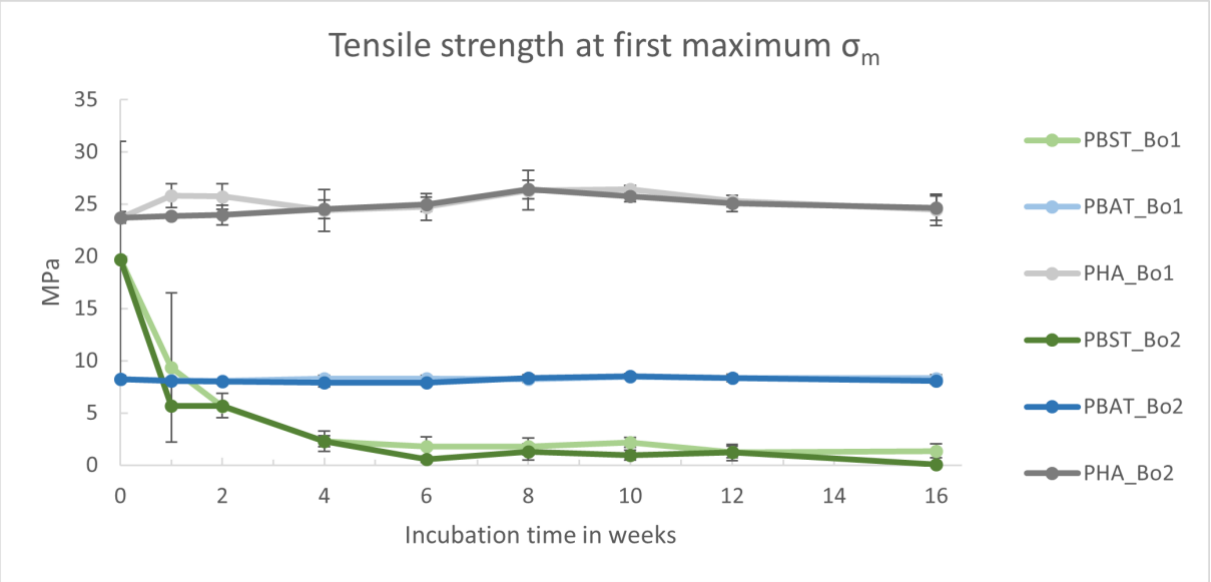

Figure 17: Tensile strength at first maximum. Results of the tensile strength at first maximum σ_m of the samples in MPa of each sampling date over the incubation time of 16 weeks. Measurements were conducted in replicates of five and the standard deviation was calculated. Small error bars may be covered by dots. According to the denomination of the samples, abbreviations in the form of "PBST_Bo1" indicate the polymer types of poly(butylene-sebacate-co-terephthalate) (PBST), poly(butylene-adipate-co-terephthalate) (PBAT) or poly(3-hydroxybutyrate-co-3-hydroxyhexanoate) (PHA), and the soil types regular topsoil (Bo1) or agricultural soil (Bo2).

incubated on the agricultural soil decreased even further ending below 0.1 MPa while the samples from the regular soil maintained some 1.4 ± 0.7 MPa.

The tensile strength of the PBAT strips remained stable during the whole experiment and showed continuously small deviation. No difference between the soil types was discovered with final measurement values of 8.3 ± 0.3 MPa for samples from the regular soil and 8.2 ± 0.3 MPa for samples from the agricultural soil.

Similar stability was also found in the measurement of the PHA strips. Although the tensile strength from regular soil samples in the first two weeks slightly increased compared to the agricultural soil samples, the tensile strength overall showed a similar stable trend. Final measurements revealed σ_m of 24.5 ± 1.5 MPa for strips from the regular soil and 24.6 ± 1.2 MPa for strips from the agricultural soil.

4.5 Thermal properties

All samples were measured with a differential scanning calorimeter one day after sampling took place. With this method material-specific properties like the glass transition temperature, the crystallization temperature and the melting point were determined to compare potential changes. An exemplary depiction of a DSC measurement of each polymer type can be found in the appendix (Figure 28, Figure 29 and Figure 30).

4.5.1 Glass transition temperature

The three different polymer types revealed three different glass transition temperatures of -36.1 ± 1.6 °C for PBST, -30.4 ± 2.1 °C for PBAT and -2.0 ± 4.4 °C for PHA, respectively. Thus, the PHA samples showed the highest T_g, the PBST samples showed the lowest T_g and the PHA samples lied in between.

Overall, the measurement points of both PBST samples from the surface of the regular and the agricultural soil remained stable with minor variations, as seen in Figure 18. In the end, the samples from the regular soil showed a glass transition temperature of -35.0 ± 1.4 °C and the samples from the agricultural soil showed a temperature of -34.5 ± 0.7 °C, being close to the reference value of week zero.

A similar pattern was observed for the PBAT samples showing almost no variation between the two soil types except for the measurement after week four. Measured glass transition temperature after 16 weeks of incubation was -28.0 ± 0.0 °C for strips from the regular soil and -28.0 ± 1.4 °C for strips from the agricultural soil. Thus, the final measurement values were around 2.4 °C higher than before the incubation.

The PHA strips followed the same trend but showed a little more variation between the measurements. Still, the glass transition temperature was very similar and ended at -5.0 ± 4.4 °C for the samples from the regular topsoil and -2.7 ± 3.1 °C for the samples from the agricultural soil. Here, the T_g decreased slightly but the deviation of the PHA samples was also the highest of all samples.

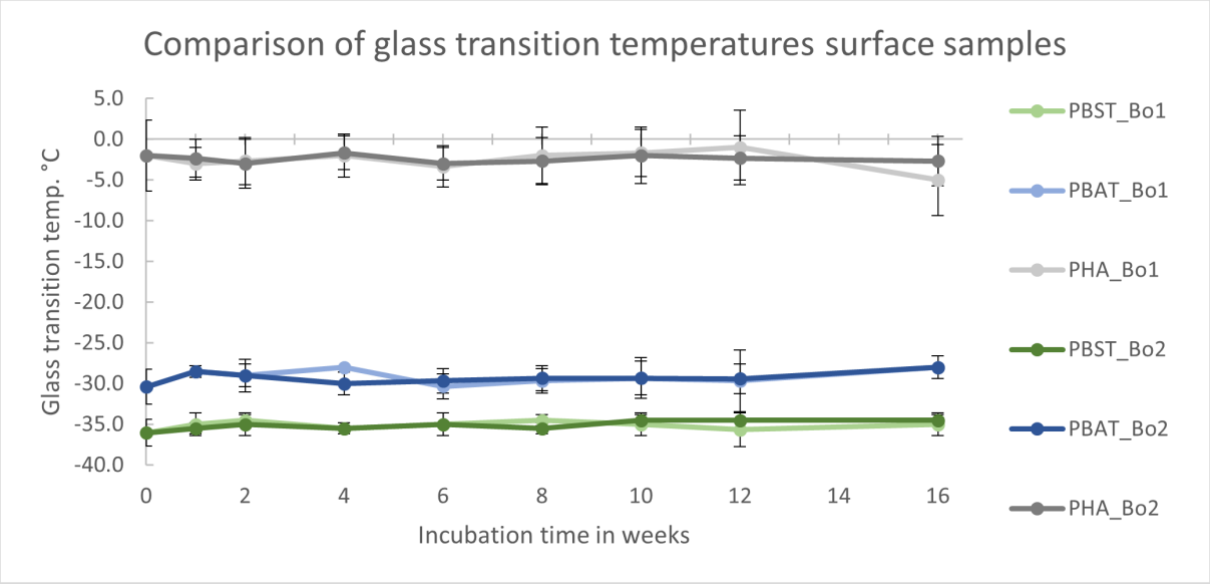

Figure 18: Comparison of the glass transition temperature of the surface samples. The glass transition temperature of the sample strips in °C is displayed over the 16 weeks of incubation time. Standard deviation was calculated from the different cycles of the measurement and is represented in error bars. According to the denomination of the samples, the abbreviations in the form of "PBST_Bo1" indicate the polymer types of poly(butylene-sebacate-co-terephthalate) (PBST), poly(butylene-adipate-co-terephthalate) (PBAT) or poly(3-hydroxybutyrate-co-3-hydroxyhexanoate) (PHA), and the soil types regular topsoil (Bo1) or agricultural topsoil (Bo2).

Measurements of the glass transition temperature of the rectangular film samples revealed comparable results to the measurements of the strips incubated on the soil surface, as Figure 19 shows. Starting from the same temperature as the surface samples, minor variations in the measurement points of the PBST samples from both soil types were found. The glass transition temperature of samples from the regular soil and from the agricultural soil after 16 weeks was -35.0 ± 1.4 °C and -34.0 ± 1.4 °C, respectively.

Likewise, the T_g of the PBAT rectangles remained relatively stable and only increased slightly during the incubation time. After 16 weeks, -29.7 ± 3.8 °C were measured for the samples in the regular soil and -29.3 ± 2.3 °C were measured for the samples in the agricultural soil.

Again, the deviation of the measured PHA samples was highest among the other polymers. The course of the measurement points remained consistent ending in a T_g of -3.3 ± 3.1 °C for rectangles from the regular topsoil and -2.0 ± 3.5 °C for rectangles from the agricultural soil.

Although all measured glass transition temperatures seemed to show a stable course during the incubation time, the values slightly raised between +0.7 °C and +2.4 °C in PBST and PBAT samples, while it decreased up to -3.0 °C in PHA samples.

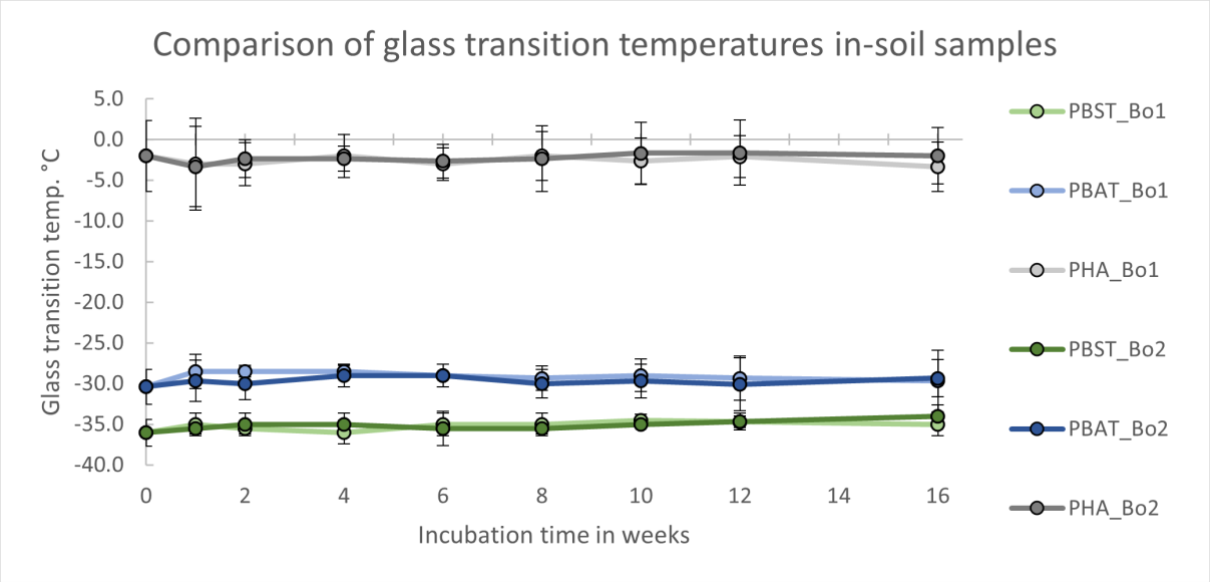

Figure 19: Comparison the glass transition temperature of the in-soil samples. The glass transition temperature of the rectangular samples in °C is displayed over the 16 weeks of incubation time. Standard deviation was calculated from the different cycles of the measurement and is represented in error bars. According to the denomination of the samples, the abbreviations in the form of "PBST_Bo1" indicate the polymer types of poly(butylene-sebacate-co-terephthalate) (PBST), poly(butylene-adipate-co-terephthalate) (PBAT) or poly(3-hydroxybutyrate-co-3-hydroxyhexanoate) (PHA), and the soil types regular topsoil (Bo1) or agricultural topsoil (Bo2).

4.5.2 Crystallization temperature

The crystallization temperatures of the samples were taken from the DSC graphs (see appendix Figure 29 for example) and were compared afterwards. Each DSC cycle resulted in one crystallization phase per sample so no standard deviation could be calculated. While the PBST and PBAT samples showed crystallization behavior during the cooling step, PHA samples showed cold crystallization during the second heating run. Starting with the sample strips on

the surface of the soil, three different crystallization temperatures were recorded for the three polymer types. As seen in Figure 20, PBST showed the lowest crystallization temperature of 33 °C, PBAT showed the next higher crystallization temperature at 39 °C and PHA showed the highest crystallization temperature of 52 °C.

The course of the measurement points of the PBST strips from the soil surface seemed constant for the first four weeks. Then, the samples incubated on the agricultural soil started to show increasing values. After week 16, the crystallization temperatures were 33 °C and 35 °C for samples from regular and agricultural soil, respectively.

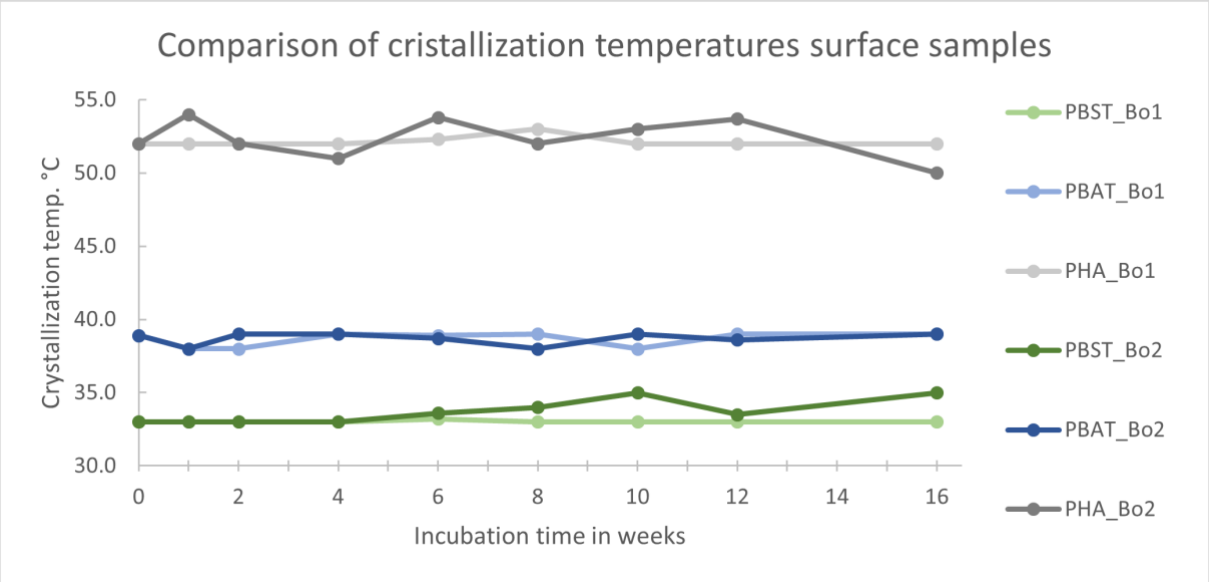

Figure 20: Comparison of the crystallization temperature of the surface samples. The crystallization temperature of the sample strips in °C is displayed over the 16 weeks of incubation time. According to the denomination of the samples, the abbreviations in the form of "PBST_Bo1" indicate the polymer types of poly(butylene-sebacate-co-terephthalate) (PBST), poly(butylene-adipate-co-terephthalate) (PBAT) or poly(3-hydroxybutyrate-co-3-hydroxyhexanoate) (PHA), and the soil types regular topsoil (Bo1) or agricultural topsoil (Bo2).

In contrast, the crystallization temperatures of the PBAT strips varied around the same temperature and ended with 39 °C from both soil types. The PHA samples, though, showed a little more variance. Particularly the samples from the agricultural soil seemed unstable while the samples from the regular soil kept a constant crystallization temperature. The incubation period resulted in 52 °C and 50 °C for regular soil and agricultural soil samples.

Measurement results of the rectangles incubated in the soil were analogous to the results of the sample incubated on the soil, as seen in Figure 21. The crystallization temperature of the PBST samples remained stable for the first two weeks, but then shifted slightly upwards before decreasing again. Final measurement values were 34 °C and 33 °C for the rectangles from the regular and agricultural soil, respectively.

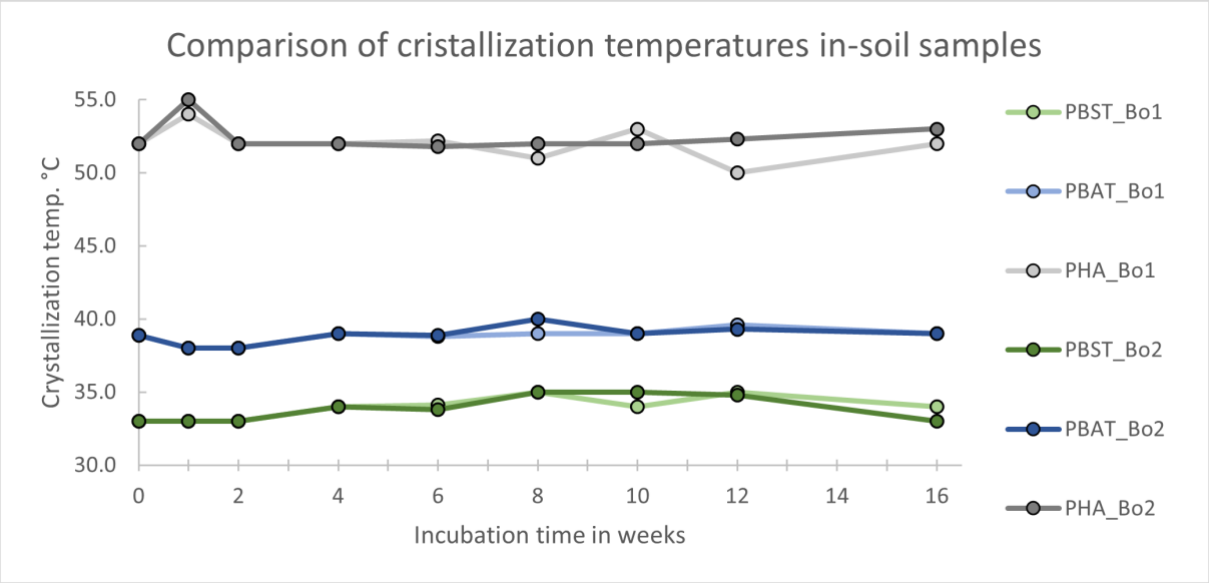

Figure 21: Comparison of the crystallization temperature of the in-soil samples. The crystallization temperature of the rectangular samples in °C is displayed over the 16 weeks of incubation time. According to the denomination of the samples, the abbreviations in the form of "PBST_Bo1" indicate the polymer types of poly(butylene-sebacate-co-terephthalate) (PBST), poly(butylene-adipate-co-terephthalate) (PBAT) or poly(3-hydroxybutyrate-co-3-hydroxyhexanoate) (PHA), and the soil types regular topsoil (Bo1) or agricultural topsoil (Bo2).

The crystallization temperatures from the PBAT samples were stable as well and both soil types resulted in a temperature of 39 °C after 16 weeks. Again, PHA samples showed a little more variation of the data points but also remained constant in general. Final measurement values were 52 °C for the samples from the regular topsoil and 53 °C for the samples from the agricultural soil.

Summing up, crystallization temperatures of the samples differed only slightly between the soil types and between surface and in-soil incubation. Trends could only be estimated with a maximum increase of +2 °C of the crystallization temperature of the PBST strips incubated on agricultural soil.

4.5.3 Melting temperature

The DSC measurement also revealed the melting temperatures of the samples. Again, three starting temperatures were observed for the three polymer types. As seen in Figure 22, samples of PBST showed the lowest melting temperature of 109.4 ± 0.8 °C, samples of PHA showed the highest melting temperature of 163.5 ± 0.7 °C and samples of PBAT showed a melting temperature of 116.3 ± 0.4 °C, being close to the ones of PBST.

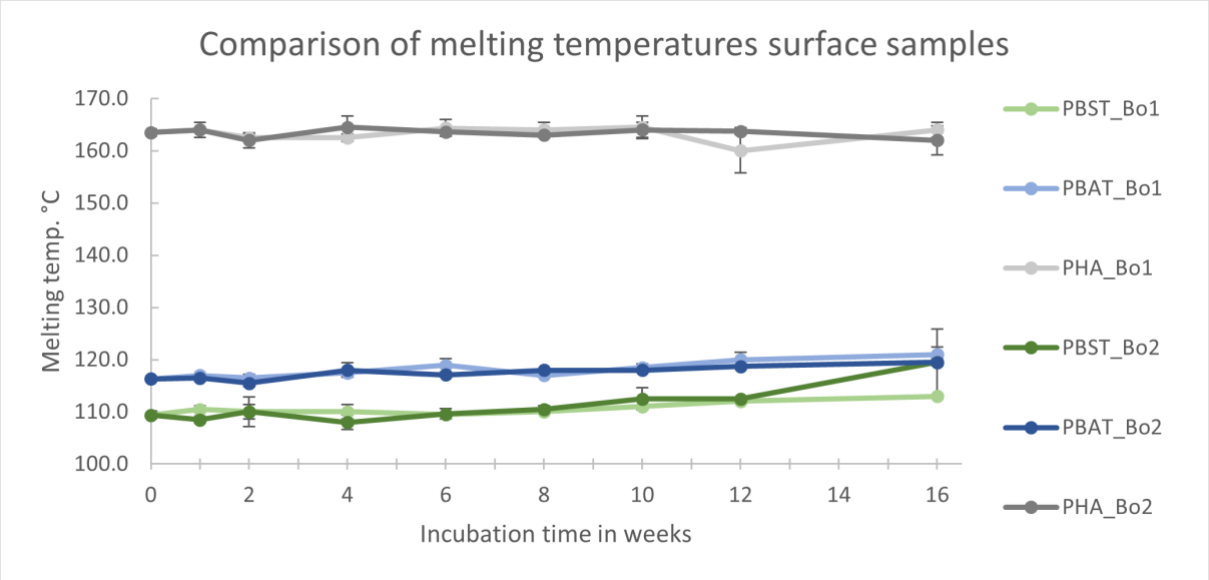

Figure 22: Comparison of the melting temperature of the surface samples. The melting temperature of the sample strips in °C is displayed over the 16 weeks of incubation time. Standard deviation was calculated from the different cycles of the measurement and is represented in error bars. According to the denomination of the samples, the abbreviations in the form of "PBST_Bo1" indicate the polymer types of poly(butylene-sebacate-co-terephthalate) (PBST), poly(butylene-adipate-co-terephthalate) (PBAT) or poly(3-hydroxybutyrate-co-3-hydroxyhexanoate) (PHA), and the soil types regular topsoil (Bo1) or agricultural topsoil (Bo2).

The measurement values of the PBST strips from both soils remained stable for the first eight weeks, but then slightly increased especially for the strips incubated on the agricultural soil. After the whole incubation time, the melting temperature was 113.0 ± 0.0 °C for the samples from regular soil and 119.5 ± 6.4 °C for the samples from agricultural soil.

PBAT samples showed a similar trend of increasing melting temperature, but the increase already started after the first two weeks in the agricultural soil. Final melting temperature of the strips from the surface of the regular soil and from the agricultural soil were 121.0 ± 1.4 °C and 119.5 ± 0.7 °C, respectively.

In contrast to the two previous polymers, PHA samples kept or slightly decreased their melting temperature during the incubation time, but the course of the measurements showed some variation. The strips from the regular soil revealed a final t_m of 164.0 ± 1.4 °C and the strips from the agricultural soil revealed a final t_m of 162.0 ± 2.8 °C.

The measurement of the rectangular samples that were incubated in the soil delivered similar results, as seen in Figure 23. Starting points were the same as for the sample strips. A final melting temperature of 113.0 ± 1.4 °C for the rectangles from the regular soil and 113.0 ± 0.0 °C for the rectangles from the agricultural soil was measured. Hence, the melting temperature slightly increased in both cases.

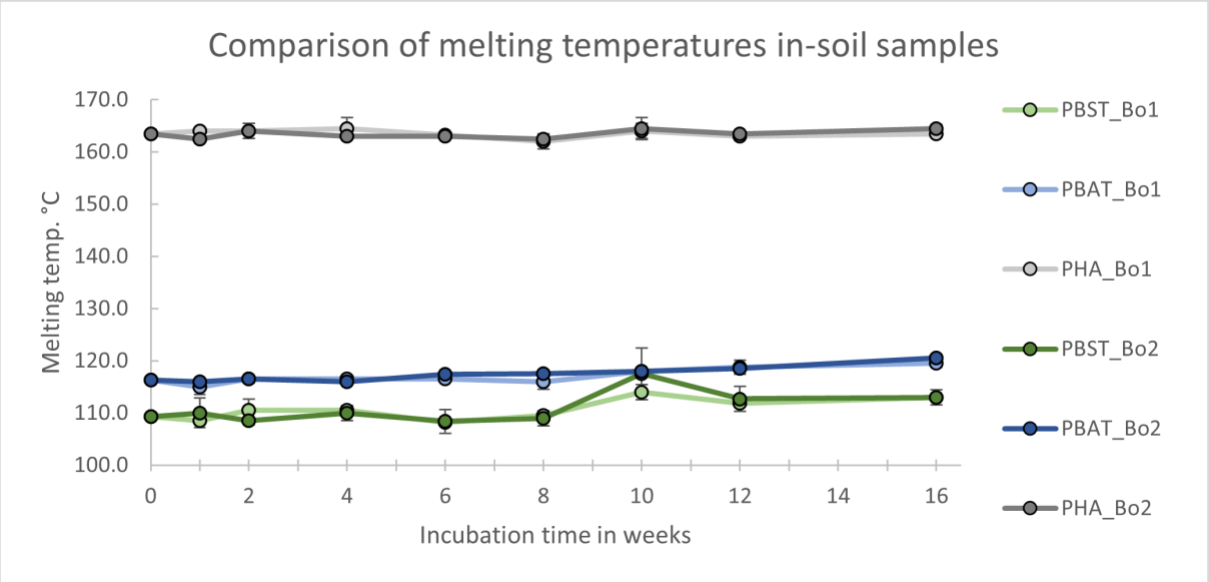

Figure 23: Comparison of the melting temperature of the in-soil samples. The melting temperature of the rectangular samples in °C is displayed over the 16 weeks of incubation time. Standard deviation was calculated from the different cycles of the measurement and is represented in error bars. According to the denomination of the samples, the abbreviations in the form of "PBST_Bo1" indicate the polymer types of poly(butylene-sebacate-co-terephthalate) (PBST), poly(butylene-adipate-co-terephthalate) (PBAT) or poly(3-hydroxybutyrate-co-3-hydroxyhexanoate) (PHA), and the soil types regular topsoil (Bo1) or agricultural topsoil (Bo2).

A similar observation was made for the measurements of the PBAT samples, which also increased their melting temperature during the incubation in the soil. Just like that, the melting temperature increased up to 119.5 ± 0.7 °C and 120.5 ± 0.7 °C for the rectangles from the regular soil and the agricultural soil, respectively.

However, stable melting temperatures were recorded for PHA samples. The melting temperature of 163.5 ± 0.7 °C for the regular soil samples and 164.5 ± 0.7 °C for the agricultural soil samples was measured after 16 weeks.

Overall, the measured melting temperatures for the different sample types and incubation types of the polymers revealed slightly increased values for PBST and PBAT samples, particularly for the samples incubated in the agricultural soil. On the contrary, the PHA samples kept a stable melting temperature which only varied around the reference value.

4.5.4 Crystallinity

Relative crystallinities could not be calculated due to imprecise peak integration caused by an unstable baseline during the DSC measurement. However, melting enthalpies from the second heating curve were compared between the measurements before and after the incubation (see appendix Table 8). The highest increase in melting enthalpy was observed in PBST samples with 46 % when incubated on the surface of the regular soil, 92 % when buried in the regular soil, 52 % when incubated on the surface of the agricultural soil and 43 % when buried in the agricultural soil. PBAT samples showed more variation with a decrease of 8 % and an increase of 73 % when incubated on and buried in the regular topsoil, respectively. The incubation on the surface of the agricultural soil promoted an increase of 23 % and the incubation buried in the agricultural soil promoted an increase of 12 %. Similarly, the PHA samples showed mixed measurement values with an increase of 2 % and a decrease of 33 % when incubated on the surface and within the regular soil, respectively. An increase of 9 % was found when incubated on the surface of the agricultural soil and increase of 44 % was found when buried in the agricultural soil.

4.6 Molecular weight

Numeric molecular weight of the samples was measured with gel permeation chromatography before and after the incubation. Start values were 75,200 g / mol, 62,820 g / mol and 293,000 g / mol for PBST, PBAT and PHA, respectively. Overall, a decrease of the molecular weight up to -28 % was determined. As direct comparison, the start measurement and the end measurement after 16 weeks of incubation time is displayed in Figure 24.

The final molecular weight of PBST surface samples from the regular soil was 72,200 g / mol and 70,100 g / mol from the agricultural soil. Rectangular samples incubated in the regular soil showed a molecular weight of 61,400 g / mol and rectangular samples buried in the agricultural soil showed 63,400 g / mol. Accordingly, the highest decrease occurred when buried in the soil.

Similarly, the measurement of PBAT samples incubated in regular soil revealed a slightly decreased molecular weight of 62,500 g / mol and 61,600 g / mol after 16 weeks on the surface of the regular and the agricultural soil. Again, the molecular weight of the rectangular samples decreased even more resulting in 59,200 g / mol from the regular soil and 58,200 g / mol from the agricultural soil, respectively.

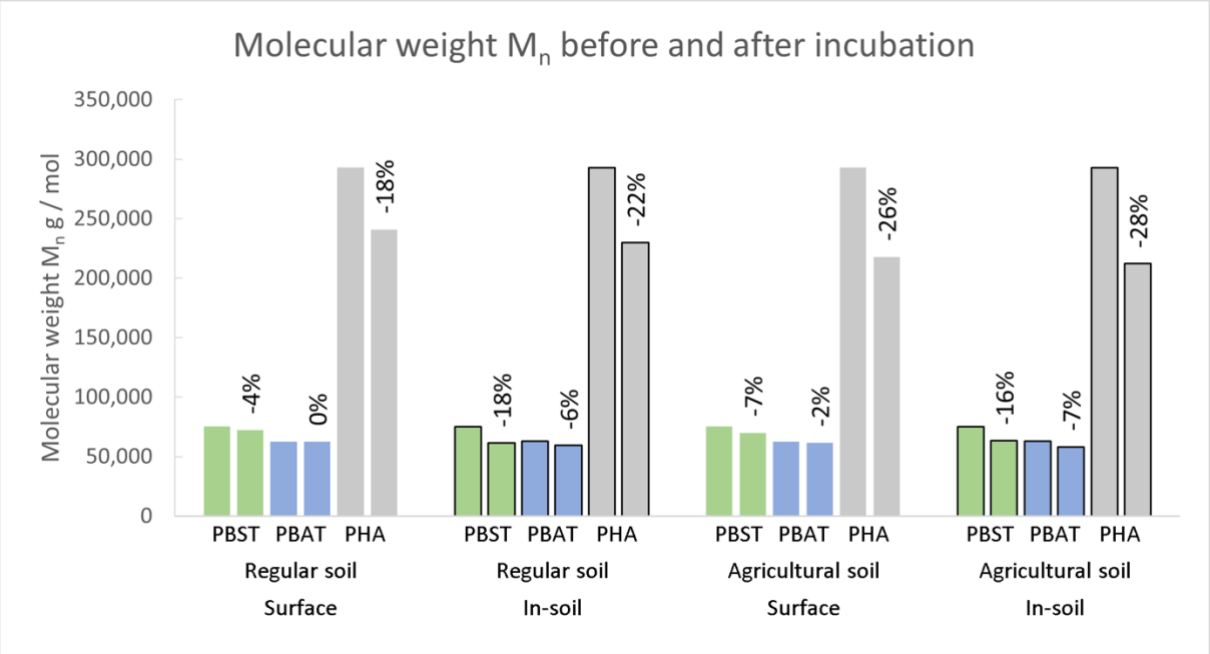

Figure 24: Comparison of the molecular weight M_n of the samples. The graph shows the molecular weight M_n in g / mol of the different samples consisting of poly(butylene-sebacate-co-terephthalate) (PBST), poly(butylene-adipate-co-terephthalate) (PBAT) and poly(3-hydroxybutyrate-co-3-hydroxyhexanoate) (PHA) before and after the 16 weeks incubation. The relative difference between the two measurement points is indicated above the corresponding data bars. Same polymers are displayed in the same color with the left bar indicating the molecular weight of the reference at start and the right bar indicating the molecular weight after 16 weeks.

The highest decrease of molecular weight was found in the PHA samples. The measurement revealed 241,000 g / mol for strips incubated on the surface and 218,000 g / mol for the strips from the agricultural soil. A molecular weight of 230,000 g / mol was found for samples buried in the regular soil and 212,000 g / mol for the samples buried in the agricultural soil. Hence,

the incubation in film holders buried in the agricultural soil influenced the molecular weight the most.

However, with a ten percent relative error of the determination of the molecular weight only a relative change of the molecular weight of more than ten percent was considered as significant. Thus, remarkable changes were observed in PBST samples buried in both, regular (-18 %) and agricultural (-16 %), soil types. All PHA samples lost -18 % to -28 % of their molecular weight, especially when exposed to the agricultural soil. A change in samples of PBAT, though, was not determined.

4.7 Functional groups

Infrared spectra were recorded for the determination of functional groups of the polymer samples. For comparison of potential changes during the incubation, spectra from the reference measurement before incubation and after 16 weeks of incubation were arranged in one depiction, as seen in Figure 25. The characteristic bands of each raw material were compared with literature and are noted in the appendix (Table 9, Table 10 and Table 11).

The IR spectra of all three polymers showed characteristic bands of CH_2 between 3000 cm^{-1} and 2800 cm^{-1}, C=O around 1720 cm^{-1} and C-O around 1260 cm^{-1}. Additionally, PHA showed a third peak at 2972 cm^{-1} referring to the presence of -CH_3 groups.

Changes in the infrared absorbance spectrum of PBST samples after the incubation showed a broad band between 3600 cm^{-1} and 3100 cm^{-1} indicating the presence of -OH groups while the increase around 870 cm^{-1} represents vibrations of carboxylic groups with hydrogen bonds. Further, the carbonyl peak at 1720 cm^{-1} decreased and the bands below 1500 cm^{-1} increased.

Measurements of PBAT samples revealed only a slightly changed absorbance spectrum. Increase bands were only found between 1500 cm^{-1} and 1350 cm^{-1} and around 870 cm^{-1}, respectively. The latter could indicate an increase of carboxylic groups with hydrogen bonds but no characteristic -OH band between 3600 cm^{-1} and 3100 cm^{-1} was found.

Bands and peaks of PHA spectra, thus, showed reduced intensity but generally no differences of characteristic bands were visible.

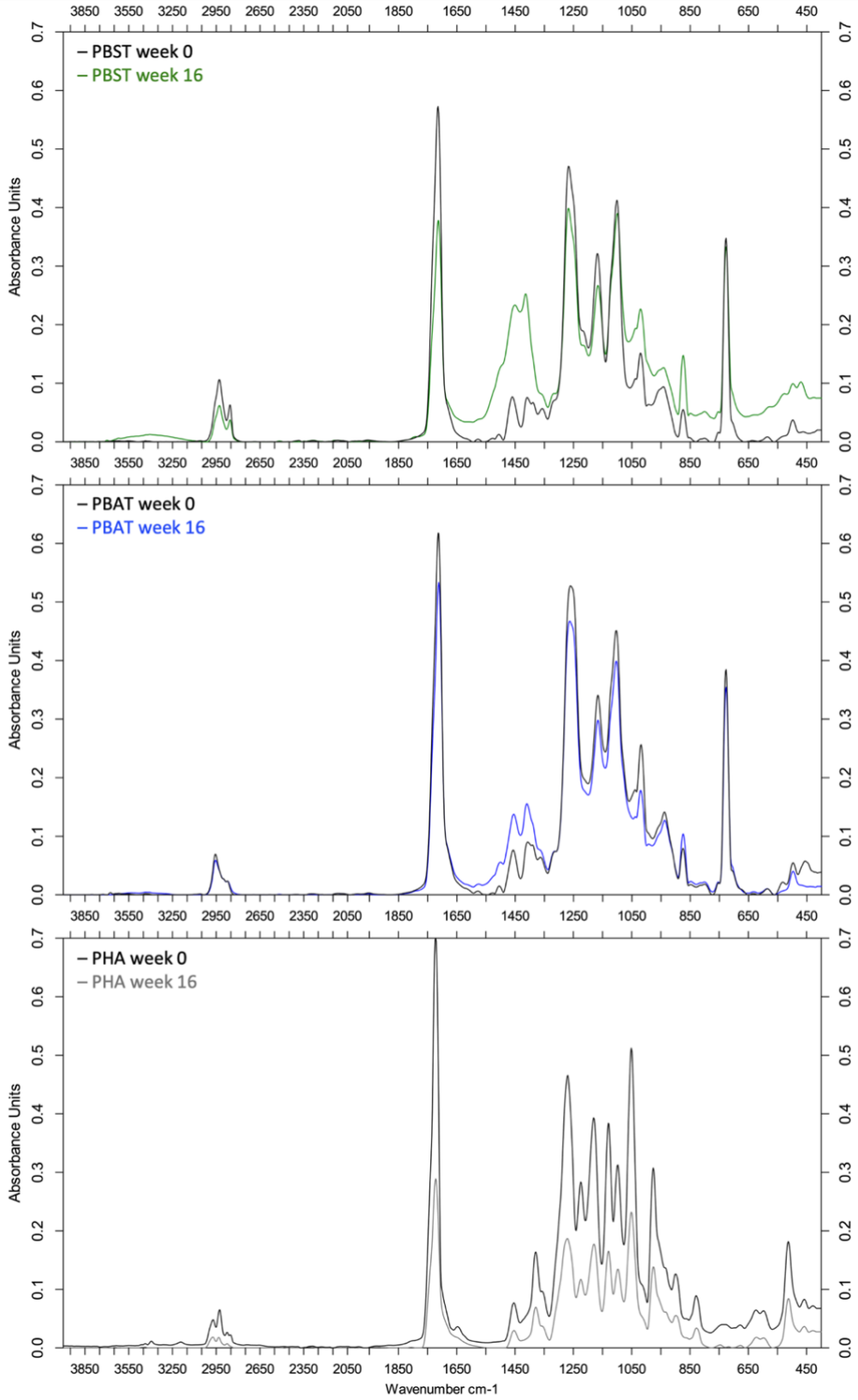

Figure 25: Infrared spectra of the three polymer types before and after incubation. The spectra show the absorbance of the samples at a corresponding wavelength in cm^{-1} and were recorded with attenuated total reflection Fourier-transformed infrared spectroscopy between 4000 and 400 cm^{-1} with 16 scans assembled to one line. Resolution was 4 cm^{-1} and the spectra of measurements before the incubation (black) and after 16 weeks of incubation (colorful) in soil were baseline corrected and normalized. Measurements are displayed in order of poly(butylene-sebacate-co-terephthalate) (PBST) in green, poly(butylene-adipate-co-terephthalate) (PBAT) in blue and poly(3-hydroxybutyrate-co-3-hydroxyhexanoate) (PHA) in light grey.

5 Discussion

Three different biodegradable polymer types were exposed to regular topsoil and regular topsoil mixed with agricultural soil from a test field for biodegradation experiments. Different methods were used to evaluate the disintegration process of the samples according to changes in morphology, mechanical and molecular properties.

5.1 Soil conditions

Plastic samples were incubated on the soil surface to reconstruct field conditions of a mulch film that is applied during the season. Rectangular samples were buried in the soil to imitate mulch film that was plowed in after harvesting (Kasirajan & Ngouajio 2012).

Further, two soil types were chosen for the experiment. Regular topsoil was compared with mixed soil consisting of the same regular topsoil and 2 % (w / w) added agricultural soil from a test field where biodegradability tests of biodegradable plastics are conducted frequently.

The incubation conditions of 23 °C and 50 % relative humidity were chosen, firstly, for the controlled storage in the measurement room with air-condition and, secondly, for slightly accelerated effects due to an increased temperature (Lucas et al. 2008). Although the average soil temperature for the year 2022 in Essen, Germany, was 13.0 °C, which is 10 K less than the incubation temperature, the average daily soil temperature in 2022 still exceeded 23 °C on 52 days (CDC 2022).

The weight of the soil boxes was measured consistently every week because the evaporation during storage caused 200 – 300 mL of water loss per box every week what was balanced out by watering. Concerning the soil moisture, the weekly watering keeping most likely was favorable for the experiment because a sufficient amount of water is a key factor for any sort of biodegradation and especially in field conditions during summer season in 2022 frequent precipitation was lacking (DWD 2023, Lucas et al. 2008). Furthermore, the relative soil humidity was measured after each sampling to check the actual moisture around the samples.

The measured pH values of the used soil fitted to an optimum pH range between seven and nine (Meereboer et al. 2020). The pH of some soil boxes first increased and then fell while others increased slowly. Towards the end of the incubation all boxes showed a higher pH

compared to the start what seemed reasonable since it was found that residues of PE and bioplastic mulch film increased soil pH (Qi et al. 2020).

Summarizing, soil conditions were favorable for abiotic and biotic material degradation with an adequate temperature and sufficient humidity.

5.2 Visual inspection and surface characterization by light microscopy

Images taken with a camera and with a digital microscope revealed different stages of surface alterations of the samples. All samples quickly turned blurry and partly showed discolorations within the first week of incubation. However, the 2 cm x 2 cm squares from the soil surface showed very different material alterations because of flowing away during watering and the buried circular microplastic samples could not be cleaned properly due to the small size. Consequently, these two sample types were not used for the assessment.

The PBST strips that were incubated on the soil surface quickly showed cracks and dark colored spots, particularly when incubated on the agricultural soil. The pictures of the PBST samples seemed to look similar to pictures of a comparable study of De Wilde et al. (2016), although the sample thickness differed by factor ten. Further, first cracks and holes were found after six weeks while the samples from De Wilde et al. (2016) were buried in soil and in this work the samples were incubated on the soil surface. The dark spots on the surface could indicate the presence of microbes in form of biofilm formation and build-up of hyphae (Oliveira et al. 2019).

Samples made from PBAT also quickly gained light brown discolorations, but cracks or holes were missing until the last sampling date after 16 weeks of incubation. Likewise, Oliveira et al. (2019) found no superficial changes in PBAT mulch film incubated in soil until the end of the 75-day incubation period when a small crack was observed. Generally, it looked like the surface incubated samples from the agricultural soil showed more discolorations compared to the regular soil and also the minor cracks were found in samples from the surface of the agricultural soil. However, findings of other studies showed strongly fragmented PBAT samples after 30 days incubated in soil (Palsikowski et al. 2017).

PHA samples, however, showed almost no surface changes during the whole incubation time. Comparison with soil incubation at similar temperatures supported the stability of the material (Gil-Castell et al. 2020). Opacity, though, may evolved from biological activity or from

superficial hydrolysis, but no clear indications could be made (Post et al. 2021). Admittedly, comparable studies of PHA showed strong differences of the disintegration behavior in soil (e.g. Emadian et al. 2017).

Images of the control PE film after 16 weeks incubated in soil indicated no surface alterations while the cellulose film could not be retrieved from the soil. Probably, the cellulose film was degraded or remained in the soil when pulling out the frame. Comparison with De Wilde et al. (2016) showed a similar observation cellulose film in film holders that could not be recovered already after eight weeks. PE films on the other hand are known to be persistent in a natural environment for which reason conventional PE mulch films are more and more replaced by biodegradable alternatives (FAO 2021).

In summary, surface images of the samples showed staining on all polymer types based on microscopic surface modifications. Especially PBST samples additionally showed dark spots resulting from biofilm formation while PBAT and PHA expressed a stable surface.

5.3 Surface characterization by SEM

More detailed examination of the sample surface was conducted with SEM images. Compared to the reference images of the materials before the incubation started, all samples showed a rough surface filled with holes and cracks after 16 weeks of incubation. The fine pitting may be a reason for the color fading observed in previous images due to increased surface roughness (Zaidi et al. 2019).

PBST samples showed the biggest holes when incubated on the soil surface, while the holes found on samples that were buried in soil seemed to be deeper instead. Further, the surface modifications seemed to be more pronounced when incubated in the agricultural soil. The holes may be attributed to microbial activity with the residues found in the holes of the sample being the residue of a biofilm (Oliveira et al. 2019). However, the cleaning procedure, especially brushing, was difficult to conduct for the porous and brittle sample strips after 16 weeks of incubation. Perhaps, the residues in the holes could not be removed sufficiently due to careful brushing. Still, the samples appeared to be similar to images of the same material after incubation in a hydrolytic medium and the incubation under the influence of a lipase enzyme (Heidarzadeh et al. 2017). The small cracks probably have originated from hydrolysis

and the deeper holes resulted from enzymes followed by microorganisms infiltrating the material (Heidarzadeh et al. 2017, Oliveira et al. 2019).

Similar observations made for PBAT samples indicate a combination of hydrolysis and microbial activity as well. Again, the formation of cavities in surface incubated samples and the formation of cracks in samples buried in soil were more distinctive when incubated in agricultural soil what supports the influence of the soil type. Interestingly, PBAT materials tend to degrade slower when covered in soil compared to being placed on the soil surface, particularly when exposed to UV-radiation like sun light (Laycock et al. 2017). Since no UV-radiation was applied in this work, the differences after the incubation period most likely were based on the soil type and not the incubation type. Still, when comparing SEM images all samples seemed to show residual artefacts of biofilm formation on the surface and specifically the samples exposed to the agricultural soil showed deeper holes not only from hydrolysis but also from enzymatic and microbial activity (Heidarzadeh et al. 2017, Oliveira et al. 2019).

Images of PHA samples revealed fine pitting on samples of all incubation types, particularly in samples incubated on the agricultural soil surface. As the proper holes in the surfaces of PBST and PBAT may resulted from enzymatic attacks, the sponge-like surface of the PHA samples could be developed by a reduced molecular weight due to hydrolysis (Zaidi et al. 2019). However, small artefacts on the sample surface reminded of biofilm fragments and some holes, primarily from the samples incubated on the surface of the agricultural soil, appeared to be similar to the ones formed by microbial activity on PBST or PBAT samples (Heidarzadeh et al. 2017, Oliveira et al. 2019).

Concluding, a rough surface on all sample surface was revealed by comparing SEM images, which suggested hydrolytic and enzymatic activity. Effects of the superficial alterations on the material properties are to be further discussed.

5.4 Mechanical properties

Mechanical properties of the sample strips were determined with a tension test. Results showed an elastic modulus Et of 61.0 $\pm$ 7.5 MPa, 96.2 $\pm$ 8.9 MPa and 802.8 $\pm$ 93.6 MPa for PBST, PBAT and PHA, respectively. Changes in the measurement values were compared relatively along the course of the incubation, since the mechanical properties can vary based on the manufacturing process. The elastic modulus of PBST samples showed the first decrease

after six weeks following the previous findings of material alteration of PBST samples, particularly in agricultural soil. Therefore, following the theory of bulk degradation, the elastic modulus first slowly decreased and then dropped towards zero (Laycock et al. 2017). For an application as biodegradable mulch film compound, PBST would only suit a short-term use due the fast decline of material strength.

In contrast, the elastic modulus of PBAT further increased during the incubation. This phenomenon may be possible due to infiltrated water molecules that led to more stable chain packing of amorphous regions (Tsuji 2002). Here, the difference between the soil types was negligible although the surface images had shown different surface alterations.

The measurement values of the PHA strips varied strongly not only between the measurement dates, but also between the replicates resulting in high standard deviations. This may be the reason for the decreased and increased results of the elastic modulus after the incubation for samples from regular and agricultural soil, respectively. Generally, PHA is said to feature high mechanical strength (Lee et al. 2022).

Tensile strength results of the samples at start were 19.7 ± 11.3 MPa, 8.2 ± 0.4 MPa and 23.7 ± 0.7 MPa for PBST, PBAT and PHA, respectively. A fast decrease of the tensile strength was reported for PBST samples after just one week of incubation in contrast to the elastic modulus that seemed to remain stable for the first five weeks. Thus, this mechanical property was the first indication revealing a change of the material due to the incubation in soil even before macroscopic changes were visible on the sample surface. This fast and unanticipated transition is correlated with abiotic factors influencing the polymeric structure (Lucas et al. 2008).

The measured tensile strength of the PBAT samples experienced no deviation during the whole incubation time. Similarly, the tensile strength measured during a degradation study with intense UV-radiation remained stable during the first 120 days, but then dropped quickly (Tang et al. 2021). Probably the incubation period was too short to affect the mechanical properties of the material. Further, the influence of UV photodegradation on PBAT has been described as relevant abiotic factor for disintegration (Kijchavengkul et al. 2008).

Throughout the incubation, no change of the mechanical properties of the PHA strips was observed what seemed likely due to the high molecular weight of the sample. Further, PHAs tend to be highly crystalline which, firstly, makes it difficult for water to infiltrate the material

and, secondly, offers less chances for enzymes to attack, because enzymatic degradation takes place preferably in amorphous regions (Chanprateep et al. 2006, Deroiné et al. 2014). Interestingly, similar findings were made by Hermida et al. (2009) reporting a stable elastic modulus and a constant percentage of crystallinity during degradation. Thus, a decrease in tensile strength was observed, but the reduced cross-sectional area from surface erosion was not considered. Therefore, the mechanical properties remained unchanged what would make the material suited for field applications that demand consistent stability (Hermida et al. 2009).

To sum up, the changing tensile strength of the PBST samples was the first indication of material alteration whilst the mechanical properties of PBAT and PHA samples remained stable.

5.5 Thermal properties

The glass transition temperature, the crystallization temperature and the melting temperature of the samples were measured according to the sampling plan. Interestingly, the incubation temperature of 23 °C exceeded the glass transition temperature of all materials what implies a rubbery state of the materials with disorganized polymer chains that are more prone to degradation (Iovino et al. 2008).

Measured glass temperatures of PBST samples were -36.1 ± 1.6 °C at start which was convenient compared to literature with values between -28 °C and -39 °C depending on the ratio of poly(butylene-sebacate) and poly(butylene-terephthalate) (Heidarzadeh et al. 2017). Similarly, the measured glass transition temperature of -30.4 ± 2.1 °C for PBAT samples at start was in accordance compared to literature values of -30 °C (Bordes et al. 2009). During the incubation, the measurement values of PBST and PBAT only increased slightly, particularly in samples incubated in the agricultural soil. However, the glass transition temperature typically decreases with decreasing molecular weight because random chain scission during hydrolytic degradation leads to free moving polymer chains (Laycock et al. 2017). Therefore, the background of the temperature shift may arose from any sort of biofilm formation on the sample surface interfering with the DSC measurement.

The glass transition temperature of the PHA samples was -2.0 ± 4.4 °C at start and met reference values from literature with -2 °C (Lee et al. 2022). Interestingly, the glass transition temperature decreased by 3 K although several deviations were observed during the

incubation time. However, it is questionable if the PHA samples experienced a slow form of hydrolysis what affected the molecular weight and the glass transition temperature, respectively, since no other forms degradation were observed and standard deviation was relatively high.

In contrast, the measurements of the crystallization temperature of the samples showed more change during the course of the incubation. Generally, changing crystallinity during degradation further influences the degradation rate as well as the mechanical properties (Laycock et al. 2017). The PBST samples, which had shown distinct changes in tensile strength, showed a crystallization temperature at start of 33 °C which fits to the range of a 50 % / 50 % molar ratio of poly(butylene-sebacate) and poly(butylene-terephthalate) co-polymers (Heidarzadeh et al. 2017, S.J. Kim et al. 2020). The molar ratio would further indicate a degree of crystallinity of around 10 %, hence supporting the fast degradation of the material due to a highly amorphous structure being preferential for abiotic and biotic degradation (S.J. Kim et al. 2020, Laycock et al. 2017). However, only PBST samples from the surface of the agricultural soil expressed an increased crystallization temperature at the end of the incubation because the crystallization temperature of the buried samples increased first but decreased towards the end.

The measurement of the PBAT samples before the incubation showed a crystallization temperature of 39 °C. In contrast to the other material properties, the crystallization temperature could not be approved by literature values with clearly higher temperatures of 60 °C (Jian et al. 2020), 74 °C (Tang et al. 2021) and 80 °C (Weng et al. 2013). It is possible that the exact same molar ratio of the poly(butylene-adipate) (PBA) and poly(butylene-terephthalate) (PBT) from the used sample was not similar to the molar ratio in literature. Nevertheless, the crystallization temperature of all PBAT samples remained unchanged during the whole incubation period indicating no molecular changes.

The measured crystallization temperature of the PHA samples of 52 °C was also found in literature with a slightly higher temperature of 56 °C (Lee et al. 2022). Interestingly, the incubation led to vaguely decreased crystallization temperatures of the samples incubated in regular soil. However, the highest deviation between the sampling weeks was also found for the PHA samples.

Despite expectations, no substantial decrease of the crystallization temperature was found in any sample as it was recorded from Santonja-Blasco et al. (2013) that the crystallization temperature of different poly(lactide)s decreased and even disappeared during degradation.

Some more variation during the incubation course was found in the results of the melting temperature. Starting at 109.4 ± 0.8 °C for PBST, similar values of the melting temperature between 106 °C and 112 °C were found assuming a 50 % / 50 % molar fraction of poly(butylene-sebacate) and poly(butylene-terephthalate) (Heidarzadeh et al. 2017, S.J. Kim et al. 2020). Additionally, a second melting temperature of 42 °C was manifested by literature and a change of the heat flow around 47 °C was also found in the measurement (Heidarzadeh et al. 2017). This thermal behavior supported the previously described molar ratio that led to the complex melting range. After the incubation period, all samples exhibited increased melting points of 3 – 10 K, pointing out the influence of the agricultural soil on the surface samples.

The melting temperature for PBAT samples at start was 116.3 ± 0.4 °C what matched with information from literature between 110 °C and 121 °C (Bordes et al. 2009, Tang et al. 2021). Overall, the melting temperature increased during the incubation by 3 – 4 K, but no specific trend was found. Further, a second melting range was discovered around 47 °C which raised up to 51 °C after the incubation period. This behavior represents the two aliphatic and aromatic phases evolving from the poly(butylene-adipate) and poly(butylene-terephthalate) structures of a 50 % / 50 % molar ratio of the polymers (H. Kim et al. 2020). Similarly, the shift of the melting point during the incubation was also discovered by Weng et al. (2013) with PBAT samples incubated in soil for four months. It was seen that the carbon content of the samples decreased while the oxygen content increased indicating chain cleavage and formation of carboxyl groups. Although no differences of the infrared measurement of the functional groups were found, degradation of the samples was assumed due to visual and thermal examination.

Furthermore, the melting temperature of the PHA samples was found to be 163.5 ± 0.7 °C before the incubation started. Because of different possible ratios of poly(3-hydroxybutyrate) and poly(3-hydroxyhexanoate) in the polymer, a molar ratio of 10 – 15 % poly(3-hydroxyhexanoate) was assumed, which implied a similar melting temperature (Volova et al. 2013). However, the melting temperature of all PHA samples remained stable throughout the

incubation period, what matches with the results from Gil-Castell et al. (2020) where PHA samples were incubated for 90 days at 25 °C in soil without change of thermal properties.

Lastly, the measured melting enthalpy of the samples was intended to be used to calculate the material crystallinity as it plays an active role for biotic and abiotic degradation. Crystalline spheres are less permeable for water and less prone to enzymatic attacks due to the dense arrangement of polymer chains. Therefore, hydrolysis and enzyme activity are slowed down in these areas (Laycock et al. 2017). Further, depending on the crystallinity, bulk eroding materials can underly surface erosion when crystalline areas are too persistent. However, relative crystallinity could not be calculated due to varying baselines of the heat flow during DSC measurement that resulted in insufficiently integrated peaks (see Appendix Figure 28 and Figure 30). When comparing (with reservations) the melting enthalpies, an increase in PBST and PBAT samples was observed during the incubation while PHA samples showed a stable or even decreasing melting enthalpy indicating a stagnation or decrease in crystallinity, respectively. Beforehand, it was expected that the crystallinity increases when amorphous regions are degraded and crystalline regions remain. Crystallinity of the polymers according to literature was 15 % for PBST, 18 % for PBAT and 55 % for PHA, respectively (Farrag et al. 2022, Feng et al. 2022, Palsikowski et al. 2017). To improve the crystallinity measurement X-ray diffraction (XRD) could be used in following experiments.

In conclusion, thermal properties of the samples were similar to reference values from literature. Some minor variations may arose from residues on the sample surface, but generally the measurement values showed stability during the incubation what was also seen in comparable studies.

5.6 Molecular weight

Results from gel permeation chromatography were compared between start and end of the incubation to directly examine the effect of the soil and incubation types on the different polymer samples. Changes most likely are a result of bond cleavage due to hydrolysis or enzymatic attacks (Lucas et al. 2008). The molecular weight of the PBST and PBAT samples with 75,200 g / mol and 62,820 g / mol, respectively, was almost similar while the molecular weight of the PHA sample with 293,000 g / mol was more than four times higher. As a simple rule, the lower the molecular weight, the faster the degradation of a polymer, because it takes less steps

to reduce the molecular weight according chain length significantly to be taken up by microorganisms (Lucas et al. 2008).

Unexpectedly, the PBST strips showed no decrease of the molecular weight above the 10 % measurement error despite losing integrity and tensile strength the most while the buried rectangular samples showed a decrease of the molecular weight up to -18 %. Furthermore, the samples that were incubated in the agricultural soil showed more surface alterations but the samples from the regular topsoil expressed a lower molecular weight at the end. Compared to the degradation in a hydrolytic medium, the decrease of the molecular weight seemed to proceed very slowly. However, a comparable study used a PBST polymer with only a tenth of the molecular weight (6,700 g / mol), what was favorable for hydrolysis (Heidarzadeh et al. 2017). Consequently, the PBST samples may have been affected by enzymatic attacks mainly on the surface since the molecular weight remained stable when incubated on the soil surface with only one side exposed to the soil but decreased when buried in the soil with both sides contacting the soil.

The measurement of the PBAT samples showed no significant decrease in molecular weight of any sample form. As photodegradation plays an important role in polymer ageing of PBAT, a study of the photodegradability of PBAT samples with a similar molecular weight was compared. It was found out that the molecular weight only decreased by 13.5 % after 120 days of exposure under direct sunlight (Tang et al. 2021). Therefore, PBAT with a similar range of the molecular weight seems to be relatively durable under certain environmental conditions. Nevertheless, a study with lower molecular weight (23,000 g / mol) and incubation in soil interestingly revealed a quickly decreasing molecular weight where 30 days were enough to lower the molecular weight by more than 50 % (Palsikowski et al. 2017). However, the degradation of PBAT polymers in soil was found to occur mainly on the sample surface caused by enzymes (Palsikowski et al. 2017). Consequently, the molecular weight and mechanical properties remained stable following the idea of the surface erosion model, although the bulk erosion model was expected (Von Burkersroda et al. 2002). In terms of future applications, either the molecular weight or the sample thickness should be reduced to improve the disintegration behavior. Further, instead of solely following the molecular weight, the mass of the samples could also be noted before and after the incubation to examine potential weight loss according to bulk or surface erosion (Laycock et al. 2017).

Despite not showing changes of the mechanical properties and only developing a rough surface under SEM observation, the PHA samples showed the highest decrease in molecular weight after the incubation. Overall, the decrease was higher in samples from the agricultural soil with the highest (-28 %) when buried in the agricultural soil. A comparable study with a smaller molecular weight at start (122,000 g / mol) showed a 40 % decrease of the molecular weight during soil incubation for 90 days (Gil-Castell et al. 2020). It was noted that the determination of the molecular weight was crucial for the observation of the degradation process since other methods like surface imaging and thermal properties led to mixed results (Gil-Castell et al. 2020). Generally, PHAs show a wide range of molecular weight since the polymers can be produced by bacteria that use them as storage molecules. Thereby the chain length can be influenced by the carbon source of the bacteria, as well as the cultivation period and the extraction method (Volova et al. 2013). The variation of molecular weight impedes the comparison of degradation because a high molecular weight will affect abiotic as well as biotic degradation (Laycock et al. 2017). However, a high molecular weight sometimes is required for suitable mechanical properties although it results in slower degradation (Jaisankar et al. 2010).

Poly(3-hydroxybutyrate-co-3-hydroxyvalerate) (PHBV) is a related polymer to the used PHA and differs by one less carbon group in the side chain. For comparison, degradation tests in sand of a PHBV sample with related molecular weight of 259,000 g / mol were conducted by Deroiné et al. (2015). Measurements after 100 days of incubation revealed a decrease of the molecular weight by 30 %. Further, similarities in the surface morphology were also observed. The authors suggested that bulk erosion may not be the main degradation pathway, but enzymatic activity might play a bigger role (Deroiné et al. 2015).

In summary, the molecular weight of all samples was relatively high compared to other degradation studies. Unexpectedly, PBST and PBAT samples showed no remarkable decrease, but PHA samples showed a decrease up to -28 % after incubation. It was suggested that superficial enzymatic attack was the reason for the stable molecular weight.

5.7 Functional groups

The comparison of the recorded infrared spectra, surprisingly, only showed minor changes of the bands. It was expected that the spectrum of the samples changes with ongoing incubation due to chemical modifications by enzymes on the sample surface. However, the recorded

spectra at start were checked with bands and peaks in literature (S.J. Kim et al. 2020, Tavares et al. 2018, Volova et al. 2013). For simplification, three representative spectra of the samples after the incubation were evaluated.

Changes of the PBST spectra showed the uptake of -OH groups as well as the presence of carboxyl groups that are connected to hydrogen bonds. Further, the carbonyl peak decreased slightly, but showed no additional shoulder. Consequently, the suggested enzymatic activity may have altered the chemical structure on the surface leading to exposed functional acid groups of the chain ends (Shah et al. 2008).

Similar to the stable mechanical and thermal properties, the infrared spectra of the PBAT samples showed almost no differences compared to the reference spectra. Only a few bands between 1500 cm^{-1} and 1350 cm^{-1} and around 870 cm^{-1} increased absorbance. Interestingly, Tavares et al. (2018) reported similar behavior of PBAT samples buried in soil. Accordingly, the degradation of the material was very slow and no products of chain cleavage were measured on the sample surface (Hamad et al. 2014, Palsikowski et al. 2017).

The measurement of the PHA samples showed no difference to the reference spectra at start. In a PHBV degradation study in sewage sludge similar behavior was observed (Gutierrez-Wing et al. 2010).

Finally, the infrared spectra were compared with literature information. However, the incubation promoted merely changed spectra for PBST indicating exposed acidic chain ends. In contrast, PBAT and PHA showed no remarkable changes of the functional groups.

6 Conclusion

This work investigated the disintegration behavior of three different polymer types that can be processed as a biodegradable mulch film compound. Therefore, film like samples were pressed and either incubated on the soil surface to imitate the application of a mulch film on the soil during service life or fixed in a film holder and buried in the soil compared to being plowed into the soil after use. Two types of soil were used to compare the influence of the soil type: Regular topsoil and a mix of regular topsoil and soil from an agricultural test field for biodegradability studies to reconstruct natural conditions. During the incubation of 16 weeks, the samples of PBST, PBAT and PHA showed a different speed of changes in morphology, mechanical and thermal properties as well as corresponding functional groups and molecular weight.

Generally, discolorations on all sample surfaces occurred already after the first week of incubation. PBST samples incubated on the soil surface continuously developed cracks already after four weeks resulting in a completely altered surface at the end of the study. Simultaneously, the tensile strength dropped after the first week of incubation and drifted towards zero. In contrast, samples of PBAT and PHA only developed superficial surface modifications like pitting that was observed with SEM. Thermal properties and infrared spectra of functional groups remained almost constant under all conditions but, interestingly, the only decline in molecular weight was found in PHA samples.

When comparing the obtained results to other studies about biodegradable plastics, firstly, the small amount of literature for PBST and, secondly, the experimental framework with its incubation and material parameters were limiting. While general theories about the steps of biodegradation are established, the observed results sometimes mismatched these models. As a consequence, the disintegration behavior of PBST, PBAT and PHA in soil needs to be further examined.

Comparing the three polymers for their potential application as biodegradable mulch film compound, a high percentage of PBST may be used for short-term application due to its quick fragmentation, PBAT may be used for short-term application as well since it is said to disintegrate faster under the influence of UV-radiation and PHA may be installed for medium-term application, because it brings along a high degree of stability. With this, a variable share

of PBST / PHA or PBAT / PHA in a compound for mulch films may facilitate processability and lead to desired biologic stability.

Along with the different speed of material alteration came the difficulty to evaluate the measurement values according to the different steps of biodegradation. It was found that results from visual examination and tensile test were important first indications for material change, therefore being essential for evaluating the behavior of the polymers. Further, the determination of the molecular weight was relevant to differ between shallow and profound material alterations.

Differences between surface incubation and soil incubation were difficult to point out. Generally, it seemed like the incubation on the soil surface led to more modifications on the sample surface while the incubation in the soil promoted the decrease of the molecular weight. Because of the rectangular sample design when buried in the soil, mechanical tests of the samples could not be conducted. Hence, information on the mechanical performance was missing what could be ameliorated with a different sample form.

Following, the influence of the soil type referring to the microbiological activity was difficult to determine, but generally it seemed like the exposure to the agricultural soil promoted faster material transformations. Additionally, experiments of enriched bacteria cultures could be useful for future experiments.

The present study was set up under temporal limitations and, therefore, the measurements were conducted according to the sampling plan. Consequently, measurement values sometimes were taken before clear evidence of abiotic or biotic influences was observed in all samples. Hence, the time frame of 16 weeks was too short to establish full models on the disintegration behavior of the tested polymers. Especially, the high molecular weight and comparatively thick sample morphology may have influenced the behavior of the materials.

Lastly, the stable incubation conditions were optimized to promote a fast disintegration of the test samples. Natural field conditions, however, would underly certain variations of soil humidity, temperature and pH. Further factors affecting the material stability like UV-radiation, mechanical stress and significant temperature changes between day and night were not tested but could show relevance. Also, different soil types containing different influential microbial communities should be further investigated.

7 Literature

Directive 2008/98/EC of the European Parliament and of the European Council of 19 November 2008 on waste, consolidated text from 05/07/2018.

Amobonye, A., Bhagwat, P., Singh, S., & Pillai, S. (2021). Plastic biodegradation: Frontline microbes and their enzymes. Science of The Total Environment, 759, 143536. doi:https://doi.org/10.1016/j.scitotenv.2020.143536.

ASTM. (2012). D6400-12 Standard Specification for Labeling of Plastics Designed to be Aerobically Composted in Municipal or Industrial Facilities. American Society for Testing and Materials.

Auras, R., Harte, B., & Selke, S. (2004). An Overview of Polylactides as Packaging Materials. Macromolecular Bioscience, 4(9), 835-864. doi:https://doi.org/10.1002/mabi.200400043.

Bandopadhyay, S., Martin-Closas, L., Pelacho, A., & DeBruyn, J. (2018). Biodegradable Plastic Mulch Films: Impacts on Soil Microbial Communities and Ecosystem Functions. Frontiers in Microbiology, 9, 819. doi:10.3389/fmicb.2018.00819.

Bonhomme, S., Cuer, A., Delort, A., Lemaire, J., Sancelme, M., & Scott, G. (2003). Environmental biodegradation of polyethylene. Polymer Degradation and Stability, 81(3), 441-452. doi:https://doi.org/10.1016/S0141-3910(03)00129-0.

Bordes, P., Pollet, E., & Avérous, L. (2009). Nano-biocomposites: Biodegradable polyester/nanoclay systems. Progress in Polymer Science, 34(2), 125-155. doi:https://doi.org/10.1016/j.progpolymsci.2008.10.002.

Briassoulis, D. (2005). The effects of tensile stress and the agrochemical Vapam on the ageing of low density polyethylene (LDPE) agricultural films. Part I. Mechanical behaviour. Polymer Degradation and Stability, 88(3), 489-503. doi:10.1016/j.polymdegradstab.2004.11.021.

Briassoulis, D., & Degli Innocenti, F. (2017). Standards for Soil Biodegradable Plastics. In *Soil Degradable Bioplastics for a Sustainable Modern Agriculture* (pp. 139-168). Springer Berlin Heidelberg. https://doi.org/10.1007/978-3-662-54130-2_6

Bucknall, D. (2020). Plastics as a materials system in a circular economy. Philosophical Transactions of the Royal Society A: Mathematical, Physical and Engineering Sciences, 378(2176), 20190268. doi:10.1098/rsta.2019.0268.

CDC. (2022). *Hourly station observations of soil temperature at the depth of 5 cm in °C for Germany, version v21.3*. DWD Climate Data Center. Retrieved 28.03.2023 from

Chanprateep, S., Shimizu, H., & Shioya, S. (2006). Characterization and enzymatic degradation of microbial copolyester P(3HB-co-3HV)s produced by metabolic reaction model-based system. Polymer Degradation and Stability, 91(12), 2941-2950. doi:https://doi.org/10.1016/j.polymdegradstab.2006.08.024.

Chivrac, F., Kadlecova, Z., Pollet, E., & Avérous, L. (2006). Aromatic Copolyester-based Nano-biocomposites: Elaboration, Structural Characterization and Properties. J. Polym. Environ, 14, 393-401. doi:10.1007/s10924-006-0033-4.

De Wilde, B., Mortier, N., Tosin, M., Pognani, M., & Degli Innocenti, F. (2016). Opening bio-based markets via standards, labelling and procurement. Environmental safety of biodegradation residuals of polymers. Retrieved 15 January 2023, from https://www.biobasedeconomy.eu/projects/open-bio/

Deroiné, M., César, G., Duigou, A., Davies, P., & Bruzaud, S. (2015). Natural Degradation and Biodegradation of Poly (3-Hydroxybutyrate-co-3-Hydroxyvalerate) in Liquid and Solid Marine Environments. Journal of Polymers and the Environment.

Deroiné, M., Le Duigou, A., Corre, Y., Le Gac, P., Davies, P., César, G., & Bruzaud, S. (2014). Accelerated ageing and lifetime prediction of poly(3-hydroxybutyrate-co-3-hydroxyvalerate) in distilled water. Polymer Testing, 39, 70-78. doi:https://doi.org/10.1016/j.polymertesting.2014.07.018.

Dilkes-Hoffman, L., Pratt, S., Lant, P., & Laycock, B. (2019). 19 - The Role of Biodegradable Plastic in Solving Plastic Solid Waste Accumulation. In S. M. Al-Salem (Ed.), *Plastics to Energy* (pp. 469-505). William Andrew Publishing. https://doi.org/https://doi.org/10.1016/B978-0-12-813140-4.00019-4

DIN. (2003). DIN EN ISO 527-3 Bestimmung der Zugeigenschaften Teil 3: Prüfbedingungen fur Folien und Tafeln. Deutsches Institut für Normung.

DIN. (2012). DIN EN ISO 527-1 Bestimmung der Zugeigenschaften Teil 1: Allgemeine Grundsätze. Deutsches Institut für Normung.

DWD. (2023). Klimastatusbericht Deutschland Jahr 2022. Deutscher Wetterdienst, Geschäftsbereich Klima und Umwelt, Offenbach, 27. https://www.dwd.de/DE/leistungen/klimastatusbericht/klimastatusbericht.html

El-Hadi, A., Schnabel, R., Straube, E., Müller, G., & Henning, S. (2002). Correlation between degree of crystallinity, morphology, glass temperature, mechanical properties and biodegradation of poly (3-hydroxyalkanoate) PHAs and their blends. Polymer Testing, 21(6), 665-674. doi:https://doi.org/10.1016/S0142-9418(01)00142-8.

Emadian, S., Onay, T., & Demirel, B. (2017). Biodegradation of bioplastics in natural environments. Waste Management, 59, 526-536. doi:10.1016/j.wasman.2016.10.006.

EUBP. (2022). *Fact sheet: What are bioplastics? Material types, terminology, and labels - an introduction*. European Bioplastics e.V. Retrieved 07.02.2023 from https://docs.european-bioplastics.org/publications/fs/EuBP_FS_What_are_bioplastics.pdf

FAO. (2021). Assessment of agricultural plastics and their sustainability - A call for action. FAO Food and Agriculture Organization of the United Nations, Rome, 160.

Farrag, Y., Barral, L., Gualillo, O., Moncada, D., Montero, B., Rico, M., & Bouza, R. (2022). Effect of Different Plasticizers on Thermal, Crystalline, and Permeability Properties of Poly(3-hydroxybutyrate-co-3-hydroxyhexanoate) Films. *Polymers*, *14*(17).

Feng, Y., Li, Y., Almalki, A., Meng, X., Alhadhrami, A., Ye, X., Ibrahim, M., Guo, X., Algadi, H., Huang, M., Winchester, W., & Wang, Z. (2022). Synthesis and characterization of poly(butanediol sebacate-butanediol) terephthalate (PBSeT) reinforced by hydrogen bond containing amide group, with good mechanical properties and improved water vapor barrier. Advanced Composites and Hybrid Materials, 5(3), 2051-2065. doi:10.1007/s42114-022-00542-y.

Francioni, M., Kishimoto-Mo, A., Tsuboi, S., & Hoshino, Y. (2021). Evaluation of the mulch films biodegradation in soil: a methodological review. Italian Journal of Agronomy. doi:10.4081/ija.2021.1936.

Gao, H., Yan, C., Liu, Q., Ding, W., Chen, B., & Li, Z. (2019). Effects of plastic mulching and plastic residue on agricultural production: A meta-analysis. Science of The Total Environment, 651, 484-492. doi:https://doi.org/10.1016/j.scitotenv.2018.09.105.

Ghosh, K., & Jones, B. (2021). Roadmap to Biodegradable Plastics—Current State and Research Needs. ACS Sustainable Chemistry & Engineering, 9(18), 6170-6187. doi:10.1021/acssuschemeng.1c00801.

Gil-Castell, O., Andres-Puche, R., Dominguez, E., Verdejo, E., Monreal, L., & Ribes-Greus, A. (2020). Influence of substrate and temperature on the biodegradation of polyester-based materials: Polylactide and poly(3-hydroxybutyrate-co-3-hydroxyhexanoate) as model cases. Polymer Degradation and Stability, 180, 109288. doi:https://doi.org/10.1016/j.polymdegradstab.2020.109288.

Gutierrez-Wing, M., Stevens, B., Theegala, C. S., Negulescu, I., & Rusch, K. (2010). Anaerobic biodegradation of polyhydroxybutyrate in municipal sewage sludge. Journal of Environmental Engineering, 136(7), 709-718.

Hamad, K., Kaseem, M., Ko, Y., & Deri, F. (2014). Biodegradable polymer blends and composites: An overview. Polymer Science Series A, 56(6), 812-829. doi:10.1134/S0965545X14060054.

Heidarzadeh, N., Rafizadeh, M., Taromi, F., del Valle, L., Franco, L., & Puiggalí, J. (2017). Biodegradability and biocompatibility of copoly(butylene sebacate-co-terephthalate)s. Polymer Degradation and Stability, 135, 18-30. doi:https://doi.org/10.1016/j.polymdegradstab.2016.11.013.

Hermida, É., Yashchuk, O., & Miyazaki, S. (2009). Changes in the mechanical properties of compression moulded samples of poly(3-hydroxybutyrate-co-3-hydroxyvalerate) degraded by Streptomyces omiyaensis SSM 5670. Polymer Degradation and Stability, 94(2), 267-271. doi:https://doi.org/10.1016/j.polymdegradstab.2008.10.019.

Iovino, R., Zullo, R., Rao, M., Cassar, L., & Gianfreda, L. (2008). Biodegradation of poly(lactic acid)/starch/coir biocomposites under controlled composting conditions. Polymer Degradation and Stability, 93(1), 147-157. doi:https://doi.org/10.1016/j.polymdegradstab.2007.10.011.

ISO. (2021a). ISO 16929 Plastics — Determination of the degree of disintegration of plastic materials under defined composting conditions in a pilot-scale test. International Organization for Standardization.

ISO. (2021b). ISO 17088 Plastics — Organic recycling — Specifications for compostable plastics. International Organization for Standardization.

Jaisankar, V., Nanthini, R., Muruganandam, K., & Ravi, A. (2010). Study on Biodegradable Random Copolyesters Derived From 1,4-Butane Diol, Terephthalic Acid and Adipic Acid/Sebacic Acid. Asian Journal of Chemistry, 22, 5077-5085.

Jian, J., Xiangbin, Z., & Xianbo, H. (2020). An overview on synthesis, properties and applications of poly(butylene-adipate-co-terephthalate)–PBAT. Advanced Industrial and Engineering Polymer Research, 3(1), 19-26. doi:https://doi.org/10.1016/j.aiepr.2020.01.001.

Johnson, M., & Fennimore, S. (2005). Weed and Crop Response to Colored Plastic Mulches in Strawberry Production. HortScience HortSci, 40(5), 1371-1375. doi:10.21273/HORTSCI.40.5.1371.

JoVE. (2023). *Bestimmung des Feuchtigkeitsgehalts im Boden*. JoVE Science Education Database. Retrieved 14.04.2023 from https://www.jove.com/de/t/10011

Kasirajan, S., & Ngouajio, M. (2012). Polyethylene and biodegradable mulches for agricultural applications: a review. Agronomy for Sustainable Development, 32(2), 501-529. doi:10.1007/s13593-011-0068-3.

Kijchavengkul, T., Auras, R., Rubino, M., Ngouajio, M., & Fernandez, R. (2008). Assessment of aliphatic–aromatic copolyester biodegradable mulch films. Part II: Laboratory simulated conditions. Chemosphere, 71(9), 1607-1616. doi:https://doi.org/10.1016/j.chemosphere.2008.01.037.

Kim, H., Kim, T., Choi, S., Jeon, H., Oh, D., Park, J., Eom, Y., Hwang, S., & Koo, J. (2020). Remarkable elasticity and enzymatic degradation of bio-based poly(butylene adipate-co-furanoate): replacing terephthalate [10.1039/D0GC01688H]. Green Chemistry, 22(22), 7778-7787. doi:10.1039/D0GC01688H.

Kim, S. J., Kwak, H., Kwon, S., Jang, H., & Park, S. (2020). Synthesis, Characterization and Properties of Biodegradable Poly(Butylene Sebacate-Co-terephthalate). Polymers (Basel), 12(10). doi:10.3390/polym12102389.

Koenders, E., Weise, K., & Vogt, O. (2020). Kunststoffe. In E. Koenders, K. Weise, & O. Vogt (Eds.), *Werkstoffe im Bauwesen: Einführung für Bauingenieure und Architekten* (pp. 245-260). Springer Fachmedien Wiesbaden. https://doi.org/10.1007/978-3-658-32216-8_4

Laycock, B., Nikolić, M., Colwell, J., Gauthier, E., Halley, P., Bottle, S., & George, G. (2017). Lifetime prediction of biodegradable polymers. Progress in Polymer Science, 71, 144-189. doi:10.1016/j.progpolymsci.2017.02.004.

Lee, J., Hikima, Y., Sekiguchi, T., & Ohshima, M. (2022). Thermal, rheological, and mechanical properties of cellulose nanofiber (CNF) and poly(3-hydroxybutyrate-co-3-hydroxyhexanoate) (PHBH) biopolymer nanocomposites. Cellulose, 29(7), 3901-3913. doi:10.1007/s10570-022-04539-0.

Lim, D., & Park, S. (2023). Solid State Polymerization of Biodegradable Poly(butylene sebacate-co-terephthalate): A Rapid, Facile Method for Property Enhancement. *Polymers*, *15*(5).

Lucas, N., Bienaime, C., Belloy, C., Queneudec, M., Silvestre, F., & Nava-Saucedo, J. (2008). Polymer biodegradation: mechanisms and estimation techniques. Chemosphere, 73(4), 429-442. doi:10.1016/j.chemosphere.2008.06.064.

Malinconico, M. (2017). Soil Degradable Bioplastics for a Sustainable Modern Agriculture (1. Ed.). Springer Verlag, Heidelberg, 185. https://doi.org/10.1007/978-3-662-54130-2

Mansoor, Z., Tchuenbou-Magaia, F., Kowalczuk, M., Adamus, G., Manning, G., Parati, M., Radecka, I., & Khan, H. (2022). Polymers Use as Mulch Films in Agriculture: A Review of History, Problems and Current Trends. Polymers, 14(23), 5062. https://www.mdpi.com/2073-4360/14/23/5062.

Martín-Closas, L., Costa, J., & Pelacho, A. (2017). Agronomic Effects of Biodegradable Films on Crop and Field Environment. In M. Malinconico (Ed.), *Soil Degradable Bioplastics for a Sustainable Modern Agriculture* (pp. 67-104). Springer Berlin Heidelberg. https://doi.org/10.1007/978-3-662-54130-2_4

Meereboer, K., Misra, M., & Mohanty, A. (2020). Review of recent advances in the biodegradability of polyhydroxyalkanoate (PHA) bioplastics and their composites. Green Chemistry, 22(17), 5519-5558. doi:10.1039/d0gc01647k.

Merck. (2023). *Product sheet: Poly((R)-3-hydroxybutyrate-co-(R)-3-hydroxyhexanoate)*. Merck KGaA. Retrieved 06.03.2023 from https://www.sigmaaldrich.com/deepweb/content/dam/sigma-aldrich/structure4/189/a_____915890.eps/_jcr_content/renditions/a_____915890-large.png

Moshood, T., Nawanir, G., Mahmud, F., Mohamad, F., Ahmad, M., & AbdulGhani, A. (2022). Sustainability of biodegradable plastics: New problem or solution to solve the global plastic pollution? Current Research in Green and Sustainable Chemistry, 5, 100273. doi:https://doi.org/10.1016/j.crgsc.2022.100273.

Oliveira, T., Oliveira Mota, I., Mousinho, F., Barbosa, R., Carvalho, L., & Alves, T. (2019). Biodegradation of mulch films from poly(butylene adipate co-terephthalate),

carnauba wax, and sugarcane residue. Journal of Applied Polymer Science, 136(47). doi:10.1002/app.48240.

Palsikowski, P., Kuchnier, C., Pinheiro, I., & Morales, A. (2017). Biodegradation in Soil of PLA/PBAT Blends Compatibilized with Chain Extender. Journal of Polymers and the Environment, 26(1), 330-341. doi:10.1007/s10924-017-0951-3.

PAPILLONS. (2021). *FAO report confirms microplastics cause damage to human cells*. Plastic in Agricultural Production: Impacts, Life-cylces and LONg-term Sustainability PAPILLONS. Retrieved 20.02.2023 from https://www.papillons-h2020.eu/news/fao-report-confirms-microplastics-cause-damage-to-human-cells/

Picuno, P. (2014). Innovative Material and Improved Technical Design for a Sustainable Exploitation of Agricultural Plastic Film. Polymer-Plastics Technology and Engineering, 53(10), 1000-1011. doi:10.1080/03602559.2014.886056.

Plastics Europe. (2022). *Plastics - the Facts 2022*. Plastics Europe Deutschland e.V. Retrieved 02.03.2023 from https://plasticseurope.org/knowledge-hub/plastics-the-facts-2022/

Post, W., Kuijpers, L., Zijlstra, M., van der Zee, M., & Molenveld, K. (2021). Effect of Mineral Fillers on the Mechanical Properties of Commercially Available Biodegradable Polymers. Polymers, 13(3), 394. https://www.mdpi.com/2073-4360/13/3/394.

Qi, Y., Ossowicki, A., Yang, X., Huerta Lwanga, E., Dini-Andreote, F., Geissen, V., & Garbeva, P. (2020). Effects of plastic mulch film residues on wheat rhizosphere and soil properties. J Hazard Mater, 387, 121711. doi:10.1016/j.jhazmat.2019.121711.

Qin, Q., Yang, Y., Yang, C., Zhang, L., Yin, H., Yu, F., & Ma, J. (2022). Degradation and adsorption behavior of biodegradable plastic PLA under conventional weathering conditions. Science of The Total Environment, 842, 156775. doi:https://doi.org/10.1016/j.scitotenv.2022.156775.

Reineke, W., & Schlömann, M. (2020). Mikrobielle Lebensgemeinschaften. Strukturelle und funktionelle Analysen mit klassischer Vorgehensweise. In W. Reineke & M. Schlömann (Eds.), *Umweltmikrobiologie* (pp. 417-441). Springer Berlin Heidelberg. https://doi.org/10.1007/978-3-662-59655-5_11

Samir, A., Ashour, F., Hakim, A., & Bassyouni, M. (2022). Recent advances in biodegradable polymers for sustainable applications. npj Materials Degradation, 6(1), 68. doi:10.1038/s41529-022-00277-7.

Santonja-Blasco, L., Ribes-Greus, A., & Alamo, R. (2013). Comparative thermal, biological and photodegradation kinetics of polylactide and effect on crystallization rates. Polymer Degradation and Stability, 98(3), 771-784. doi:https://doi.org/10.1016/j.polymdegradstab.2012.12.012.

Schettini, E., & Vox, G. (2010). Greenhouse Plastic Films Capable Of Modifying The Spectral Distribution Of Solar Radiation. Journal of Agricultural Engineering, 41(1), 19-24. doi:10.4081/jae.2010.1.19.

Schyns, Z., & Shaver, M. (2021). Mechanical Recycling of Packaging Plastics: A Review. Macromolecular Rapid Communications, 42(3), 2000415. doi:https://doi.org/10.1002/marc.202000415.

Shah, A., Hasan, F., Hameed, A., & Ahmed, S. (2008). Biological degradation of plastics: A comprehensive review. Biotechnology Advances, 26(3), 246-265. doi:https://doi.org/10.1016/j.biotechadv.2007.12.005.

Tang, D., Zhang, C., & Weng, Y. (2021). Effect of multi-functional epoxy chain extender on the weathering resistance performance of Poly(butylene adipate-co-terephthalate) (PBAT). Polymer Testing, 99, 107204. doi:https://doi.org/10.1016/j.polymertesting.2021.107204.

Tavares, L., Ito, N., Salvadori, M., dos Santos, D., & Rosa, D. (2018). PBAT/kraft lignin blend in flexible laminated food packaging: Peeling resistance and thermal degradability. Polymer Testing, 67, 169-176. doi:https://doi.org/10.1016/j.polymertesting.2018.03.004.

Tsuji, H. (2002). Autocatalytic hydrolysis of amorphous-made polylactides: effects of l-lactide content, tacticity, and enantiomeric polymer blending. Polymer, 43(6), 1789-1796. doi:https://doi.org/10.1016/S0032-3861(01)00752-2.

Velandia, M., Galinato, S., & Wszelaki, A. (2020). Economic Evaluation of Biodegradable Plastic Films in Tennessee Pumpkin Production. *Agronomy*, *10*(1).

Volova, T., Zhila, N., Shishatskaya, E., Mironov, P., Vasilev, A., Sukovatyi, A., & Sinskey, A. (2013). The physicochemical properties of polyhydroxyalkanoates with different chemical structures. Polymer Science Series A, 55(7), 427-437. doi:10.1134/S0965545X13070080.

Von Burkersroda, F., Schedl, L., & Göpferich, A. (2002). Why degradable polymers undergo surface erosion or bulk erosion. Biomaterials, 23(21), 4221-4231.

Vox, G., Loisi, R., Blanco, I., Mugnozza, G., & Schettini, E. (2016). Mapping of Agriculture Plastic Waste. Agriculture and Agricultural Science Procedia, 8, 583-591. doi:https://doi.org/10.1016/j.aaspro.2016.02.080.

Wang, K., Sun, X., Long, B., Li, F., Yang, C., Chen, J., Ma, C., Xie, D., & Wei, Y. (2021). Green Production of Biodegradable Mulch Films for Effective Weed Control. ACS Omega, 6(47), 32327-32333. doi:10.1021/acsomega.1c05725.

Wei, R., & Zimmermann, W. (2017). Microbial enzymes for the recycling of recalcitrant petroleum-based plastics: how far are we? [https://doi.org/10.1111/1751-7915.12710]. Microbial Biotechnology, 10(6), 1308-1322. doi:https://doi.org/10.1111/1751-7915.12710.

Weng, Y., Jin, Y., Meng, Q., Wang, L., Zhang, M., & Wang, Y. (2013). Biodegradation behavior of poly(butylene adipate-co-terephthalate) (PBAT), poly(lactic acid) (PLA), and their blend under soil conditions. Polymer Testing, 32(5), 918-926. doi:https://doi.org/10.1016/j.polymertesting.2013.05.001.

Xu, P., Cao, Y., Lv, P., Ma, P., Dong, W., Bai, H., Wang, W., Du, M., & Chen, M. (2018). Enhanced crystallization kinetics of bacterially synthesized poly(3-hydroxybutyrate-co-3-hydroxyhexanate) with structural optimization of oxalamide compounds as nucleators. Polymer Degradation and Stability, 154, 170-176. doi:https://doi.org/10.1016/j.polymdegradstab.2018.06.001.

Zaidi, Z., Mawad, D., & Crosky, A. (2019). Soil Biodegradation of Unidirectional Polyhydroxybutyrate-Co-Valerate (PHBV) Biocomposites Toughened With Polybutylene-Adipate-Co-Terephthalate (PBAT) and Epoxidized Natural Rubber (ENR). Frontiers in Materials, 6. doi:10.3389/fmats.2019.00275.

8 Appendix

Sample layout diagram

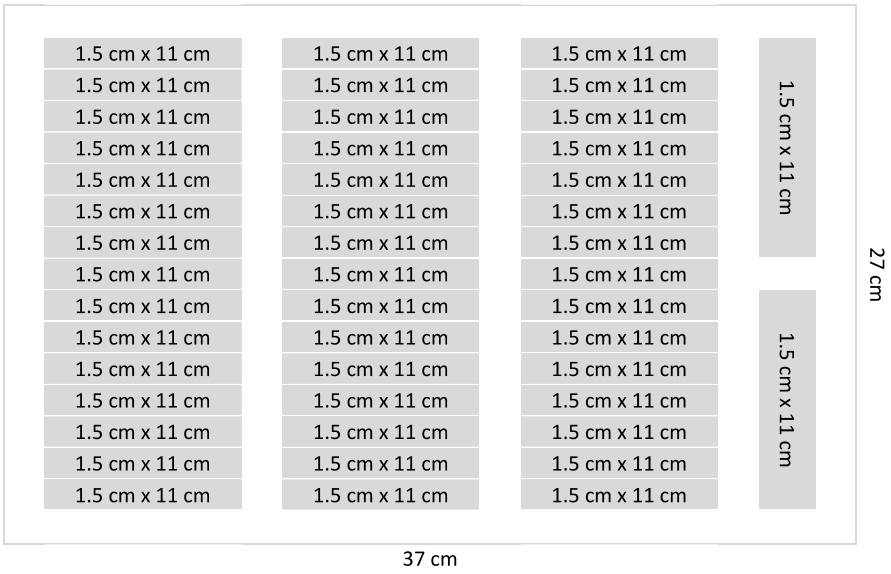

Figure 26: Layout diagram of the samples incubated on the soil surface (1.5 cm x 11 cm strips).

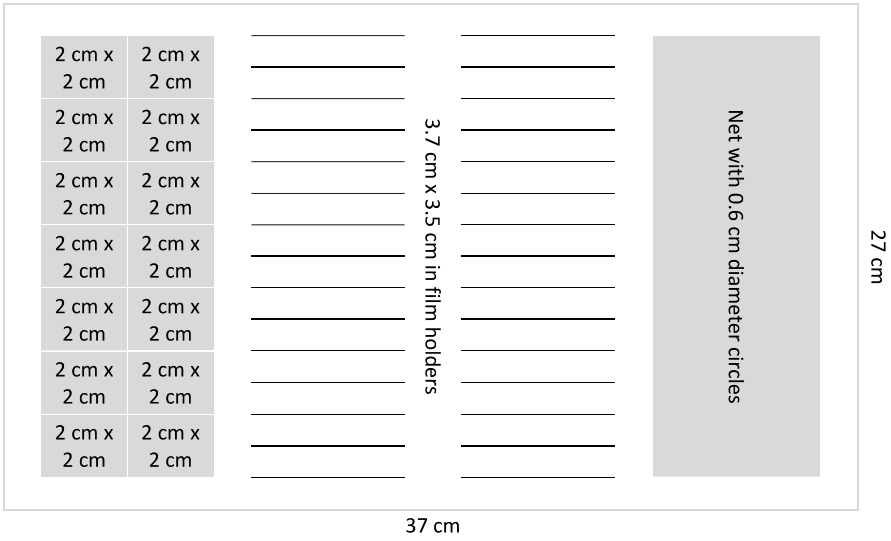

Figure 27: Layout diagram of the samples incubated on the soil surface (2 cm x 2 cm plates) and buried in the soil (3.7 cm x 3.5 cm rectangles fixed in film holders and 0.6 cm diameter circles collected in a net).

Sampling plan

Table 6: Measurement plan according to the sampling weeks. The samples were taken after one, two, four, six, eight, ten, twelve and 16 weeks. Abbreviations equal scanning electron microscopy (SEM), differential scanning calorimetry (DSC), gel permeation chromatography (GPC) and Fourier-transform infrared spectroscopy (FT-IR).

Week	0	1	2	4	6	8	10	12	16
Soil moisture	x	x	x	x	x	x	x	x	x
pH	x					x			x
Light microscopy	x	x	x	x	x	x	x	x	x
SEM	x	x	x	x	x	x	x	x	x
Tensile test	x	x	x	x	x	x	x	x	x
DSC	x	x	x	x	x	x	x	x	x
GPC	x								x
FT-IR	x								x

DSC temperature profile

Table 7: Overview of the temperature course during the measurement.

Mode	Final temperature °C	Temperature change K / min	Measurement points / min	Duration min
Start	25	-	-	-
Cool down	-60	10	600	9
Hold	-60	-	85.71	10
Heat up	200	10	600	26
Hold	200	-	600	3
Cool down	-60	10	600	26
Hold	-60	-	50	15
Heat up	200	10	600	26

Cool down	25	30	600	6
Hold	50	-	50	8

Exemplary DSC measurements

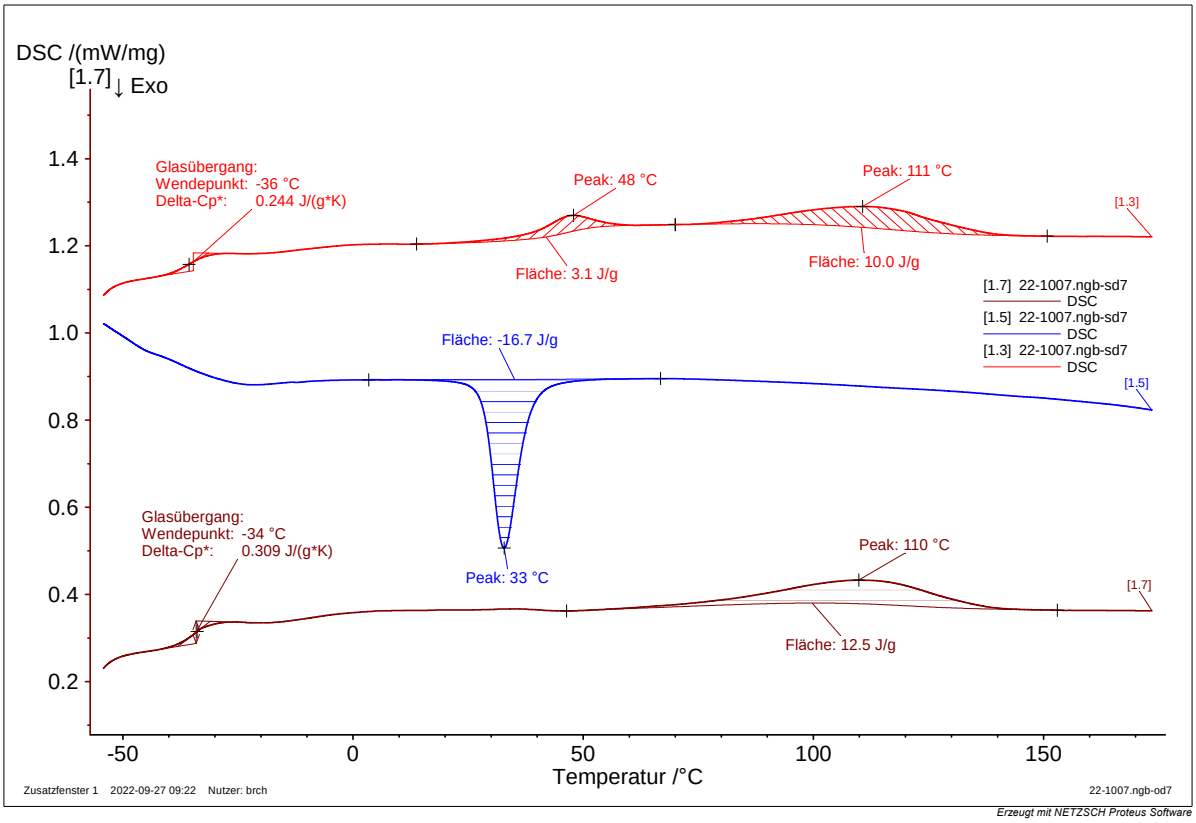

Figure 28: The diagram shows the heat flow of the sample chamber compared to the reference chamber according to the set temperature. Sample material were 5 mg of poly(butylene-sebacate-co-terephthalate) after one week of incubation. Due to the curved baseline, the peak areas corresponding to the melting enthalpy in both heating curves (1.3 and 1.7) were smaller than the crystallization enthalpy which is questionable.

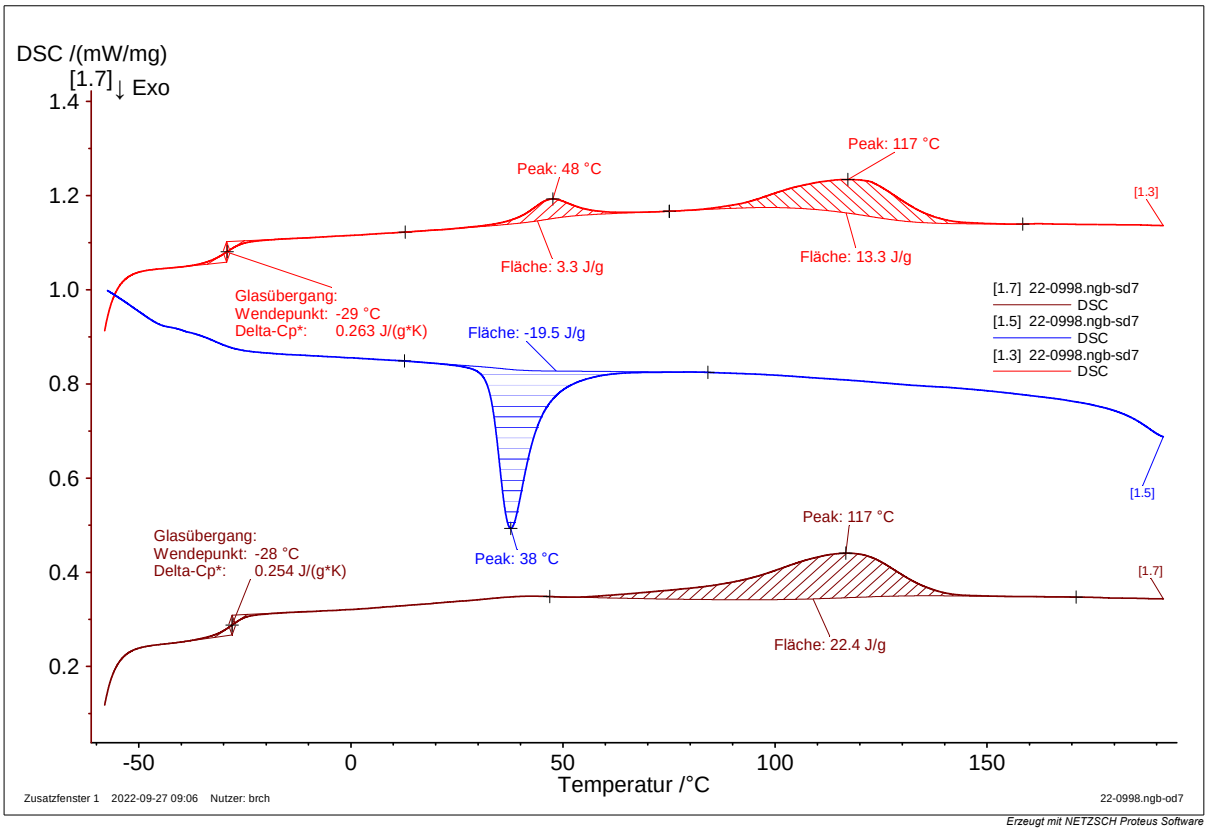

Figure 29: The diagram shows the heat flow of the sample chamber compared to the reference chamber according to the set temperature. Sample material were 5 mg of poly(butylene-adipate-co-terephthalate) after one week of incubation. The first heating curve (1.3) probably shows cold crystallization of amorphous areas around 48 °C that occurred during storage. The melting range resulted in a peak at 117 °C in both heating curves (1.3 and 1.7). In the course of the cooling curve (1.5) the crystallization can be found around 38 °C and around -29 °C and -28 °C the glass transition temperatures are marked.

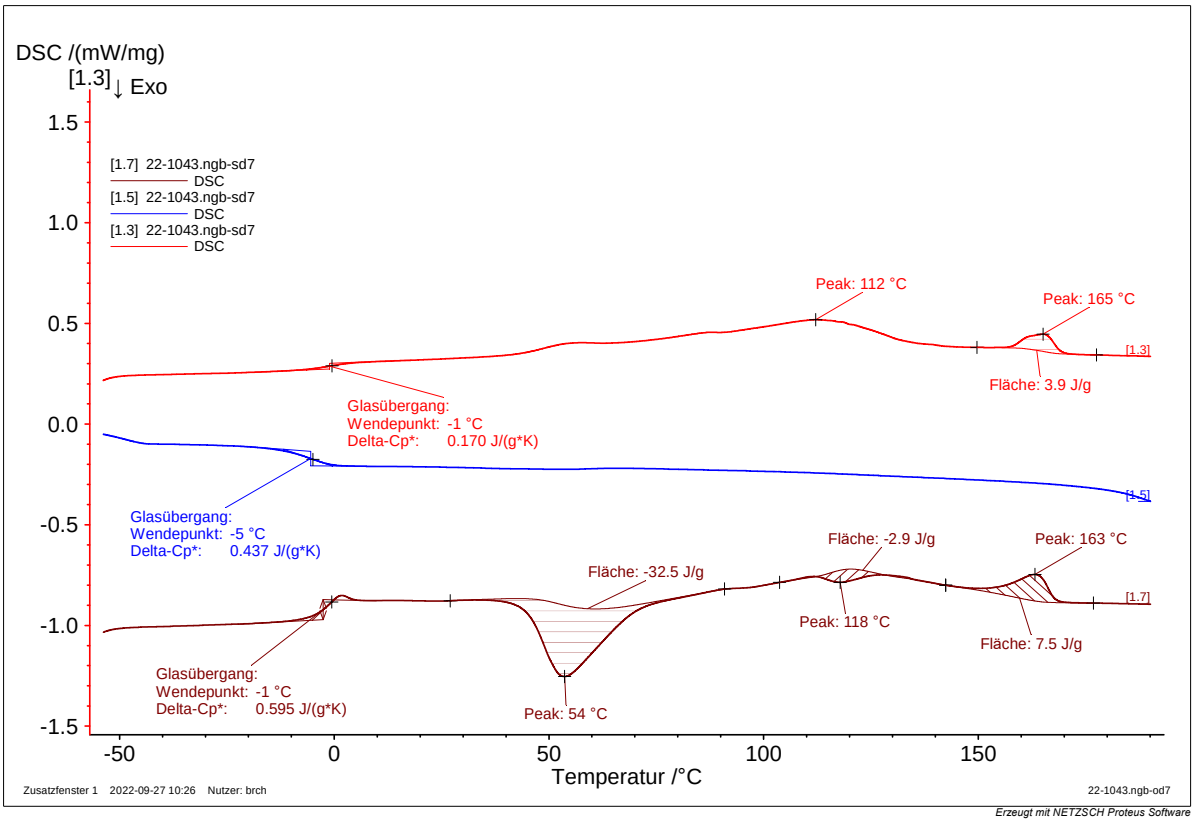

Figure 30: The diagram shows the heat flow of the sample chamber compared to the reference chamber according to the set temperature. Sample material were 5 mg of poly(3-hydroxybutyrate-co-3-hydroxyhexanoate) after one week of incubation. Due to the curved baseline, the peak areas corresponding to the melting enthalpy in both heating curves (1.3 and 1.7) were smaller than the crystallization enthalpy which is questionable.

Melting enthalpies of the samples

Table 8: Melting enthalpies in J / g from the second heating curve. Samples consisting of poly(butylene-sebacate-co-terephthalate), poly(butylene-adipate-co-terephthalate) and poly(3-hydroxybutyrate-co-3-hydroxyhexanoate) were declared as PBST, PBAT and PHA, respectively. The abbreviations in form of "Bo1_OF" indicate the soil types of regular soil (Bo1) or agricultural soil (Bo2) and sample location on the surface (OF) or buried in the soil (IN).

Week	0	1	2	4	6	8	10	12	16
PBST_Bo1_OF	10	12.5	13.4	20.6	12	14.2	18.3	14.1	18.2
PBAT_Bo1_OF	18	22.4	18.2	22.6	20	16.1	26.3	25.3	20.5
PHA_Bo1_OF	7	5	3.8	4.6	4	7	5	8	5.1
PBST_Bo1_IN	10	11.1	8.9	9.6	20	20	15.2	16	21.3
PBAT_Bo1_IN	18	9.7	12.9	10.5	18	13.8	25.8	24	16.8
PHA_Bo1_IN	7	7.5	5.2	7.8	5	7.6	8.5	4	5
PBST_Bo2_OF	10	13.2	20.9	8.2	15	18.7	22.2	16	20.1

PBAT_Bo2_OF	18	17	15.6	6.9	19	21.9	25	26	20.9
PHA_Bo2_OF	7	5.5	4.5	7.9	5	5	4.8	9	6
PBST_Bo2_IN	10	13.6	21.4	8.9	18	13.1	13.7	15	19.4
PBAT_Bo2_IN	18	21.2	13.2	17.5	15	17.1	18.5	19	23.8
PHA_Bo2_IN	7	5.2	4.4	8.7	4	5.4	4.8	5	7.5

Images of the samples incubated in film holders

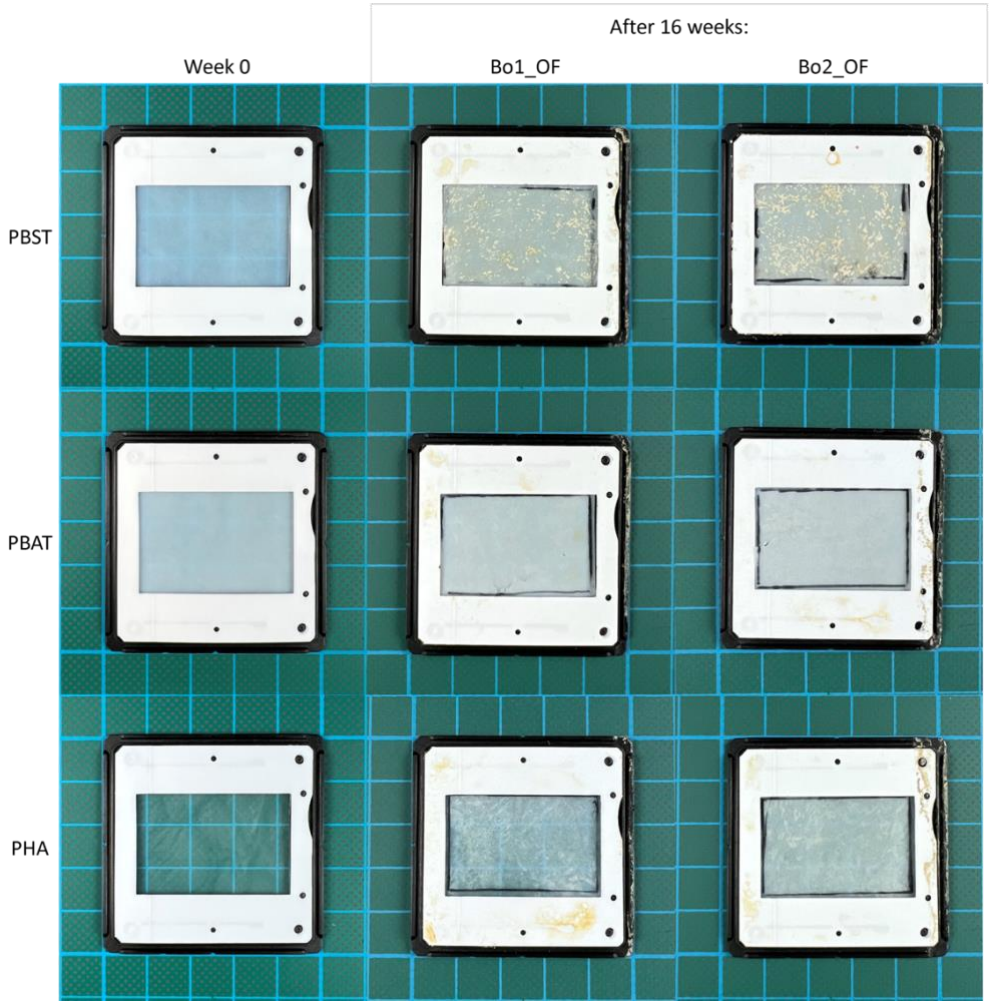

Figure 31: Images of the samples incubated in film holders in the soil before the incubation and after 16 weeks. According to the denomination of the samples, abbreviations indicate poly(butylene-sebacate-co-terephthalate) (PBST), poly(butylene-adipate-co-terephthalate) (PBAT) and poly(3-hydroxybutyrate-co-3-hydroxyhexanoate) (PHA) as well as the soil types of regular soil (Bo1) or agricultural soil (Bo2). One square of the scale paper equals 1 cm^2.

Identified peaks from the IR measurement

Table 9: Identified peaks in the IR spectrum of poly(butylene-sebacate-co-terephthalate) (PBST). *According to S.J. Kim et al. (2020) the following absorption bands were found in the PBST reference material: δ = bending, v = stretching; as = asymmetric, s = symmetric.*

Number	**Wave number cm^{-1}**	**Assignment**
1	727, 874	δ out-of-plane vibrations (Rosa)
2	1022	δ in-plane vibrations (Rosa)
3	1103	ν C-O (Rosa)
4	1168, 1264	ν C-O
5	1717	ν C=O
6	2857, 2929	$\nu_{s/as}$ $-CH_2-$ slightly shifted

Table 10: Identified peaks in the IR spectrum of poly(butylene-adipate-co-terephthalate) (PBAT). *According to Tavares et al. (2018) the following absorption bands were found in the PBAT reference material: δ = bending, v = stretching; as = asymmetric, s = symmetric.*

Number	**Wave number cm^{-1}**	**Assignment**
1	727, 875	δ out-of-plane vibrations
2	1020	δ in-plane vibrations
3	1107	ν C-O
4	1167, 1258	ν_s C-O
5	1458, 1506	ν C=C phenylene
6	1715	ν C=O
7	2873, 2955	$\nu_{s/as}$ $-CH_2-$

Table 11: Identified peaks in the IR spectrum of poly(3-hydroxybutyrate-co-3-hydroxyhexanoate) (PHA). *According to Volova et al. (2013) the following absorption bands for PHA were found in the reference material: δ = bending, ν = stretching; as = asymmetric, s = symmetric.*

Number	**Wave number cm^{-1}**	**Assignment**
1	975	$\delta_{nonplanar}$, C-H
2	1051	ν C-O secondary OH-group
3	1097	CH_2-O-CH_2 vibrations from the interaction of C=O and C-C
4	1130	-CH_2- rocking vibrations
5	1181	Skeletal ν C=O
6	1223	ν C-O
7	1269	ν_{as} C-O
8	1379	δ_s -CH_3, δ -CH_2- -CH_3
9	1455	δ_{as} -CH_3, δ -CH -CH_2- -CH_3
10	1723	ν C=O
11	2927	ν_{as} -CH_2-
12	2972	ν_{as} -CH_3